Nucleobase functionalized polymers prepared by ATRP
Toward DNA mimetic materials

Een wetenschappelijke proeve op het gebied van
Natuurwetenschappen, Wiskunde en Informatica

Proefschrift

ter verkrijging van de graad van doctor
aan de Radboud Universiteit Nijmegen
op gezag van de rector magnificus prof. dr. C. W. P. M. Blom
volgens besluit van het College van Decanen
in het openbaar te verdedigen op donderdag 26 april 2007
om 13:30 uur precies

door
Henri Johannes Spijker

Geboren op 31 maart 1976 te Enschede

Promotor: Prof. Dr. Ir. Jan C. M. van Hest

Manuscript commissie: Prof. Dr. Alan E. Rowan
Prof. Dr. Rint P. Sijbesma (TUE)
Dr. Jeroen J. L. M. Cornelissen

De uitgave van dit proefschrift is mede gerealiseerd met financiële steun van Syntarga bv.

Omslag: Ton Dirks

Uitgeverij: Ponsen & Looijen bv, Wageningen

ISBN: 978-90-6464-095-7

Elk afscheid betekent de geboorte van een herinnering.
(S.Dali)

Ter nagedachtenis aan mijn vader,
voor mijn moeder

Contents

Chapter 1

Nucleobase functionality in materials science

1 Nucleobase functionality in materials science

The ability of nature to control the structure and properties of biomolecules is at a level which is still unsurpassed by anything accomplished by current synthetic techniques. A classic example in this respect is DNA. Since the publication of the DNA model by Watson and Crick half a century ago[1], major advances in understanding the structural build up of this natural material have been made. Cornerstone for the information pathway from DNA to RNA to functional proteins is the specific reversible recognition between the four nucleobases thymine, adenine, cytosine and guanine (figure 1). The self assembly of single stranded DNA into a double stranded helix or other DNA folding motifs are driven by many intermolecular forces.

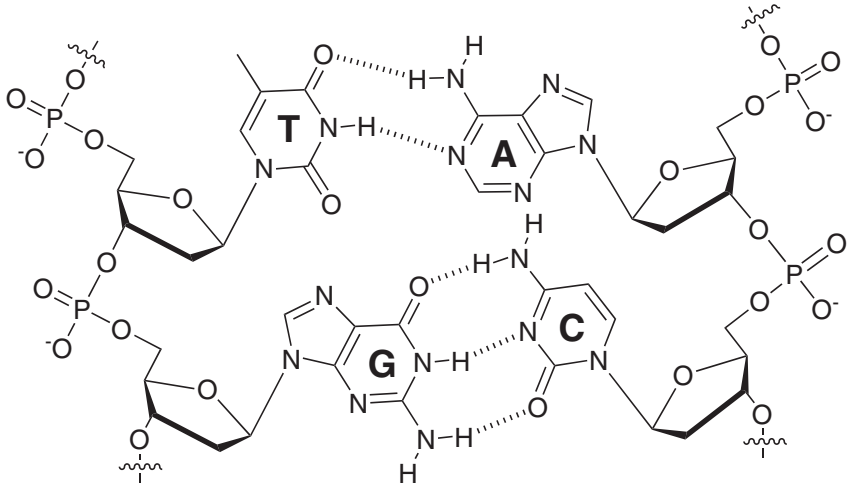

Figure 1. Watson-Crick base pairing between the four nucleotides Thymine (**T**), Adenine (**A**), Guanine (**G**) and Cytosine (**C**).

These include π-stacking interactions, hydrophobic and van der Waals forces (figure 2)[2]. Of these forces, the Watson-Crick hydrogen bonding interactions that dictate specific base-pairing are the most crucial for establishing the fidelity required for efficient storage, replication, and transcription of genetic information. However, there are 28 base-pairing motifs that involve at least two hydrogen bonds which can be formed between the four common nucleobases[2]. This has inspired researchers to investigate the use of hydrogen bonding driven base pairing for purposes other than those intended by nature.

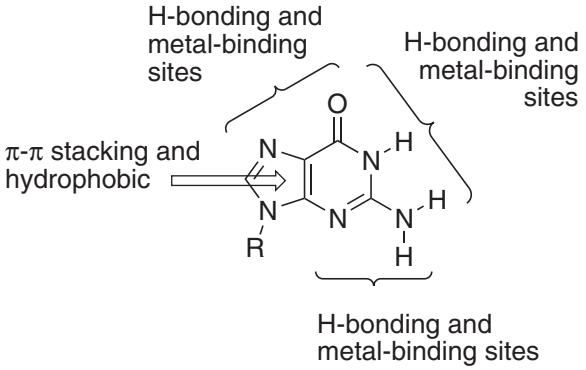

Figure 2. Some of the non-covalent interactions which are present in the nucleobase guanine

Nowadays, (bio)chemical techniques have been developed that enable convenient synthesis of DNA molecules in relatively small quantities. These techniques therefore allow researchers to create DNA strands that can be programmed to self assemble in a highly specific way. The hybridization of these synthetic DNA strands can then be used to create e.g. supramolecular materials, perform template assisted coupling reactions between different substrates, or create well-defined nanoscaled aggregates and molecular machines. Not only DNA strands are of great interest, but also synthetic analogues of the nucleotides have been prepared and used in the field of supramolecular chemistry to enhance material properties or to increase the level of control of e.g. synthetic polymerization reactions. In the following paragraphs some of the many examples in which properties of DNA or DNA-like materials have been exploited will be discussed.

1.1 Natural DNA as a building material for nanomechanical devices.

The best known form of DNA is the unbranched double helix structure proposed by Watson and Crick in 1953[1]. However, conformational variability and backbone flexibility permit the formation of branch points (junctions) which are crucial to the biological role played by nucleic acids. The replicational and Holliday junction[3] are naturally occurring examples of these branched DNA motifs and have inspired materials scientists to make artificial analogues by careful design of complementary DNA strands. The construction of immobile junctions relies on unique base pairing sequences which should obey a certain set of rules[4]. Immobile junctions can be transformed into networks by facilitating sticky end cohesion. Initial endeavors in structural DNA nanotechnology, in which these types of

immobile junctions were applied, have been directed at constructing DNA objects such as a cube[5] or a truncated octahedron[6] (figure 3 A and B respectively).

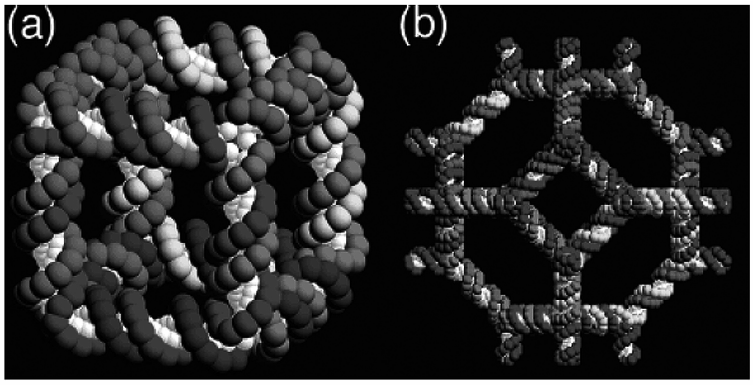

Figure 3. Ligated products prepared from flexible DNA components. A) a cube and B) a truncated octahedron.

Besides DNA, the often unique sequence-dependent folding motifs of RNA makes this polynucleobase also an appealing material for the construction of well defined nanoscaled architectures, as was shown by Jeager and others[7, 8].

DNA polyhedra and arrays are static objects that represent an approach towards nanoscaled structures. Another opportunity DNA-based materials offer is to not only control their basic structure, but also to induce well-defined structural changes. In principle, objects that can change shape, in response to an external stimulus, can function as a device or machine. The past few years have therefore seen an increasing activity in the area of nucleic acid based nanomachines.

Some of the first controlled DNA-based devices were based on structural changes in DNA induced by changing the salt concentration in the environment. Mao et al used fluorescence resonance energy transfer (FRET) to monitor the transitions in DNA folding from right handed B-DNA to left handed Z-DNA[9, 10]. Another example is a device prepared by Niemeyer et al[11], which was based on the structural transition between supercoiling of two DNA molecules[12]. It was found that the transition could be induced by varying the magnesium concentration.

More complex DNA based devices could be made by making full use of the sequence specificity associated with DNA hybridization. The first hybridization-based device was created by Yurke et al[13] (figure 4). This device consisted out of three DNA strands (A, B and C) which were hybridized in the form of a pair of tweezers. It could be closed and opened by addition of auxiliary so-called fuel strands (F) of DNA. The efficiency of the tweezers was

demonstrated by fluorescence resonance energy transfer (FRET) between the two fluorophores TET and TAMRA.

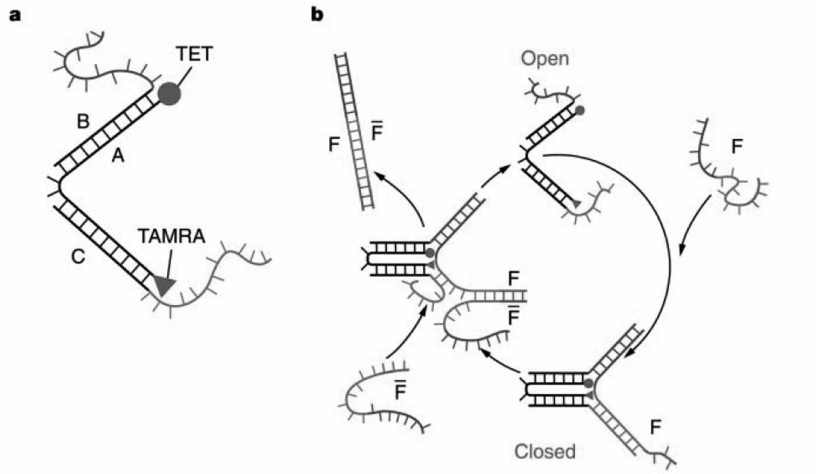

Figure 4. Construction and operation of the molecular tweezers. **A)** molecular tweezers structure formed by hybridization of oligonucleotide strands A, B and C. **B)**, closing and opening the molecular tweezers. Closing strand F hybridizes with the dangling ends of strands B and C to pull the tweezers closed. Hybridization with the overhanging section of F allows F̲ strand to remove F from the tweezers, forming a double-stranded waste product FF̲ and allowing the tweezers to open.

Seeman et al[14] created a more robust so called "PX-JX2 device", where PX is paranemic crossover DNA (two coiled double stranded DNA strands) and JX2 is its topoisomer, one end of which is rotated relative to the other by 180°. The device uses two different so called "set strands" to establish the state of the device, in either the PX or the JX2 conformation. A system to demonstrate the motion of the PX–JX2 device is shown in figure 5A and C. Four DNA trapezoids (three fused DNA triangles) are joined to three PX-JX device strands. When the system is in the PX state, all trapezoids point in the same direction, but they point in opposite directions in the JX2 state. The device is operated by addition and removal of different set strands, and is demonstrated by the AFM images of the molecules (figure 5c).

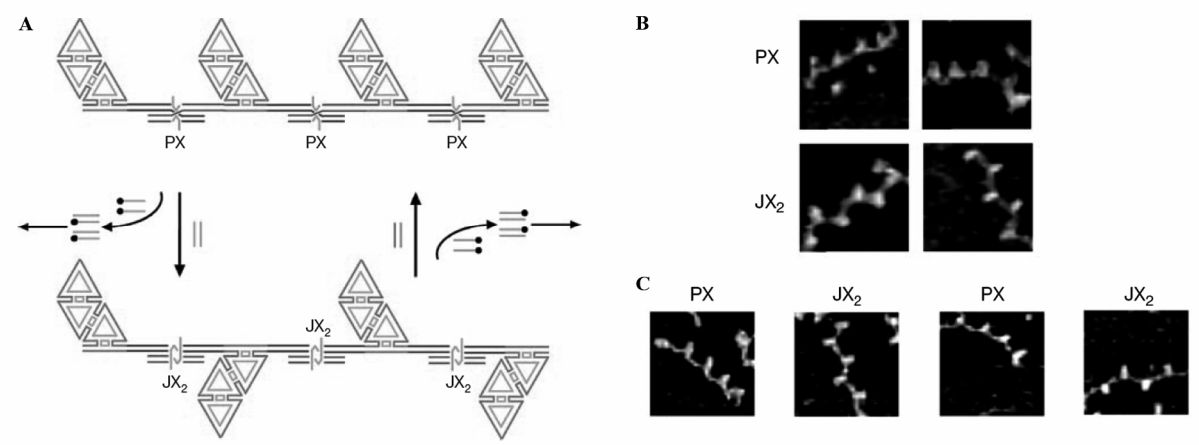

Figure 5. A) a simplified schematic representation of the device consisting of four DNA trapezoids which are joined to three PX-JX2 device strands. B) control AFM images of the DNA molecules locked in either the PX or JX2 state (not a device). C) AFM images taken at different stages during cycling of the device.

These abovementioned examples describe the use of double stranded DNA motifs to create stable sequence-specific predefined constructs. Smart hybridization between two DNA strands can even cause specific motion to occur. Cornerstone for these DNA constructs and machines is of course the specific recognition capability of DNA. Another direction researchers are investigating is the use of the sequence specific hybridization of DNA for the organization of nanoscaled objects.

1.2 DNA-assisted organization of nanoscaled aggregates.

The sequence specificity of the self aggregation process of DNA strands into different morphologies has stimulated chemists to explore the possibilities of utilizing these features for development of advanced artificial systems for various applications[11].

Material scientists have focused on DNA as a synthetically programmable interconnect for the preparation of new nanoscaled materials with preconceived architectural parameters and properties[15-17]. Most of the research has focused on the use of inorganic nanoparticles as building blocks for larger structures.

DNA hybridization was used to generate repetitive nanocluster materials[15, 18, 19]. Two non-complementary oligonucleotides were coupled in separate reactions with gold nanoparticles. A DNA strand containing regions complementary to both particle-bound DNAs was added as a linker. The addition of the linker led to sequence-specific assembly of

the oligonucleotide modified colloids. The reversibility of the process was demonstrated by the temperature dependent changes of the UV/Vis spectroscopic properties. The work was expanded by generating binary networks consisting of two types of gold clusters as shown in figure 6.

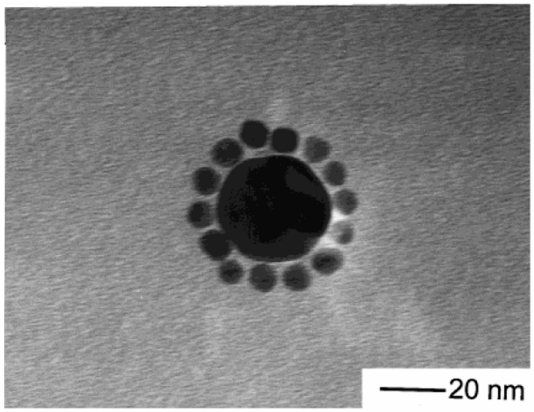

Figure 6. TEM images of binary DNA-linked network materials. A satellite structure formed by using a 60-fold excess of the 8-nm particles[18].

A different approach to control the spatial arrangement of molecular devices was investigated by Schultz and coworkers[20, 21]. They attached single stranded DNA oligonucleotides of defined length and sequence to individual nano-crystals, which were subsequently assembled into dimers and trimers on addition of a complementary single stranded DNA template (figure 7).

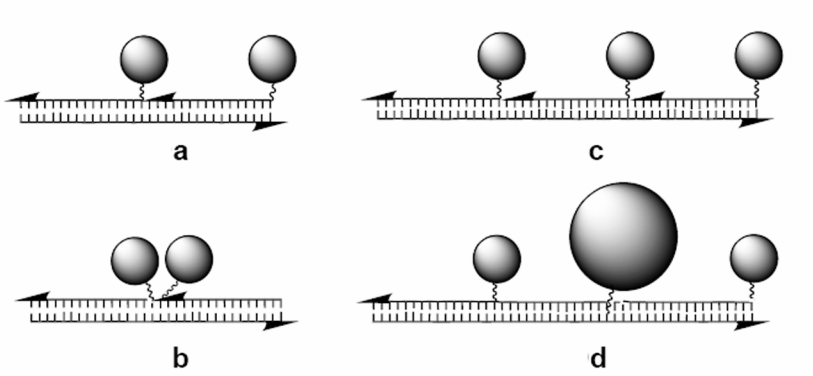

Figure 7. Assembly of conjugates from gold particles and thiolated oligonucleotides allowed formation of head to tail or head to head dimers (a, b), trimers (c) or hetero trimers (d) by means of DNA hybridization.

Besides controlling the spatial arrangement of inorganic nanoparticles, the control over spatial arrangement of functional chemical groups like fluorescent probes has also been developed. These types of DNA or RNA molecules are often referred to as molecular probes

and ever since their first report in 1996[22], molecular beacons (MBs) have become a class of DNA probes that are widely used in chemistry, biology, biotechnology and medical sciences for biomolecular recognition[23-25]. In the traditional format, MBs act like switches that are normally closed — or 'off'. Binding induces conformational changes that open the hairpin and, as a result, the fluorescence is turned 'on'. The stem structure (figure 8a) holds the fluorophore and the quencher in close proximity to one another, preventing the fluorophore from emitting a signal as a result of resonance energy transfer (RET). Once the single stranded loop portion of the MB hybridizes to the target, the stem melts and the resulting spatial separation of the fluorophore from the quencher leads to an enhancement in fluorescence signal (figure 8b).

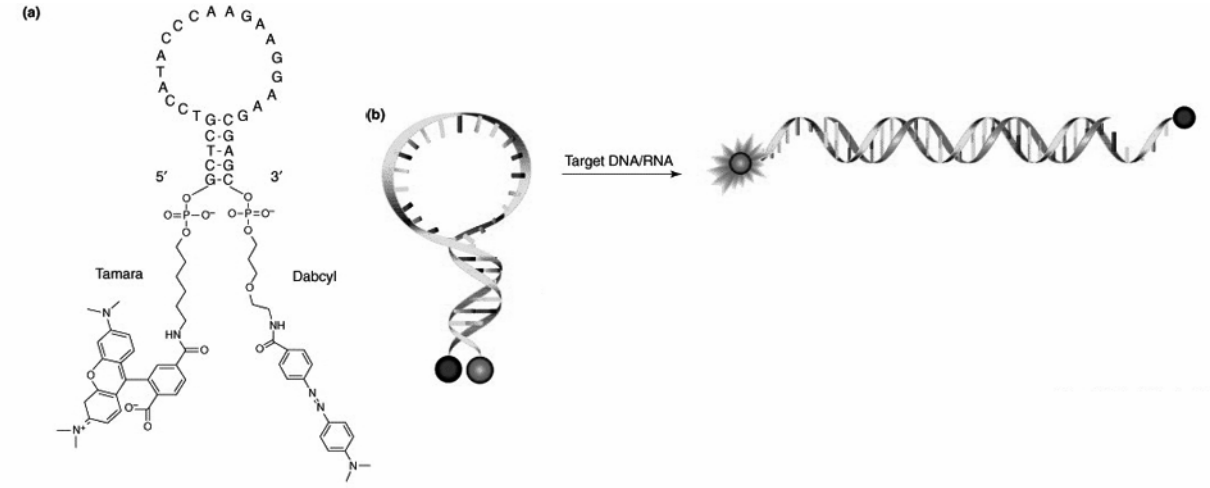

Figure 8. Structural characteristics of molecular beacon probes. (a) A typical molecular beacon DNA probe. (b) Molecular beacon working principle.

An alternative for DNA-based binding scaffolds was explored by McIntosh[26] and others[27]. They fabricated Mixed Monolayer Protected Gold Clusters (MMPCs) functionalized with tetraalkylammonium ligands that can interact with the DNA backbone via charge complementarity. Binding studies indicated that the MMPCs and DNA form a charge-neutralized, non-aggregated assembly as was shown by monitoring DNA UV/Vis absorption after removal of the MMPC/DNA particles by centrifugation. The interactions controlling these assemblies are highly efficient, completely inhibiting transcription by T7 RNA polymerase in vitro. These MMPCs are potential leads for the creation of biosensors and for chemotherapeutics.

Mirkin et al.[28] created a polystyrene-DNA conjugate using solid-phase synthesis on controlled pore glass beads. The key reagent in the synthesis was a phosphoramidite modified polystyrene chain, which was coupled to alcohol-terminated oligonucleotides directly on the glass beads. The resulting amphiphilic molecules yielded micelles, which were studied using AFM and light scattering studies.

So far most examples discussed here have focused on using hybridization between two single stranded DNA chains attached to different materials. This concept is however not limited to the use of DNA strands. Rotello and coworkers[29, 30], developed a "brick and mortar" system in which colloidal gold particles functionalized with single nucleobase recognition elements serve as bricks, while polymers bearing a complementary functionality serve as mortar. Complementarity between colloid and polymer was achieved using the diaminotriazine-thymine three-point hydrogen bonding interaction of which an example is depicted in figure 9.

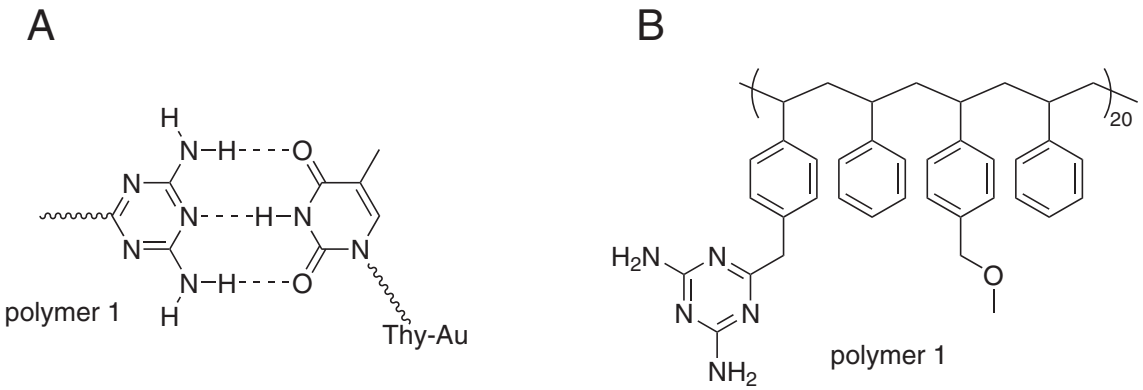

Figure 9. Recognition motif and polymer mortar. **A)** diaminotriazine-thymine recognition **B)** triazine functionalized random copolymer 1.

It was observed with small angle X-ray scattering (SAXS) that after aggregation induced by polymer 1 (figure 9), the observed interparticle distance of 4.4 nm was in good agreement with distances calculated by molecular modeling. Large scale ordering of the Au particles was also observed with TEM. In addition, it was found that the self-assembly process is temperature dependent, since larger aggregates were obtained at lower temperatures.

1.3 Supramolecular materials based upon nucleobase functionality

Synthetic macromolecules bearing oligonucleobase moieties are very appealing candidates for application in molecular nanotechnology, biotechnology or gene delivery. However, since most specific DNA sequences are often produced in only μg scale quantities, DNA functionalized macromolecules are limited with respect to their use in materials science. Therefore scientists are investigating the use of synthetically more easily accessible nucleobase functionalized materials of which some examples will be discussed.

The typical melting behavior of DNA and PNA[31, 2], caused by breaking up of the intermolecular forces involved with base pairing, has also been exploited to create thermo responsive materials by side chain modification of polymer materials. Armitage and coworkers[32] created, using Atom Transfer Radical Polymerization (ATRP), well defined water soluble polymers with end groups designed to couple reversibly with complementary PNA groups connected to a small core (figure 10).

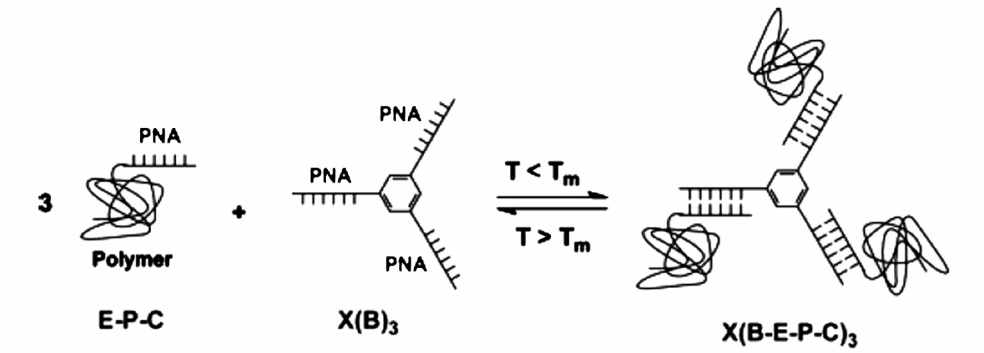

Figure 10. Reversible coupling via PNA moieties on a crosslinker (XB3) and the complementary groups on the polymer (P) end group (E)

Polymerization from a PNA initiator resulted in a PNA polymer hybrid (figure 10 E-P-C) which could be reversibly coupled to a three arm PNA crosslinker ($X(B)_3$). Thermoreversible duplex formation was shown by a transition in absorbance at 260 nm, and additional light scattering measurements indicated the formation of star-shaped polymers at lower temperatures.

Several research groups prepared materials functionalized with single nucleobases for use in biotechnological applications[33, 34]. Puskas et al[35, 36] synthesized and characterized a polystyrene resin carrying thymine functionality, obtained via free radical emulsion copolymerization of styrene, thymine-functionalized monomer and divinylbenzene

(figure 11a). Bioseparation studies with these materials were analyzed using FTIR spectroscopy. It was shown that both bovine serum albumin (BSA) and bovine hemoglobin (BHb) were chemisorbed via hydrogen bonding interactions onto the thymine functionalized PS copolymer beads. Additionally, good separation of binary mixtures of the enzymes via adsorption onto the polymer beads could be achieved for both enzymes.

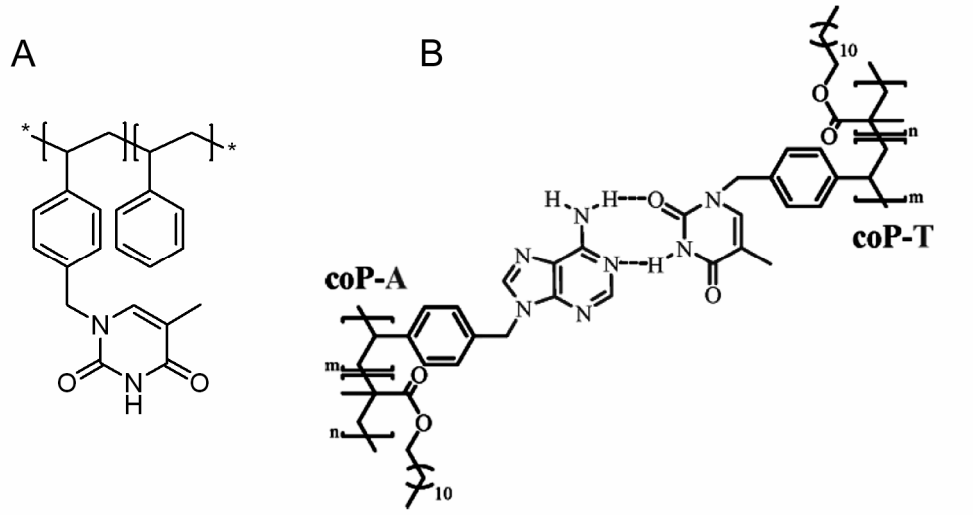

Figure 11. Nucleobase functionalized styrene copolymers. A) thymine functionalized styrene used by Puskas et al. for bioseparation studies. B) mixture of random copolymers containing adenine (A) or thymine (T) functionalization used by Lutz et al.

Lutz and coworkers[37] prepared adenine and thymine functionalized styrene monomers and copolymerized them using conventional free radical polymerization (figure 11b). Preliminary investigations showed that the adenine functionalized copolymer self-assembled with the complementary thymine copolymer. The supramolecular aggregates obtained showed a DNA like melting behavior in nonpolar solvents.

Sleiman and coworkers[38, 39] were the first to use ring opening metathesis polymerization (ROMP) to prepare block copolymers containing adenine or thymine[40] functionality. In order to improve solubility of the adenine monomer and increase the degree of polymerization they employed the hydrogen bonding capability of adenine with complementary succinimide. Initial studies on the self assembly behavior of the block copolymers revealed a cylindrical morphology in THF.

Meijer et al[41-45] showed that reversible polymers may possess properties that are similar to traditional covalent polymers despite the short-lived non-covalent interactions (lifetime on the order of seconds) defining the main chain. In line with this work, several researchers demonstrated that chain end functionalization of oligomethylene spacers with nucleobase functionality[46, 47] resulted in the formation of supramolecular fibers[48]. Iwaura et al[49] prepared oligomethylene spacers with oligonucleotides and confirmed with microscopy studies that the hydrogels consisted of intertwined nanofibers. It was found that these bola-amphiphiles without the ribose and phosphate units (figure 12A) self assembled into water to produce fibers in the crystalline state without forming a hydrogel[48].

Low molecular weight macromonomers that had single protected nucleobases placed on both chain ends resulted in materials behaving like high molecular weight polymers[50-53]. It was found that supramolecular telechelic adenine functionalized polymer self assembled in the solid state, to yield materials with high mechanical stability. Interestingly, the thymine derivative did not show these types of properties, due to a high crystallization temperature which prevented any film or fiber-forming ability. The weak association constant between the adenine moieties suggests that other factors such as π-π stacking interactions may play a crucial role in this self assembly process.

Oligonucleotide-based monomers prepared by Craig et al[54, 55] were intensively studied as models to gain more insight in the thermodynamics and kinetics of reversible polymers. They found that slight changes in the primary base sequence resulted in varied thermodynamics of association, which were reflected in the molecular weights of resulting polymeric assemblies. Incorporation of synthetic spacers between the oligonucleotides within a monomer had a substantial influence on the conformational properties of the monomer and resulting assemblies. They reasoned that the lower molecular weights found for the more flexible monomers was the result of the presence of more cyclic structures.

Sivakova et al[56] showed that attachment of nucleobase derivatives to a functional mesogenic fluorescent core can have drastic effects on the liquid crystalline behavior of the material. Attachment of the thymine or a protected adenine nucleobase to a mesogenic alkoxy-substituted bis(phenylethynyl)benzene results in a loss of LC behavior. Upon mixing and annealing the complementary monomers results in the formation of relative stable LC phases. Additionally, the material showed polymer-like properties like fiber formation.

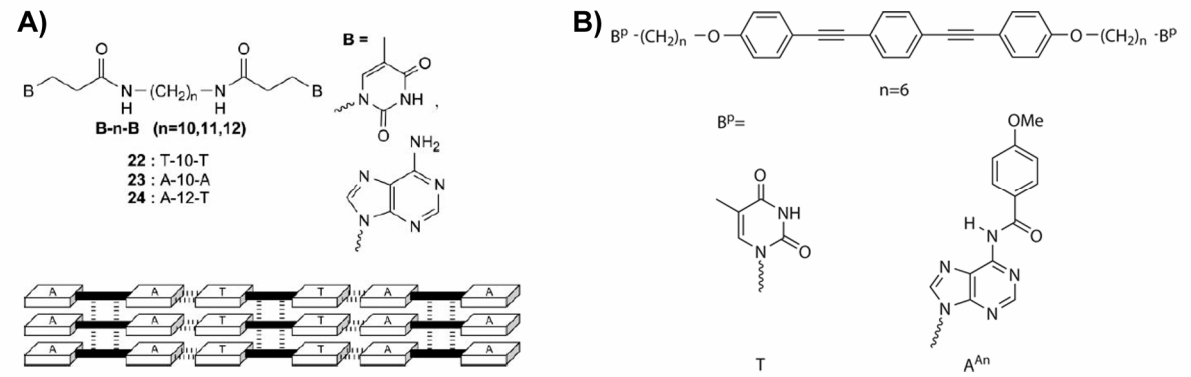

Figure 12. **A**) nucleobase functionalized Bola-amphiphiles and a possible hydrogen bonding scheme. **B**) nucleobase functionalized liquid crystalline materials prepared by Sivakova

1.4 DNA aided synthesis and templating

In many processes occurring in nature, a template is used for the preparation of a new molecule. A beautiful example is of course DNA replication and transcription. Upon DNA replication the double helix DNA strand unfolds into two single stranded DNA molecules. Both DNA strands can then act as a template for the preparation of an RNA or new DNA molecule. By making use of a template, nature is able to accurately use the information stored in the DNA molecule towards all kinds of processes occurring in living organisms.

The recognition that templating might also be useful for organic reactions has captured the imagination of chemists. The first examples of nucleic acid templated synthesis used DNA or RNA templates to mediate ligation reactions that generate oligomers of DNA, RNA, or structural analogues of nucleic acids[57-62]. More recently, Liu et al started to probe the structural requirements for DNA templated synthesis (DTS) by generating products that do no relate to the DNA backbone[63]. Different DNA architectures were equipped with electrophiles and treated with nucleophiles linked to a complementary DNA oligonucleotide (figure 13). This led to the formation of the expected reaction products, whereas little non-templated intermolecular product formation was observed. Remarkably, the reported DNA-templated reactions include a variety of reaction types and reactant structures, despite considerable variations in their transition-state geometry, steric hindrance, and conformational flexibility. The possible ligation reactions compatible with DNA templated synthesis were gradually expanded from nucleophilic substitution and conjugate addition to

amine acylation, reductive amination, nitro-aldol and nitro-Michael addition, Wittig olefination, transition metal-catalyzed cross-coupling[64]; heterocycle formation[65]; cycloadditions[64, 66], and metal coordination complex formation[67, 68]. The development of cleavable linkers enabled multi step small molecule synthesis [69].

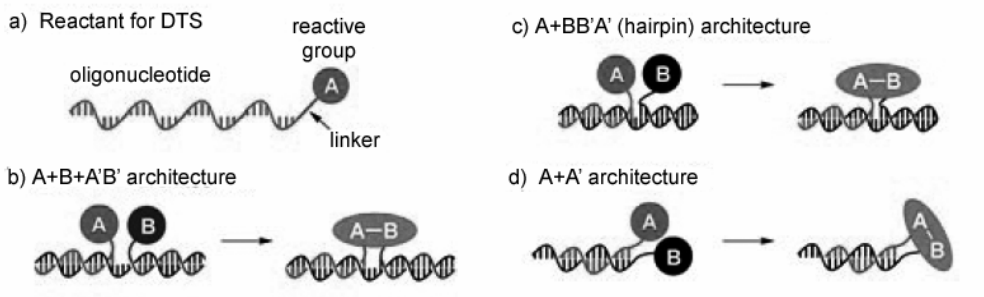

Figure 13. a) The three components of a reactant for DTS. b)–d) Template architectures for DTS. A/B and A′/B′ refer to reactants containing complementary oligonucleotides, and + symbols indicate separate molecules.

Using these features of DTS, libraries of DNA sequences were translated into synthetic small molecule macrocycles (figure 14). In the first step, a starting library was annealed with a different complementary reagent library after which the first templated reaction took place. Repeating these steps with different reagent libraries completed the macrocycle after three templated steps. The resulting DNA-macrocycle conjugates were subjected to in vitro selections for protein affinity. PCR amplification and DNA sequence characterization were used to identify a single macrocycle possessing known target affinity.

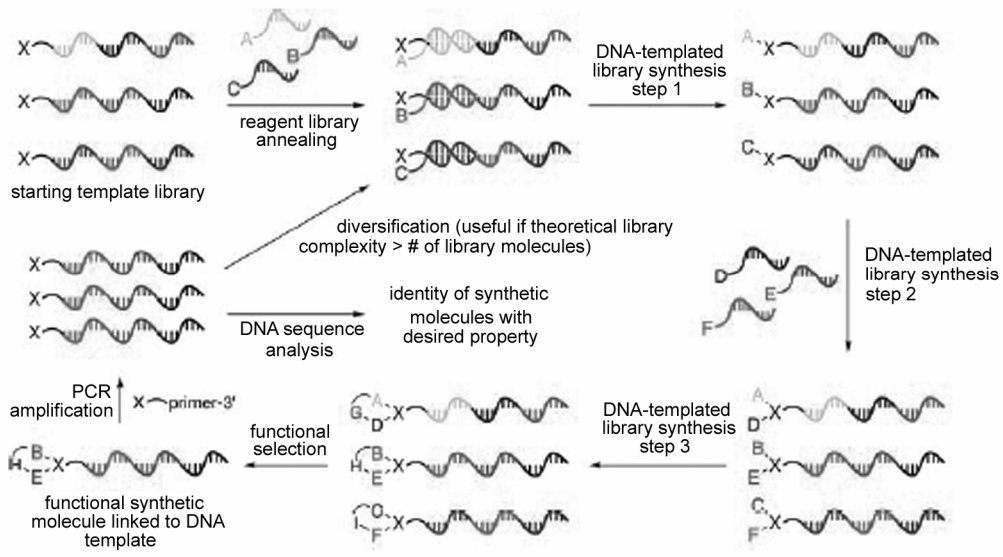

Figure 14. Scheme for translation, selection, and amplification of libraries of DNA templates encoding synthetic small molecules.

Besides using DNA or RNA for templating organic coupling reactions, already in the seventies polymer chemists were interested in studying the use of base-base interaction between different nucleic acid analogues for polymerization purposes. One of the first examples of template polymerization used nucleobase containing polymers such as poly-N-vinyl derivatives of adenine, uracil and protected cytosine nucleobases[70, 71]. Initially only polymer-polymer interactions were studied between premade polymers using different spectroscopic techniques and compared with monomeric and dimeric model compounds[72]. Later methacryloyl and methacrylamide type polymers containing adenine, uracil and thymine moieties were also prepared[73-77] and used in initial template polymerization studies. Those investigations involved free radical copolymerization of the different monomers in the presence of the complementary polymers. It was observed that the copolymerization proceeds predominantly under the influence of base-base pairing between the adenine and uracil rings.

In a more recent investigation Marsh and coworkers[78, 79] prepared protected nucleoside acrylate and methacrylate type monomers, and used free radical polymerization to prepare homo and co polymers. They investigated the effect of these nucleobase functionalized polymers on the free radical polymerization of complementary nucleobase monomers. They showed by careful analysis of the products that only uracil functionalized polymer can act as a template for the polymerization of the complementary adenine monomer in the presence of the noncomplementary uracil monomer (figure 15). They reasoned that intramolecular interactions of the adenine polymer hindered this polymer to function as a suitable template for the polymerization of uracil monomer.

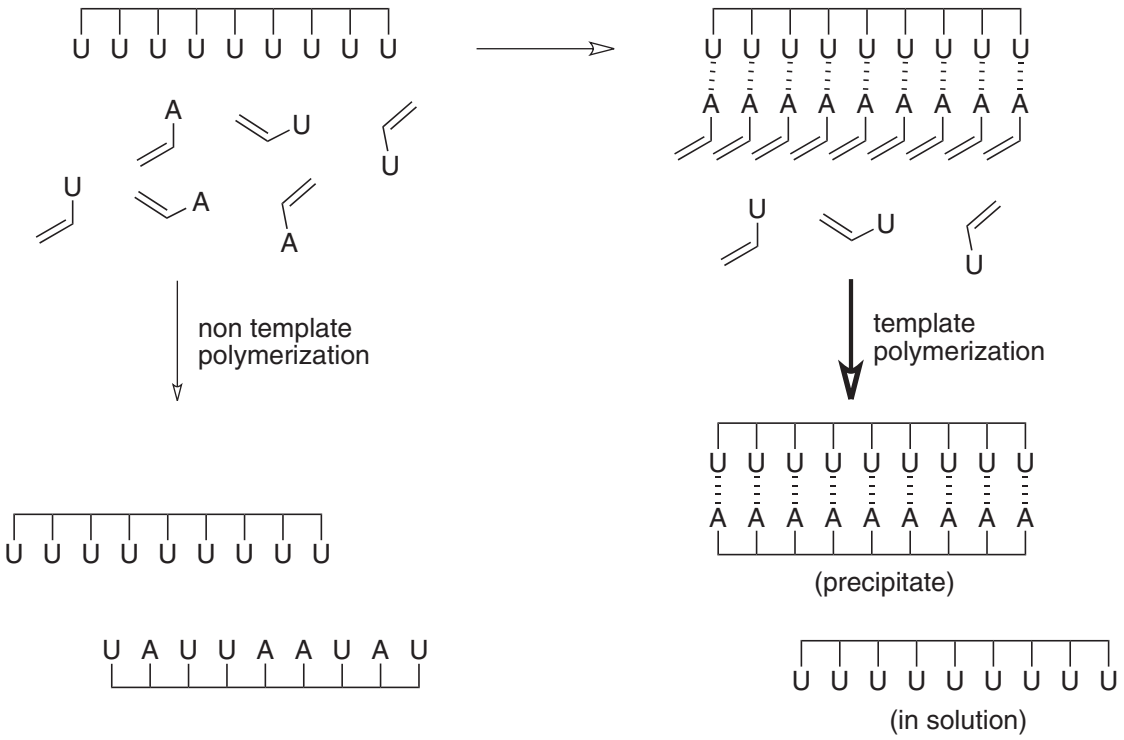

Figure 15. Schematic representation of the possible routes during the template polymerization of adenine (A) monomer in the presence of a uracil (U) functionalized polymer template.

1.5 Outline of this thesis

From a polymer chemist's point of view, the DNA molecule can be regarded as a copolymer, which has a highly defined monomer composition and polymer chain length. Using this DNA molecule as a template, nature can produce a new DNA strand that has the same chain length and exact complementary monomer sequence. Cornerstone for the high level of accuracy and specificity at which this process is performed is the recognition between the four nucleobases, which is also known as Watson-Crick base pairing. As described above already in the seventies researchers started to investigate the use of nucleobase functionalized monomers for template polymerizations. However, often they were hampered in their analysis by poor control over the polymerization and poor solubility of the materials that were obtained.

The development of controlled radical polymerization techniques, like atom transfer radical polymerization (ATRP)[80-82] opens possibilities for well-defined polymers containing biofunctional monomers. These findings inspired us to investigate the use of ATRP to

prepare nucleobase containing polymer architectures, and study their assembly and template polymerization behavior.

In chapter 2 the synthesis and controlled polymerization of all four nucleobase monomers using ATRP is described. Although ATRP has proven itself as a versatile polymerization technique which tolerates nucleobase functionality[78, 79], this is the first time that it has been used to polymerize in a controlled fashion all four nucleobase monomers (thymine, adenine, cytosine and guanine) without any need for protective groups[85].

Chapter 3 describes the initial template polymerization studies using adenine and thymine monomers. To circumvent possible solubility problems, PEG block copolymers were also prepared and used as template polymers for the polymerization of the complementary monomers[83].

The PEG – nucleobase block copolymers prepared in chapter 3 were found to have amphiphilic character. The self aggregation behavior of these materials was further investigated in chapter 4 using techniques such as dynamic light scattering and UV/vis spectroscopy[84].

The recognition properties of complementary nucleobase functionalized polymer materials were further exploited by preparing linear ABA-type triblock copolymers. Different synthetic methods are described in chapter 5, as well as their use as supramolecular polymer materials.

Finally in chapter 6 the nucleobase functional PEG block copolymers aggregates were probed for their ability to bind natural single stranded DNA and double stranded plasmid DNA. Additionally, a preliminary study to use these materials as gene transfection vehicles was performed.

1.6 References

1. J. D. Watson and F. H. C. Crick. *Nature* **1953**, *171*, 737-738.
2. W. Saenger. *Principles of Nucleic Acid Structure*, ed.; Springer-Verlag: New York, 1984; Vol.
3. R. Holliday. *Genet Res* **1964**, *5*, 282.
4. N. C. Seeman. *J. Theor. Biol.* **1982**, *99*, 237-247.
5. J. H. Chen and N. C. Seeman. *Nature* **1991**, *350*, 631-633.
6. Y. W. Zhang and N. C. Seeman. *J. Am. Chem. Soc.* **1994**, *116*, 1661-1669.
7. A. Chworos, I. Severcan, A. Y. Koyfman, P. Weinkam, E. Oroudjev, H. G. Hansma and L. Jaeger. *Science* **2004**, *306*, 2068-2072.
8. P. X. Guo. *J. Nanosci. Nanotechnol.* **2005**, *5*, 1964-1982.
9. W. Zacharias, J. E. Larson, J. Klysik, S. M. Stirdivant and R. D. Wells. *J. Biol. Chem.* **1982**, *257*, 2775-2782.
10. C. D. Mao, W. Q. Sun, Z. Y. Shen and N. C. Seeman. *Nature* **1999**, *397*, 144-146.
11. C. M. Niemeyer. *Angew. Chem., Int. Ed.* **2001**, *40*, 4128-4158.
12. C. M. Niemeyer, M. Adler, S. Lenhert, S. Gao, H. Fuchs and L. F. Chi. *ChemBioChem* **2001**, *2*, 260-264.
13. B. Yurke, A. J. Turberfield, A. P. Mills, F. C. Simmel and J. L. Neumann. *Nature* **2000**, *406*, 605-608.
14. H. Yan, X. P. Zhang, Z. Y. Shen and N. C. Seeman. *Nature* **2002**, *415*, 62-65.
15. C. A. Mirkin, R. L. Letsinger, R. C. Mucic and J. J. Storhoff. *Nature* **1996**, *382*, 607-609.
16. N. L. Rosi and C. A. Mirkin. *Chem. Rev.* **2005**, *105*, 1547-1562.
17. J. Xu and S. L. Craig. *J. Am. Chem. Soc.* **2005**, *127*, 13227-13231.
18. C. A. Mirkin. *Inorg. Chem.* **2000**, *39*, 2258-2272.
19. S. J. Park, A. A. Lazarides, C. A. Mirkin and R. L. Letsinger. *Angew. Chem., Int. Ed.* **2001**, *40*, 2909-2912.
20. A. P. Alivisatos, K. P. Johnsson, X. G. Peng, T. E. Wilson, C. J. Loweth, M. P. Bruchez and P. G. Schultz. *Nature* **1996**, *382*, 609-611.
21. C. J. Loweth, W. B. Caldwell, X. G. Peng, A. P. Alivisatos and P. G. Schultz. *Angew. Chem., Int. Ed.* **1999**, *38*, 1808-1812.
22. S. Tyagi and F. R. Kramer. *Nat. Biotechnol.* **1996**, *14*, 303-308.
23. C. Tse and J. Capeau. *Annales De Biologie Clinique* **2003**, *61*, 279-293.
24. W. H. Tan, K. M. Wang and T. J. Drake. *Curr. Opin. Chem. Biol.* **2004**, *8*, 547-553.
25. G. Goel, A. Kumar, A. K. Puniya, W. Chen and K. Singh. *Journal of Applied Microbiology* **2005**, *99*, 435-442.
26. C. M. McIntosh, E. A. Esposito, A. K. Boal, J. M. Simard, C. T. Martin and V. M. Rotello. *J. Am. Chem. Soc.* **2001**, *123*, 7626-7629.
27. R. R. Arvizo, A. Verma and V. M. Rotello. *Supramol. Chem.* **2005**, *17*, 155-161.
28. Z. Li, Y. Zhang, P. Fullhart and C. A. Mirkin. *Nano Letters* **2004**, *4*, 1055-1058.
29. A. K. Boal, F. Ilhan, J. E. DeRouchey, T. Thurn-Albrecht, T. P. Russell and V. M. Rotello. *Nature* **2000**, *404*, 746-748.
30. R. Shenhar, T. B. Norsten and V. M. Rotello. *Adv. Mater.* **2005**, *17*, 657-669.
31. D. Voet, W. B. Gratzer, R. A. Cox and P. Doty. *Biopolymers* **1963**, *1*, 193-208.
32. Y. Wang, B. A. Armitage and G. C. Berry. *Macromolecules* **2005**, *38*, 5846-5848.
33. F. Ilhan, M. Gray and V. M. Rotello. *Macromolecules* **2001**, *34*, 2597-2601.
34. R. Shenhar and V. M. Rotello. *Acc. Chem. Res.* **2003**, *36*, 549-561.
35. Y. Dahman, J. E. Puskas, A. Margaritis, Z. Merali and M. Cunningham. *Macromolecules* **2003**, *36*, 2198-2205.
36. J. E. Puskas, Y. Dahman and A. Margaritis. *Biomacromolecules* **2004**, *5*, 1412-1421.
37. J.-F. Lutz, A. F. Thuenemann and K. Rurack. *Macromolecules* **2005**, *38*, 8124-8126.
38. H. S. Bazzi and H. F. Sleiman. *Macromolecules* **2002**, *35*, 9617-9620.
39. J. Dalphond, H. S. Bazzi, K. Kahrim and H. F. Sleiman. *Macromol. Chem. Phys.* **2002**, *203*, 1988-1994.
40. W. H. Binder and C. Kluger. *Macromolecules* **2004**, *37*, 9321-9330.
41. R. P. Sijbesma, F. H. Beijer, L. Brunsveld, B. J. B. Folmer, J. Hirschberg, R. F. M. Lange, J. K. L. Lowe and E. W. Meijer. *Science* **1997**, *278*, 1601-1604.
42. B. J. B. Folmer, R. P. Sijbesma, R. M. Versteegen, J. A. J. van der Rijt and E. W. Meijer. *Adv. Mater.* **2000**, *12*, 874-878.
43. L. Brunsveld, B. J. B. Folmer, E. W. Meijer and R. P. Sijbesma. *Chem. Rev.* **2001**, *101*, 4071-4097.
44. R. P. Sijbesma and E. W. Meijer. *Chem. Commun.* **2003**, 5-16.
45. G. Ligthart, H. Ohkawa, R. P. Sijbesma and E. W. Meijer. *J. Am. Chem. Soc.* **2005**, *127*, 810-811.
46. W. H. Binder, M. J. Kunz, C. Kluger, G. Hayn and R. Saf. *Macromolecules* **2004**, *37*, 1749-1759.

47. D. Farnik, C. Kluger, M. J. Kunz, D. Machl, L. Petraru and W. H. Binder. *Macromolecular Symposia* **2004**, *217*, 247-266.
48. T. Shimizu, R. Iwaura, M. Masuda, T. Hanada and K. Yase. *J. Am. Chem. Soc.* **2001**, *123*, 5947-5955.
49. R. Iwaura, K. Yoshida, M. Masuda, M. Ohnishi-Kameyama, M. Yoshida and T. Shimizu. *Angew. Chem., Int. Ed.* **2003**, *42*, 1009-1012.
50. S. J. Rowan, P. Suwanmala and S. Sivakova. *J. Polym. Sci., Part A: Polym. Chem.* **2003**, *41*, 3589-3596.
51. S. Sivakova and S. J. Rowan. *Abstr. Pap. Am. Chem. Soc.* **2004**, *227*, U215-U215.
52. S. Sivakova, D. A. Bohnsack, M. E. Mackay, P. Suwanmala and S. J. Rowan. *J. Am. Chem. Soc.* **2005**, *127*, 18202-18211.
53. S. Sivakova and S. J. Rowan. *Chem. Soc. Rev.* **2005**, *34*, 9-21.
54. E. A. Fogleman, W. C. Yount, J. Xu and S. L. Craig. *Angew. Chem., Int. Ed.* **2002**, *41*, 4026-4028.
55. J. Xu, E. A. Fogleman and S. L. Craig. *Macromolecules* **2004**, *37*, 1863-1870.
56. S. Sivakova and S. J. Rowan. *Chem. Commun.* **2003**, 2428-2429.
57. G. Vonkiedrowski. *Angew. Chem., Int. Ed.* **1986**, *25*, 932-935.
58. T. Wu and L. E. Orgel. *J. Am. Chem. Soc.* **1992**, *114*, 7963-7969.
59. T. F. Wu and L. E. Orgel. *J. Am. Chem. Soc.* **1992**, *114*, 5496-5501.
60. R. K. Bruick, P. E. Dawson, S. B. Kent, N. Usman and G. F. Joyce. *Chem. Biol.* **1996**, *3*, 49-56.
61. Y. Z. Xu and E. T. Kool. *Nucleic Acids Res.* **1999**, *27*, 875-881.
62. Y. Z. Xu and E. T. Kool. *J. Am. Chem. Soc.* **2000**, *122*, 9040-9041.
63. Z. J. Gartner and D. R. Liu. *J. Am. Chem. Soc.* **2001**, *123*, 6961-6963.
64. Z. J. Gartner, M. W. Kanan and D. R. Liu. *Angew. Chem., Int. Ed.* **2002**, *41*, 1796-1800.
65. X. Y. Li, Z. J. Gartner, B. N. Tse and D. R. Liu. *J. Am. Chem. Soc.* **2004**, *126*, 5090-5092.
66. A. T. Poulin-Kerstien and P. B. Dervan. *J. Am. Chem. Soc.* **2003**, *125*, 15811-15821.
67. D. Summerer and A. Marx. *Angew. Chem., Int. Ed.* **2002**, *41*, 89-90.
68. X. Y. Li and D. R. Liu. *Angew. Chem., Int. Ed.* **2004**, *43*, 4848-4870.
69. Z. J. Gartner, M. W. Kanan and D. R. Liu. *J. Am. Chem. Soc.* **2002**, *124*, 10304-10306.
70. K. Kondo, H. Iwasaki, N. Ueda, K. Takemoto and M. Imoto. *Makromol. Chem.* **1968**, *120*, 21-26.
71. N. Ueda, K. Kondo, M. Kono and K. Takemoto. *Makromol. Chem.* **1968**, *120*, 13-20.
72. F. Kawakubo, K. Kondo and K. Takemoto. *Makromol. Chem.* **1973**, *169*, 37-44.
73. M. Akashi, T. Okimoto, Y. Inaki and K. Takemoto. *J. Polym. Sci., Part A: Polym. Chem.* **1979**, *17*, 905-916.
74. M. Akashi, H. Takada, Y. Inaki and K. Takemoto. *J. Polym. Sci., Part A: Polym. Chem.* **1979**, *17*, 747-757.
75. K. Takemoto and Y. Inaki. *Adv. Polym. Sci.* **1981**, *41*, 1-51.
76. Y. Inaki, K. Ebisutani and K. Takemoto. *J. Polym. Sci., Part A: Polym. Chem.* **1986**, *24*, 3249-3262.
77. Y. Inaki, S. Sugita, T. Takahara and K. Takemoto. *J. Polym. Sci., Part A: Polym. Chem.* **1986**, *24*, 3201-3217.
78. A. Khan, D. M. Haddleton, M. J. Hannon, D. Kukulj and A. Marsh. *Macromolecules* **1999**, *32*, 6560-6564.
79. A. Marsh, A. Khan, D. M. Haddleton and M. J. Hannon. *Macromolecules* **1999**, *32*, 8725-8731.
80. J. S. Wang and K. Matyjaszewski. *Macromolecules* **1995**, *28*, 7901-7910.
81. K. Matyjaszewski, D. A. Shipp, J. L. Wang, T. Grimaud and T. E. Patten. *Macromolecules* **1998**, *31*, 6836-6840.
82. K. Matyjaszewski. *Curr. Org. Chem.* **2002**, *6*, 67-82.
83. H. J. Spijker, A. T. J. Dirks and J. C. M. van Hest. *Polymer* **2005**, *46*, 8528-8535.
84. H. J. Spijker, A. J. Dirks and J. C. M. van Hest. *J. Polym. Sci., Part A: Polym. Chem.* **2006**, *44*, 4242-4250.
85. H.J.Spijker, F.L. van Delft, J.C.M. van Hest. *Macromolecules* **2007**, *40*, 12-18.

Chapter 2

Atom Transfer Radical Polymerization of Adenine, Thymine, Cytosine and Guanine Nucleobase Monomers

2 Atom Transfer Radical Polymerization of Adenine, Thymine, Cytosine and Guanine Nucleobase Monomers

2.1 Introduction

The high fidelity and specificity of the DNA replication and transcription process has been a source of inspiration for materials scientists for many years, resulting in a range of well-defined DNA-based molecular architectures and devices[1-5]. The specific hydrogen bond interaction between the nucleotide pairs adenine–thymine and guanine–cytosine, also known as Watson-Crick base pairing, has also been employed in polymer chemistry. Already in the early seventies Inaki and coworkers[6-9] conducted free radical polymerization of nucleobase functionalized monomers in DMSO/ethylene glycol mixtures in order to use hydrogen bonding interactions to control the sequence of monomer units in a polymer chain via a templated polymerization mechanism. The DNA recognition concept has also been applied for the construction of supramolecular polymers[10-13] and polymer assemblies[14-16] by introduction of complementary single DNA strands, and even single nucleobase moieties, to the chain ends of synthetic polymers.

Recent developments in controlled metathesis and radical polymerization techniques have enlarged the ability of polymer scientists to create better defined polymers containing nucleobase functionality. Several research groups[17, 18] polymerized nucleobase monomers using ring-opening metathesis polymerization (ROMP). (Non covalent) protection of the adenine and thymine monomers was necessary to obtain high conversions. In case of cytosine, however, solubility problems hindered further analysis of polymer; guanine-functionalized norbornene derivatives could not be polymerized successfully using ROMP.

Haddleton et al[19, 20] used free radical polymerization and atom transfer radical polymerization (ATRP) to polymerize protected adenosine and uridine monomers and demonstrated it to be possible to polymerize via ATRP methyl methacrylate (MMA) using unprotected adenosine and uridine initiators. In addition, a remarkable template effect was observed when adenosine and uridine monomers were polymerized in the presence of uridine polymer as template using a free radical polymerization technique. Lutz and coworkers[21] used ATRP to prepare nucleobase functionalized styrene-like copolymers and demonstrated the DNA like melting behavior in nonpolar solvents. Gross et al[22] polymerized

with ATRP unprotected adenosine and thymidine monomers using polyethylene glycol macroinitiators in order to obtain amphiphilic block copolymers. These diblock copolymers showed an assembly behavior which was affected by the presence of complementary nucleobases.

As aforementioned well-defined polymers based on nucleobase monomers adenine, uracil and thymine have been prepared. However, to the best of our knowledge the controlled polymerization of the remaining two nucleobases cytosine and guanine has been unreported. The ability to polymerize also these monomers facilitates the use of the stronger triple hydrogen bonds for template polymerizations and polymer assemblies. Moreover, it enables in combination with the adenine-thymine base pair the construction of more complex systems and fully exploit the complementary nature of Watson-Crick base pairing.

In this chapter we describe the synthesis and controlled polymerization of all four nucleobase methacrylate monomers. We have used a convenient two step synthetic route for the synthesis of thymine, adenine and cytosine methacrylate monomers. The guanine monomer synthesis was more elaborate and involved several protection and deprotection steps. All four monomers were polymerized in a controlled fashion using ATRP while kinetics were monitored using ^{1}H NMR spectroscopy.

2.2 Results and discussion

2.2.1 Monomer synthesis

Thymine monomer **2** was synthesized using 3-bromopropanol as starting material (Scheme 1). Treatment of this alcohol with methacryloyl chloride under basic conditions resulted in 3-bromopropyl methacrylate **1**[25]. Reaction of thymine with K_2CO_3 in DMF, followed by addition of **1** and a catalytic amount (10 mol%) of tetra butyl ammonium iodide (TBAI) gave thymine monomer **2** in 38% yield. The yield for monomer **2** was rather low due to side reactions such as dialkylation at the N1 and N3 position. Several attempts to increase the yield using a literature procedure that involved protection of thymine with trimethylsilyl groups prior to alkylation[26-28] in order to prevent dialkylation, did not increase the yield, since the bis-(trimethylsilyl)thymine was readily hydrolyzed back to its starting compound.

Adenine and cytosine monomers were obtained using a modified procedure of Gokel et al[27, 23] in which the nucleobase was deprotonated by treatment with sodium hydride

(NaH) in DMF. The subsequent addition of **1** resulted in nucleobase monomer **3** and **4** in reasonable yields of 69% and 48% respectively.

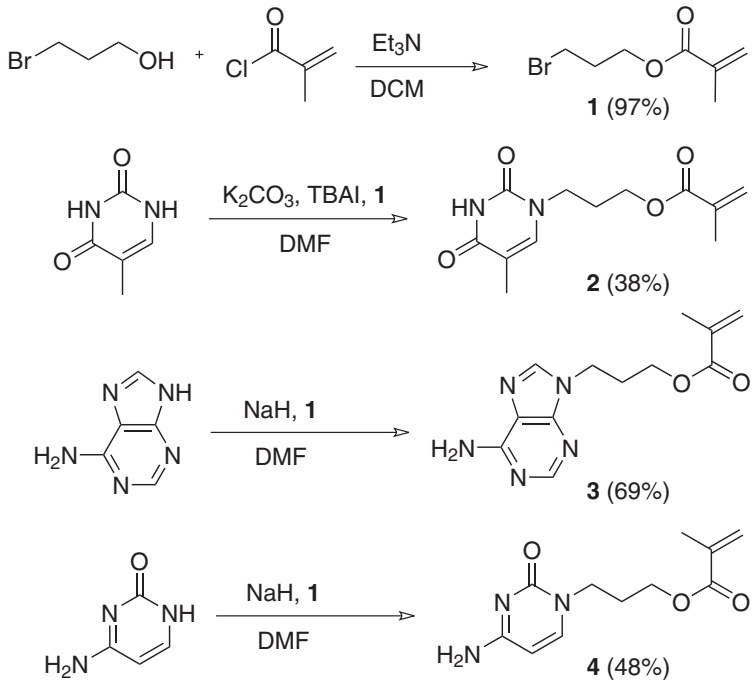

scheme 1. Synthesis of thymine, adenine and cytosine methacrylate monomers **2-4**

The synthesis of guanine monomer **5** was more elaborate since direct alkylation leads to a virtually inseparable mixture of N7 and N9 alkylated products[29, 30]. In order to obtain the desired guanine monomer, we therefore adapted a procedure described by Benner *et al*[31] for selective N9 alkylation of guanine using Mitsunobu-type conditions, as depicted in scheme 2. For selective N9 alkylation an O6 and N2 protected guanine precursor was needed. In particular the appropriate choice of the protective groups for the N2 position was crucial, since most protective groups described in literature[32] require deprotection conditions that would also hydrolyze the methacrylate ester function in the final monomer. In order to prevent this unwanted side reaction, a protective group that could be removed under mild conditions was necessary. Since enzymatic protecting group techniques have proven their efficiency with complete selective removal under mild conditions we chose the enzyme-labile phenyl acetyl moiety as a protective group[33-35] which could be removed efficiently using penicillin acylase.

Therefore, phenylacetic anhydride **11**, freshly prepared by treatment of phenylacetic acid with acetic anhydride, was condensed with guanine in refluxing DMF, followed by

acylation at N9 to obtain 9-acetyl-*N*-phenylacetylguanine **6** in 83% yield for the two steps. Purine ether derivative **7** was obtained from **6** by Mitsunobu coupling with 2-(*p*-nitrophenyl)ethanol followed by N7 deacetylation upon refluxing in a water/ethanol mixture (87% yield overall). For the next step, 3-hydroxypropylmethacrylate **10** was prepared by esterification of 1,3-propanediol with methacryloyl chloride under basic conditions. The second Mitsunobu condensation under strictly anhydrous conditions with intermediate **7**, performed immediately after purification of alcohol **10** due to its rather low stability, alkylated exclusively at the 9-position, resulting in the protected guanine methacrylate ester **8**. In the final two steps of the sequence, smooth deprotection of the 2-(*p*-nitrophenyl)ethyl group with 1,8-Diazabicyclo[5.4.0]undec-7-ene (DBU) followed by enzymatic removal of the phenylacetyl protective group using penicillin acylase, resulted in the unprotected 3-(guanin-9-yl)-propyl methacrylate **5** in an overall yield of 14%.

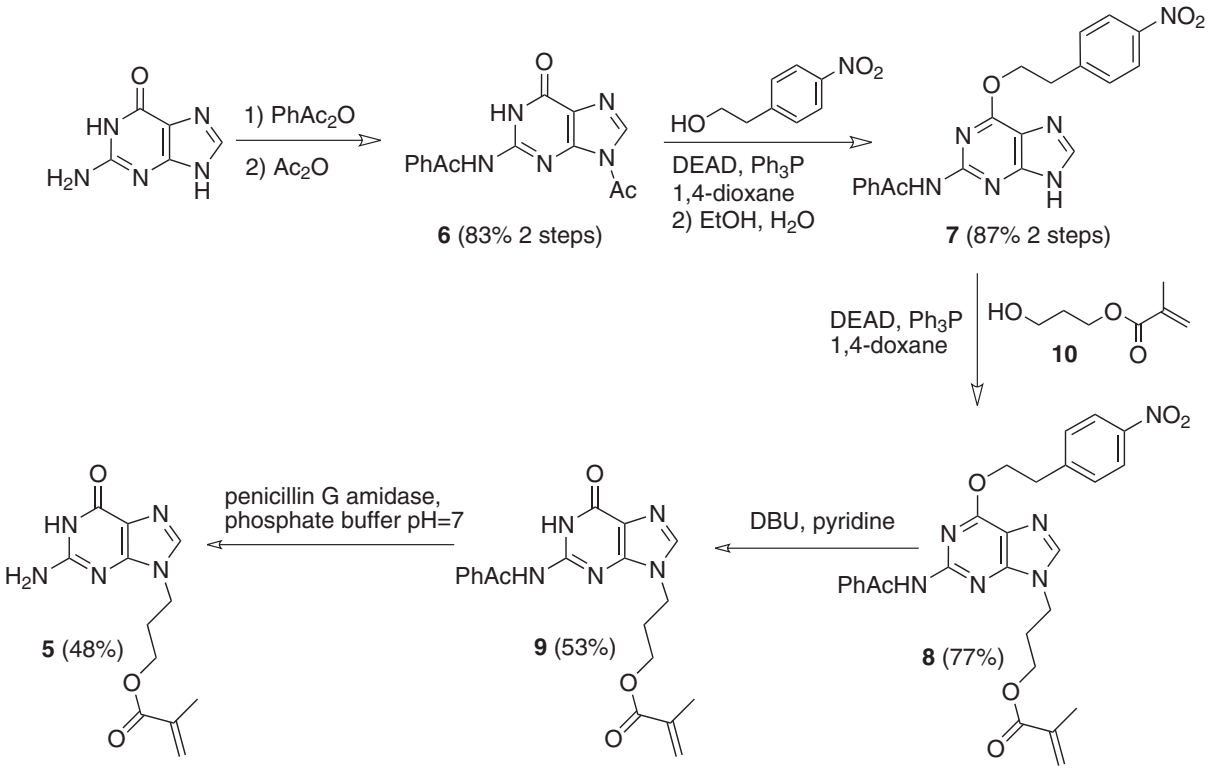

scheme 2. Guanine monomer **5** synthesis

2.3 Polymerization

Due to the relative low solubility of the nucleobase monomers in organic solvents commonly used for ATRP, and the anticipated solubility problems of the nucleobase polymers, polymerizations were performed in DMSO. Previous research in our group with peptide-based monomers[36] has already established DMSO as an adequate solvent for ATRP. Furthermore, the use of deuterated DMSO-d_6 offers the possibility to monitor kinetics directly by following the reaction with NMR spectroscopy. Thus, ATRP of monomer **2** was performed under the action of cuprous chloride (CuCl) and 2,2'-bipyridine (bpy) as catalyst and ethyl 2-bromoisobutyrate (EBiB) as initiator.

The polymerizations were monitored using ^{1}H-NMR spectroscopy by comparison of the integrals of the methacrylate proton at 6.11 ppm with the thymine H6 proton signal at 6.94 ppm for monomer **2** and the methacrylate proton at 5.91 ppm with the adenine H2 and H8 signals at 8.14 ppm in case of monomer **3**. Initially the thymine monomer polymerization was carried out at 80°C, but due to the fact that at this temperature polymerization proceeded extremely fast –reaching 92% conversion in 60 minutes– the polydispersity of the polymer was rather high (PDI > 1.3). Therefore, reaction temperature was lowered to ambient temperature and initial monomer concentration lowered to 0.5 mol/L to obtain a controlled polymerization rate. It was found that under these conditions the polymerization of thymine monomer **2** proceeded smoothly and with first order kinetics (figure 1).

Under identical conditions, 3-(adenine-9-yl)propyl methacrylate **3** also polymerized in controlled fashion, supported by the narrow molecular weight distribution (PDI=1.19) of the polymer, as was found by GPC. As can be seen in figure 1, good first order kinetics were obtained during the polymerization of both the thymine and adenine functionalized monomers.

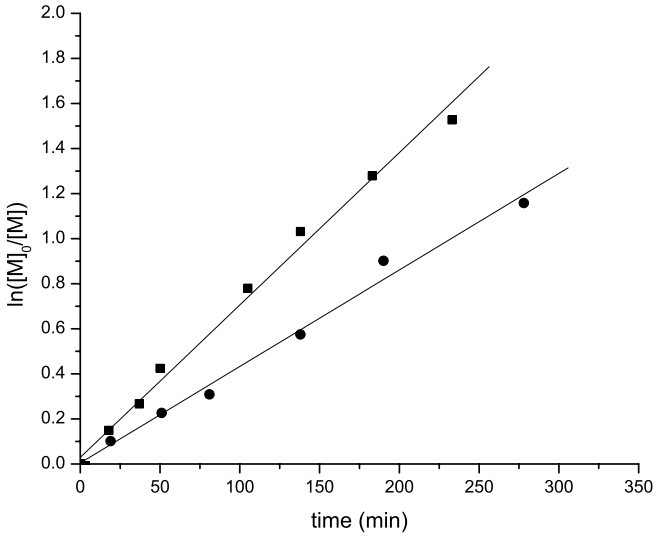

Figure 1. Kinetic plot of ATRP of thymine monomer (■, **2** = 0.58 M, CuCl = 0.020 M, bpy = 0.037 M, EBiB = 0.017 M) and adenine monomer (●, **3** = 0.36 M, CuCl = 0.013 M, bpy = 0.027 M, EBiB = 0.011 M) monomers.

For the polymerization of the guanine monomer similar ATRP conditions were applied. Because the guanine monomer **5** has a relative low solubility even in DMSO-d_6 a maximum monomer concentration of 0.13 M could be obtained. Furthermore, the reaction was performed in an NMR tube in order to scale down the reaction and still be able to monitor the polymerization kinetics in more detail. In an NMR tube, a solution of monomer **5** in DMSO-d_6 and the CuBr/bpy catalyst was deoxygenated by purging with argon for a few minutes. Surprisingly, the ^{1}H NMR spectrum of guanine monomer showed disappearance of the H8 (8.67 ppm) signal and broadening of other peaks upon addition of the catalyst stock solution as can be seen in figure 2. Also bipyridine signals (6.83 and 7.34 ppm) could be observed, indicating a chelating effect of guanine monomer with copper replacing the 2,2'-bipyridine as ligand. Interestingly, complex formation had no significant negative effect on the polymerization of **5**.

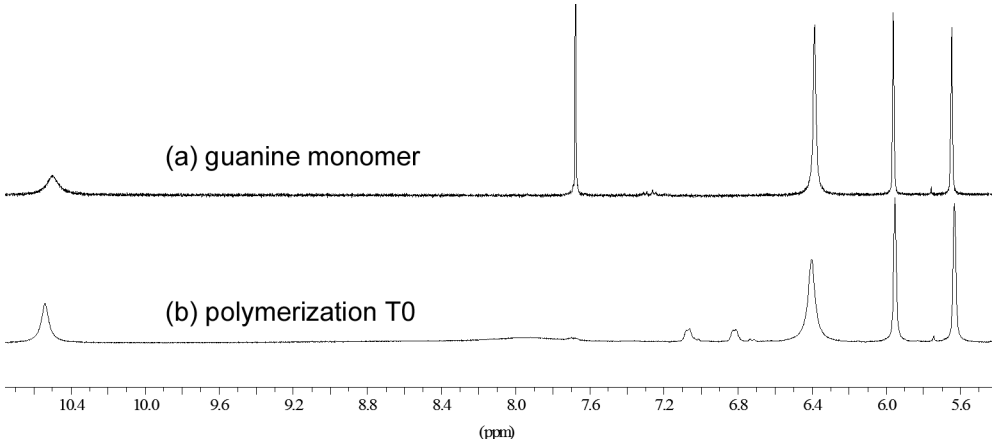

Figure 2. Part of the ^{1}H NMR spectrum of guanine monomer **5** (upper trace) and T0 of the polymerization of **5** with CuBr/2 bpy in DMSO-d_6 (lower trace).

Polymerization was started by addition of initiator followed by immediate recording of the first ^{1}H NMR spectrum (T0) after which at different time intervals more ^{1}H NMR spectra were recorded. Relative monomer concentrations could be determined from these spectra by comparing the methacrylate proton at 5.96 ppm of the monomer with the NH_2 protons at 6.37 ppm of guanine in monomer and polymer. The kinetic plot depicted in figure 3 shows that polymerization proceeded with relative good first order kinetics. GPC analysis revealed a discrepancy between the theoretical and observed molecular weight, which is indicative for a low initiation efficiency. Nevertheless a good polydispersity, indicating control over the polymerization was observed.

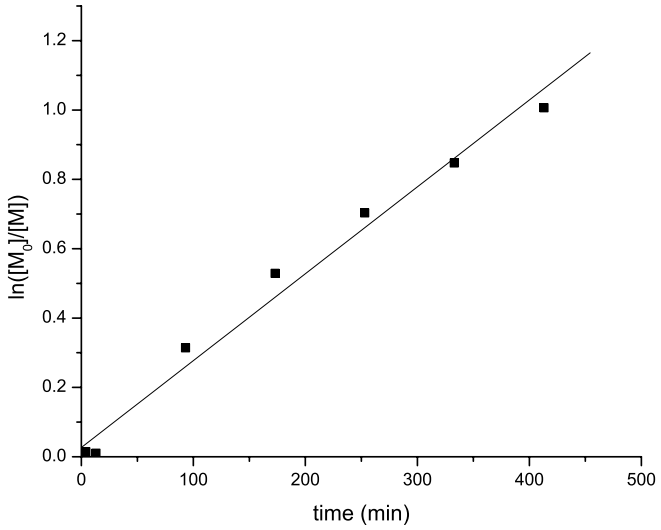

Figure 3. Kinetic plot of ATRP of guanine monomer (**5** = 0.13 M, CuBr = 9.4 mM, bpy = 18.8 mM, EBiB = 8.5 mM).

Table 1. Polymerization of thymine and adenine monomers

Polymer	Monomer	Temp (°C)	[M] (mol/L)	$M_{n\ theo}$[a] Kg/mol	M_n[b] Kg/mol	M_w/M_n[b]
12	**2**	ambient	0.58	6.4	6.8	1.21
13	**3**	ambient	0.36	5.8	6.9	1.19
15	**5**	40	0.13	3.2	6.5	1.15

a) Determined from conversion, b) determined by GPC with PEG calibration and RID detection

When the same ATRP-conditions used for monomer **2** and **3** were applied to cytosine monomer **4** no polymerization occurred even after the temperature was increased from 25 to 80°C. Detailed analysis of the 1H NMR spectrum showed also in this case broadening, *i.e.* the NH_2 signal at 7.0-7.2 ppm changed from a broad doublet to a broad singlet. In contrast, the H6 proton at 7.59 ppm remained a sharp doublet, whereas the H5 proton at 5.65 ppm of cytosine disappeared (figure 4). These findings indicate chelation of the cytosine monomer to copper, and are in line with literature where addition of only a small amount of copper(I) ($6x10^{-5}$ M) already completely broadens the H5 proton in a ^{1}H NMR spectrum[37, 38].

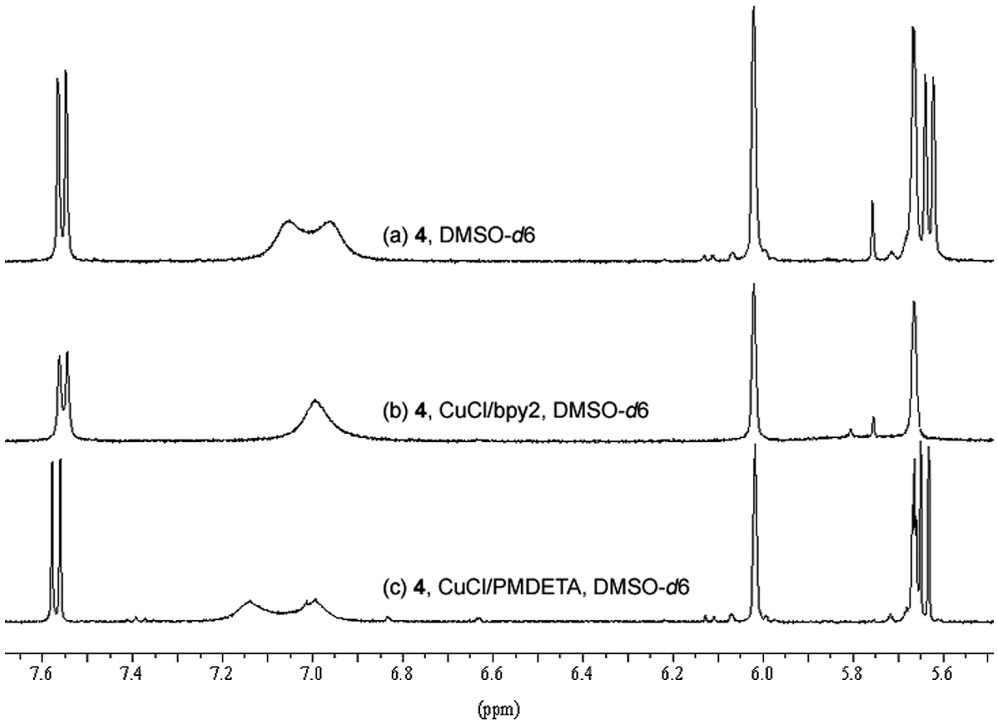

Figure 4. Part of ^{1}H NMR spectra of (**a**) cytosine monomer **4** (**b**) **4** with CuCl/2 bpy as catalyst (**c**) **4** with CuCl/PMDETA as catalyst.

Unfortunately, complex formation of cytosine with copper renders the catalyst inactive and consequently no polymerization occurs. We therefore decided to use the tridentate ligand N,N,N',N",N"-pentamethyldiethylenetriamine (PMDETA) instead of bipyridine, because PMDETA is known to bind more strongly to copper[39]. However, due to the high activation constant of the CuCl/PMDETA catalyst in polar solvents, the polymerization rate at room temperature was already very high and the kinetics did not show first order behavior (figure 5). Consequently, to lower the polymerization rate and improve control over the polymerization, the amount of catalyst (CuCl/PMDETA) was lowered. Although the polymerization rate was effectively lowered, still no good first order kinetics were observed, and the measured polydispersities remained relatively high (PDI = 1.29). Better first order kinetics were observed, determined by NMR, when 7.5 mol% cupric chloride ($CuCl_2$) was added to the catalyst. In addition, GPC analysis gave a molecular weight distribution (PDI) of 1.17, DP = 8, confirming the observations of the kinetics experiment.

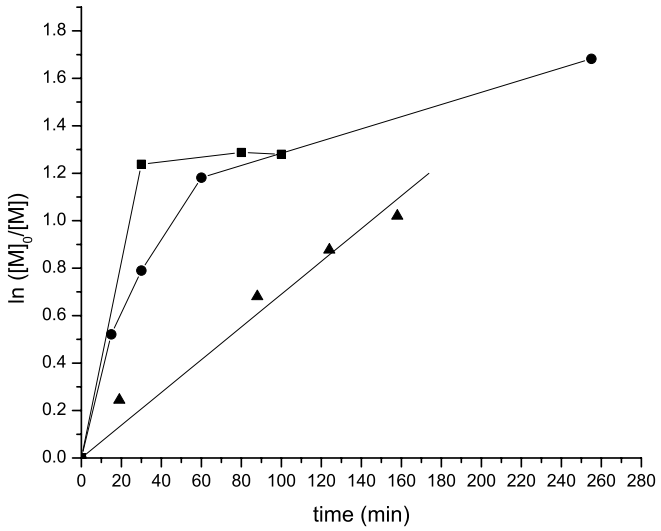

Figure 5. Kinetic plot for the polymerization of **4** with different CuCl:PMDETA ratios and weight % $CuCl_2$: (■, 1:2, 0%), (●, 1:0.3, 0%), (▲, 1:0.4, 10%).

Table2 polymerization conditions for cytosine monomer **4**

Ligand	Ratio [EBiB]/[Cu(I)Cl]/[Cu(II)Cl_2]/[Ligand]				Temp (°C)	Conv. (%)	M_n	M_w	M_w/M_n
bpy	1.00	1.13	0	2.25	rt - 80	0	-	-	-
PMDETA	1.00	1.08	0	2.02	rt	74	7.2	9.7	1.35
PMDETA	1.00	0.50	0	0.50	rt	54	5.6	7.2	1.29
PMDETA	1.00	0.66	0.05	0.40	30	65	4.5	5.2	1.15

2.4 conclusions

All four unprotected methacrylate nucleobase monomers were successfully synthesized. Thymine, adenine and cytosine monomers could be obtained via direct alkylation of the unprotected free nucleobase with 3-bromopropyl methacrylate **1**. Guanine monomer **5** was obtained after several protection and deprotection steps in an overall yield of 24%. Furthermore, all four unprotected nucleobase monomers were polymerized in a controlled fashion using ATRP. Conveniently, DMSO-d_6 was used as a solvent to enable monitoring of kinetics using ^{1}H NMR spectroscopy. Complex formation of guanine and cytosine monomer with copper(II) could be observed by NMR analysis and in case of cytosine the use of PMDETA as ligand and addition of 10 mol% copper(II) was necessary to obtain a sufficiently active catalytic system that allowed control over the polymerization. Since all four nucleobase monomers can now be polymerized in a controlled fashion, exploitation of the specific and complementary nature of base pairing for template polymerizations or supramolecular polymers can be achieved.

2.5 Experimental Section

Materials

All reactions were performed under a nitrogen atmosphere, unless otherwise stated. DMF was dried over anhydrous $MgSO_4$ followed by distillation under reduced pressure and stored under an argon atmosphere. Dichloromethane (DCM), heptane and ethyl acetate (EtOAc) were distilled over calcium hydride (CaH_2) prior to use. 1,4-dioxane was distilled over $LiAlH_4$. Copper bromide (CuBr) and copper chloride (CuCl) were purified according to literature procedures[40]. Triphenylphosphine (Ph_3P) was recrystallized from MeOH. Other chemicals were used as received unless otherwise stated.

Instrumentation

^{1}H NMR spectra were recorded on a Varian inova400 instrument at 400 MHz and ^{13}C NMR spectra were recorded on Bruker DPX300 instrument at 75 MHz. Chemical shifts (δ) are given in ppm relative to the internal standard (Me_4Si or DMSO-d_6). IR spectra were recorded on an ATI Matson Genesis Series FTIR spectrometer with fitted ATR cell. GPC measurements were performed using a Shimadzu LC-10ADvp system equipped with PL gel 5 μm guard column, a PL gel 5 μm mixed D column, differential refractive index detector (Shimadzu RID-10A) at 38°C and a UV detector (Shimadzu SPD-10AVvp). The system was operated either using

dimethylsulfoxide as an eluent, with a flow of 0.8 mL·min^{-1} at 70°C (DMSO, 0.02 M LiCl) and with polyethylene glycol standards in the range 1900 to 124700 Da to calibrate, or using THF as an eluent with a flow of 1 mL·min^{-1} at 35°C and polystyrene standards in the range of 580 to 377400 Da to calibrate the GPC. High resolution mass spectroscopy (HRMS) was performed on a VG7070. Silica gel column chromatography (SGCC) was performed using Acros or Merck silica gel (0.035-0.070 mm, pore diameter ca. 6 nm). TLC was carried out on Merck precoated silica gel 60 F-254 plates. Compounds were visualized using UV and permanganate staining agent.

3-bromopropyl methacrylate (1)

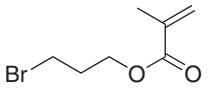

To a solution of 3-bromopropanol (15.1 mL, 0.174 mol) and triethylamine (25 mL, 0.180 mmol) in 350 mL DCM methacryloyl chloride (16.9 mL, 0.174 mmol) was added drop wise, while cooling the reaction mixture with an ice bath (0°C). After complete addition the reaction mixture was allowed to warm up to ambient temperature overnight, followed by quenching the excess methacryloyl chloride by addition of 10 mL MeOH. After 30 min the clear solution was poured into 100 mL saturated aqueous $NaHCO_3$, followed by 2 washing steps with 70 mL water. The organic layer was dried with anhydrous $MgSO_4$, filtered and concentrated *in vacuo* to give a pink oil. This was further purified by column chromatography (10% EtOAc/heptane) to give 34.82 g (0.168 mol, 96.6%) of the desired product as a colorless oil; R_f = 0.36 (10% EtOAc/heptane); ^{1}H NMR ($CDCl_3$) δ 6.11 (s, 1H, O_2C-C(CH_3)=C$\underline{H}_B$), 5.58 (s, 1H, O_2C-C(CH_3)=C$\underline{H}_A$), 4.29 (t, *J* = 6.0 Hz, 2H, -O-CH_2-), 3.49 (t, *J* = 6.6 Hz, 2H, Br-CH_2-), 2.24 (quintet, *J* = 6.3 Hz, 2H, -CH_2-C$\underline{H}_2$-CH_2-), 1.95 (s, 3H, O_2C-C(C$\underline{H}_3$)=CH_2); ^{13}C NMR ($CDCl_3$) δ 167.3, 136.3, 125.8, 62.5, 31.9, 29.5, 18.4; IR (oil) ν 2962, 1718, 1637.

3-(thymin-1-yl)propyl methacrylate (2)

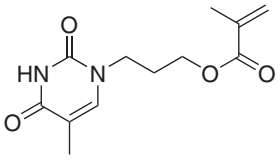

To a solution of thymine (3.58 g, 28.4 mmol) in 200 mL DMF was added anhydrous potassium carbonate (3.96 g, 28.6 mmol), tetrabutylammonium iodide (TBAI, 0.66 g, 1.80 mmol) and compound **1** (4.04 g, 19.5 mmol). The resulting suspension was stirred at ambient temperature for 24 h. The reaction was quenched by addition of 25 mL water, followed by evaporation to dryness *in vacuo*. The resulting light yellow solid was two times subjected to column chromatography (2% MeOH/DCM) to yield 1.87 g (7.40 mmol, 37.9%) of **2** as a white solid. mp = 119.7 ± 0.07 °C; R_f = 0.2 (2% MeOH/DCM); ^{1}H NMR (300MHz, $CDCl_3$): δ 8.11 (br s, 1H, pyrimidine NH), 6.94 (q, *J* = 1.2 Hz, 1H, pyrimidine H-6), 6.11 (quintet, *J* = 1.0 Hz, 1H, O_2C-C(CH_3)=C$\underline{H}_B$), 5.58 (quintet, *J* = 1.6 Hz, 1H, O_2C-C(CH_3)=C$\underline{H}_A$), 4.21 (t, *J* = 6.0 Hz, 2H, -O-CH_2-), 3.80 (t, *J* = 6.9 Hz, 2H, N-CH_2-), 2.09 (quintet, *J* = 6.3 Hz, 2H, -CH_2-CH_2-CH_2-), 1.95 (q, *J* = 1.0 Hz, 3H, O_2C-C(C$\underline{H}_3$)=CH_2), 1.91 (d, *J* = 1.2 Hz, 3H, pyrimidine-CH_3); ^{13}C NMR (DMSO-d_6): δ 166.42, 164.26, 150.90, 141.37, 135.76, 125.68, 108.50, 62.06, 44.83, 27.47, 17.90, 11.90. IR (solid) ν 3175, 3044, 2970, 2891, 2813, 1715,1665.

3-(adenin-9-yl)propyl methacrylate (3)

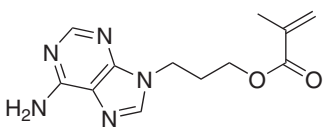

To a suspension of adenine (2.50 g, 18.5 mmol) in 125 mL DMF was slowly added NaH (0.82 g, 20.6 mmol). The reaction mixture was stirred at ambient temperature for 1 h until no more gas evolved, followed by addition of compound **1** (4.96 g, 24.0 mmol). After stirring at ambient temperature for 17 h the excess NaH was quenched with 10 mL saturated aqueous NH_4Cl solution. The resulting suspension was filtered and concentrated *in vacuo*. The resulting solid was subjected to column chromatography with eluent 7% MeOH/DCM to yield 3.34 g (12.7 mmol, 69 %) of **3** as a white solid. mp = 137.0 ± 0.28 °C; R_f = 0.12 (5% MeOH/DCM); ^{1}H NMR (DMSO-d_6): δ 8.14 (s, 1H, purine H-2), 8.11 (s, 1H, purine H-8), 7.16 (s, 2H, NH_2), 5.91 (s, 1H, O_2C-C(CH_3)=C$\underline{H}_A$), 5.62 (s, 1H, O_2C-C(CH_3)=C$\underline{H}_B$), 4.25 (t, *J* = 6.8 Hz, -O-CH_2-), 4.09 (t, *J* = 6.1 Hz, 2H, -N-CH_2-), 2.20 (quintet, *J* = 6.4 Hz, 2H, -CH_2-CH_2-CH_2-), 1.81 (s, 3H, O_2C-C(C$\underline{H}_3$)=CH_2); ^{13}C NMR (DMSO-d_6): δ 166.39, 155.93, 152.36, 149.58, 140.78, 135.66, 125.67, 118.80, 61.86, 40.33, 28.39, 17.86; IR (solid) ν 3372, 3313, 3155, 1710, 1642, 1592.

3-(cytosin-1-yl)propyl methacrylate (4)

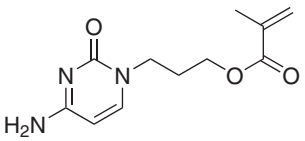

To a suspension of cytosine (5.00 g, 45.0 mmol) in 125 mL DMF was slowly added NaH (2.41 g, 60.3 mmol). The suspension was stirred at room temperature for 1 h until no more gas evolved. The resulting thick slurry was diluted with 40 ml DMF, followed by addition of 3-bromopropyl methacrylate **1** (9.71 g, 46.9 mmol). After 24 h the excess NaH was quenched with 50 mL saturated aqueous NH_4Cl solution. The reaction mixture was concentrated in vacuo and subjected to column chromatography (eluens 10 % MeOH/DCM) to yield 5.10 g (21.5 mmol, 47.7 %) of **4** as a white solid. R_f = 0.20 (10% MeOH/DCM). mp = 146.8 ± 0.42°C. HRMS (EI+) calculated for $C_{11}H_{15}N_3O_3$ 261.1113, found 261.1113. ^{1}H NMR (DMSO-d_6): δ 7.57 (d, J = 7.2 Hz, 1H, pyrimidine-H6), 7.07 (br d, NH2), 6.02 (s, 1H, O_2C-C(CH_3)=C$\underline{H}_A$), 5.66 (s, 1H, O_2C-C(CH_3)=C$\underline{H}_B$), 5.64 (d, J = 7.2 Hz, 1H, pyrimidne-H5), 4.09 (t, J = 6.3 Hz, 2H, O-CH_2-), 3.73 (t, J = 6.7 Hz, 2H, N-CH_2-), 1.97-1.90 (m, 2H, -CH_2-C$\underline{H}_2$-CH_2-), 1.87 (s, 3H, O_2C-C(C$\underline{H}_3$)=CH_2). ^{13}C NMR (DMSO-d_6): δ 165.98, 165.05, 154.90, 145.86, 135.42, 125.42, 93.10, 61.88, 46.16, 27.74, 18.03. FTIR (solid): ν 3348, 3104, 1888, 1713, 1659, 1608, 1527.

Phenylacetic anhydride (11)

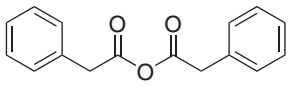

Phenyl acetic acid (14.22 g, 0.1045 mol) was suspended in acetic anhydride (25 mL) and heated to reflux for 18 h. The resulting clear yellow solution was concentrated in vacuo after which it was precipitated into water. The product was then filtered off and washed two more times followed by three washing steps with petroleum ether (80-100), after which 11.96 g (0.04598 mol, 88.0%) of product was obtained as a white powder after drying in vacuum. mp = 68.9±0.1 °C. HRMS (EI+) calculated for $C_{16}H_{14}O_3$ 254.0943, found 254.0951. ^{1}H NMR ($CDCl_3$): δ 7.32-7.18 (m, 10H, Ar$\underline{H}$), 3.71 (s, 4H, C$\underline{H}_2$). ^{13}C NMR ($CDCl_3$): δ 166.68, 131.89, 129.30, 128.69, 127.52, 42.29. FTIR (solid): ν 3030, 1812, 1739, 1497, 1454.

***N*-(9-acetyl-6-oxo-6,9-dihydro-1*H*-purin-2-yl)-2-phenylacetamide (6)**

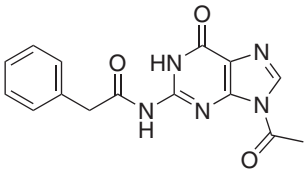

To a suspension of 5.02 g (33.2 mmol) guanine in 150 mL N,N-dimethyl acetamide (DMA) was added 22.72 g (89.3 mmol) phenylacetyl anhydride. The reaction mixture was heated to reflux until a clear solution was obtained, after which heating was continued for 30 min. After cooling to room temperature the reaction mixture was concentrated in vacuo, suspended in EtOAc, filtered and dried to obtain crude N-(2-phenylacetyl)guanine. To a suspension of crude N-(2-phenylacetyl)guanine in 41 mL DMF was added 6.77 g (66.4 mmol) acetic anhydride. The reaction mixture was heated to 105°C until a clear solution was obtained (30 min). Solvent was removed in vacuo, followed by washing of the solid on a filter with abs. EtOH and subsequent drying to yield 8.64 g, (27.7 mmol, 83.4%) **6** as an off-white powder. R_f = 0.22 (10% MeOH/DCM). HRMS (EI+) calculated for $C_{15}H_{13}N_5O_3$ 311.1018, found 311.10185. ^{1}H NMR (300 MHz, DMSO-d_6): δ 12.96 (br s, 2H, purine-NH, NH-C=O), 8.46 (s, 1H, purine-H8), 7.27-7.35 (m, 5H, ArH), 3.85 (s, 2H, O=C-C$\underline{H}_2$-), 2.83 (s, 3H, -CH_3). ^{13}C NMR (DMSO-d_6): δ 173.79, 167.55, 154.18, 147.96, 147.40, 137.24, 133.74, 129.06, 128.11, 126.68, 121.35, 42.50, 24.79. FTIR (solid): ν 3133, 1749, 1697, 1672, 1597, 1541.

***N*-[6-(4-nitrophenethoxy)-9*H*-purin-2-yl]-2-phenylacetamide (7)**

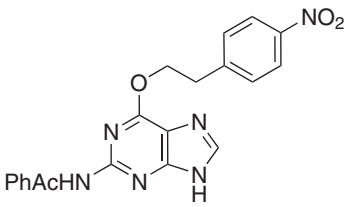

To a suspension of 1.96 g (6.29 mmol) **6** in 70 mL 1,4-dioxane was added 3.30 g (12.58 mmol) Ph_3P and 2.11 g (12.60 mmol) 2-(p-nitrophenyl)ethanol. The reaction mixture was cooled with a cold-water bath before adding 2.37 g (13.63 mmol) diethyl azodicarboxylate (DEAD) dropwise. After addition of DEAD the mixture was allowed to stir overnight at room temperature. TLC indicated incomplete conversion, therefore additional Ph_3P (0.359, 1.4 mmol) and DEAD (0.293, 1.7 mmol) were added, resulting in a clear solution. After 7 h the reaction mixture was concentrated in vacuo to 1/2 of its volume and added to 750 mL EtOH/H_2O (1/1, v/v) mixture, followed by heating to reflux until a clear solution was obtained. Upon cooling to room temperature and then to -18°C for 18 h product was obtained as crystals. Filtration and drying yielded 2.28 g (5.45 mmol, 86.7 %) of **7**. R_f = 0.43 (10%MeOH/DCM). HRMS (EI+) calculated for $C_{21}H_{19}N_6O_4$ 419.1468, found 419.14758. ^{1}H NMR (DMSO-d_6): δ 13.19 (s, 1H, purine-NH), 10.56 (s, 1H, amide-NH), 8.16 (s, 1H, purine-H8), 8.15 (d, J = 8.4 Hz, 2H, Ar$\underline{H}$-NO_2), 8.63 (d, J = 8.4 Hz, 2H, Ar$\underline{H}$-NO_2), 7.35-7.21 (m, 5H, -CH_2-Ar$\underline{H}$), 4.76 (t, J = 6.7 Hz, 2H, O-C$\underline{H}_2$-), 3.81 (s, 2H, -C$\underline{H}_2$-Ar), 3.30 (t, J = 6.7 Hz, 2H, -C$\underline{H}_2$-Ar-

NO_2). ^{13}C NMR (DMSO-d_6): δ 168.56, 159.11, 153.42, 151.27, 146.14, 145.88, 140.75, 135.49, 130.02, 128.98, 127.90, 126.16, 123.08, 116.56, 66.18, 43.13, 34.28. FTIR (solid): ν 3315, 3059, 1678, 1589, 1517, 1429, 1409, 1344.

3-hydroxypropyl methacrylate (10)

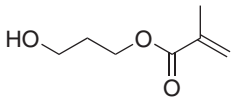

To a cooled solution (0°C) of 1,3-propanediol (14.62 g, 0.192 mol) and triethylamine (10 mL, 0.072 mol) in 100 mL DCM was added dropwise a solution of methacryloyl chloride (3.0 mL, 0.174 mmol) in 30 mL DCM while stirring vigorously. After complete addition the reaction mixture was allowed to heat up to room temperature. The reaction mixture was poured into 110 mL saturated aqueous $NaHCO_3$, followed by three washing steps with 100 mL water. The organic layer was dried with anhydrous $MgSO_4$, filtered and concentrated in vacuo to give a light yellow oil. This was further purified by column chromatography (33% EtOAc/heptane) to give 2.519 g (0.017 mol, 50.9%) of **10** as colorless oil. R_f = 0.19 (33% EtOAc/heptane). ^1H NMR (DMSO-d_6): δ 6.02-6.00 (m, 1H, O_2C-C(CH_3)=C$\underline{H}_A$), 5.67-5.65 (m, 1H, O_2C-C(CH_3)=C$\underline{H}_B$), 4.53 (t, J = 5.2 Hz, 1H, $\underline{H}$O-CH_2-), 4.15 (t, J = 6.5 Hz, 2H, -C$\underline{H}_2$-O_2C-), 3.48 (dt, 2H, J = 5.2 Hz, J = 6.3 Hz, HO-C$\underline{H}_2$-), 1.88 (dd, 3H, J = 1.0 Hz, J = 1.6 Hz, O_2C-C(C$\underline{H}_3$)=CH_2), 1.79-1.72 (m, 2H, CH_2-C$\underline{H}_2$-CH_2-). ^{13}C NMR ($CDCl_3$): δ 167.60, 136.14, 125.65, 61.75, 59.20, 31.97, 18.67. FTIR (oil): ν 3503, 3173, 3037, 2987, 2886, 2827, 1891, 1759, 1716, 1608.

3-[6-(4-nitrophenethoxy)-2-(2-phenylacetamido)-9*H*-purin-9-yl]propyl methacrylate (8)

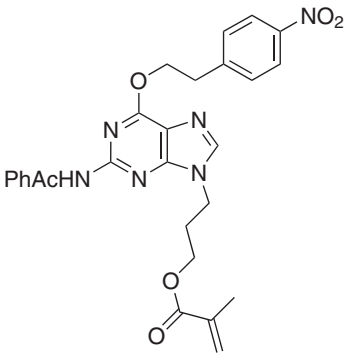

1.18 mL DEAD was added to a stirred suspension of **7** (2.10 g, 5.01 mmol), Ph_3P (1.97 g, 7.51 mmol) and **10** (0.86 g, 5.97 mmol) in 50 mL dry dioxane. The solution was allowed to stir at room temperature for 18 h. The resulting orange, yellow clear reaction mixture was concentrated *in vacuo* after which the crude product was further purified with column chromatography. (EtOAc/heptane 4/1) to yield 2.20 g of pure **8**. R_f = 0.48 (5% MeOH/DCM). mp = 230.4 ± 0.78°C. ^1H NMR (DMSO-d_6): δ 10.61 (s, 1H, N$\underline{H}$), 8.23 (s, 1H, purine-$\underline{H}$8), 8.15 (d, 2H, Ar$\underline{H}$-NO_2), 7.63 (d, 2H, CH_2-Ar$\underline{H}$-NO_2), 7.29 (m, 5H, Ar$\underline{H}$-CH_2), 5.85 (s, 1H, O_2C-C(CH_3)=C$\underline{H}_A$), 5.54 (s, 1H, O_2C-C(CH_3)=C$\underline{H}_B$), 4.76 (t, J = 6.8 Hz, 2H, O-C$\underline{H}_2$-), 4.25 (t, J = 6.8 Hz, 2H, O-C$\underline{H}_2$-), 4.09 (t, J = 6.0 Hz, 2H, N-C$\underline{H}_2$-), 3.85 (s, 2H C$\underline{H}_2$-Ar), 3.30 (t, J = 6.8 Hz, 2H, Ar-C$\underline{H}_2$), 2.21 (m, 2H, CH_2-C$\underline{H}_2$-CH_2), 1.76 (s, 3H,). ^{13}C NMR ($CDCl_3$): δ 168.63, 165.79, 162,06, 155.47, 151,24, 146.26, 145.86, 135.57, 135.15, 129.89, 129.03, 127.89, 126.14, 125.40, 123,11, 108.67, 66.46, 61.62, 44.26, 43.11, 34.07, 29.39, 17.90.

3-(6-oxo-2-(2-phenylacetamido)-6,9-dihydro-1*H*-purin-9-yl)propyl methacrylate (9)

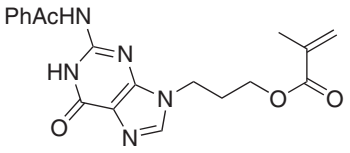

8 (520 mg, 0.95mmol) containing triphenylphosphine oxide was dissolved in a 0.5 M DBU solution in pyridine and stirred at ambient temperature for 18 h. The solvent was removed in vacuo and crude product was further purified by means of column chromatography (2 - 5% MeOH/DCM) to yield 200 mg (0.506 mmol, 53 %) of pure **9** as a white solid. R_f = 0.46 (10% MeOH/DCM). mp = 165.0 ± 1.0°C. HRMS (EI+) calculated for $C_{20}H_{21}N_5O_4$ 395.1594, found 395.15793. ^1H NMR (DMSO-d_6): δ 11.91 (br s, 2H, 2x N$\underline{H}$), 8.00 (s, 1H, purine-$\underline{H}$8), 7.30 (m, 5H, Ar$\underline{H}$), 5.90 (s, 1H, O_2C(CH_3)=C$\underline{H}_A$), 5.62 (s, 1H, O_2C(CH_3)=C$\underline{H}_B$), 4.18 (t, J = 6.7 Hz, 2H, O-C$\underline{H}_2$-), 4.12 (t, J = 6.7 Hz, 2H, N-C$\underline{H}_2$-), 3.81 (s, 2H, Ar-C$\underline{H}_2$-) 2.22-2.15 (m, 2H, CH_2-C$\underline{H}_2$-CH_2-), 1.81 (s, 3H, O_2C(C$\underline{H}_3$)=CH_2). ^{13}C NMR ($CDCl_3$): δ 173.51, 165.88, 154.37, 148.16, 147.08, 139.47, 135.22, 133.91, 129.00, 128.09, 126.64, 125.45, 120.02, 61.81, 42.48, 40.83, 28.35, 17.94. FTIR (solid): ν 3223, 3084, 2955, 1714, 1665, 1598, 1557.

3-(2-amino-6-oxo-purin-9-yl)propyl methacrylate (5)

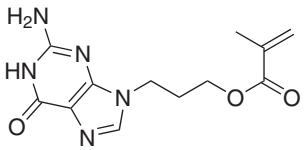

To a suspension of 0.5 g penicillin amidase on Eupergit® C in 20 mL phosphate buffer (0.07 M, pH 7.0) was added a solution of compound **9** (87 mg, 0.152 mmol) in 2 mL MeOH. The suspension was shaken at 250 rpm at 28°C for 24 h until TLC indicated complete conversion. The Eupergit was filtered off, after which the filtrate was freeze-dried. The resulting crude product was purified by column chromatography (eluens 10% MeOH/DCM) to yield 20 mg (0.072 mmol, 48%) of product **5** as a white solid. R_f = 0.19 (10% MeOH/DCM). ^1H NMR (DMSO-d_6): δ 10.52 (s, 1H, purine-

NH), 7.73 (s, 1H, purine-H8), 6.37 (s, 2H, purine-NH$_2$), 5.96 (s, 1H, O_2C-C(CH_3)=CH_A), 5.63 (s, 1H, O_2C-C(CH_3)=CH_B), 4.09 (t, J = 6.3 Hz, 2H, O-CH$_2$-), 4.05 (t, J = 6.8 Hz, 2H, N-CH$_2$-), 2.15-2.09 (m, 2H, CH_2-CH$_2$-CH_2), 1.84 (s, 3H, O_2C(CH$_3$)=CH_2). ^{13}C NMR (DMSO-d_6): δ 167.12, 156.43, 146.72, 145.12, 139.54, 134.49, 125.33, 120.02, 61.78, 41.04, 28.39, 18.02.

Poly[3-(thymin-1-yl)propyl methacrylate] (general procedure) (12)

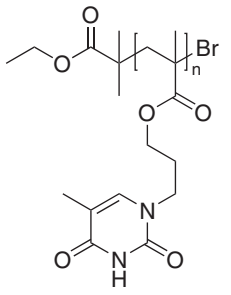

Compound **2** (436 mg, 1.73 mmol), CuCl (6 mg, 0.06 mmol) and 2,2'-bypyridine (bpy) (17 mg, 0.11 mmol) were added to a Schlenk tube, followed by three cycles of evacuation and nitrogen refilling. Deoxygenated DMSO-d_6 (3 mL) was added and the polymerization was started by addition of 8 μL (0.05 mmol) ethyl bromo isobutyrate (EBiB). During the reaction samples were taken and conversion was determined using ^{1}H NMR spectroscopy by comparing the acrylate signal with the thymine H6 signal. After polymerization the reaction mixture was precipitated in an aqueous solution of EDTA (0.07 M), the precipitate was re-dissolved in DMSO and precipitated again to yield 345 mg of polymer. $M_{n\ theo}$ = 6.4 kg/mol. SEC (DMSO): M_n = 6.8 kg/mol, M_w/M_n = 1.21. ^{1}H NMR (DMSO-d_6): δ 11.15 (br s, pyrimidine-NH), 7.45 (br s, pyrimidine-H6), 3.92 (br s, O-CH$_2$-CH$_2$), 3.71 (br s, CH$_2$-CH$_2$-N), 1.95-1.60 (br m, {CH$_2$-C(CH_3)}, pyrimidine-CH_3, CH$_2$-CH$_2$-CH$_2$-N), 1.20-0.65 (br m, {CH$_2$-C(CH_3)}).

Poly[3-(adenin-9-yl)propyl methacrylate] (13)

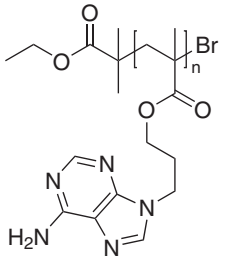

Using the procedure described for polymer **12**, a reaction mixture composed of **3** (347 mg, 1.33 mmol), CuCl (5 mg, 0.05 mmol), bpy (15 mg, 0.10 mmol) DMSO-d_6 (3.7 mL) and EBiB (6 μL, 0.04 mmol) gave 147 mg polymer. $M_{n\ theo}$ = 5.7 kg/mol. SEC (DMSO): M_n = 6.9 kg/mol, M_w/M_n = 1.19. ^{1}H NMR (DMSO-d_6): δ 8.15 (br s, purine-H2,8), 7.25 (br s, purine-NH$_2$), 4.23 (br s, O-CH$_2$-CH$_2$), 3.90 (br s, CH$_2$-CH$_2$-N), 2.16 (br s, O-CH$_2$-CH$_2$-CH$_2$-N), 1.89-1.55 (br s, {CH$_2$-C(CH_3)}), 1.10-0.55 (br m, {CH$_2$-C(CH_3)}).

Poly[3-(cytosin-1-yl)propyl methacrylate] (14)

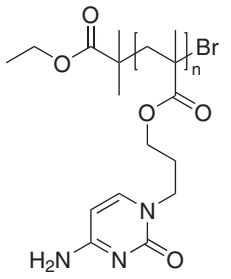

CuCl (16 mg, 0.16 mmol) and $CuCl_2$ (2 mg, 0.02 mmol) were premixed, after which 4 mg (0.04 mmol CuCl, 0.003 mmol $CuCl_2$) of copper mixture was added to a Schlenk tube containing compound **4** (325 mg, 1.37 mmol). This was followed by three cycles of evacuation and nitrogen refilling. Deoxygenated DMSO-d_6 (6.086 g, 5.12 mL), 5 μL (0.02 mmol) N,N,N',N",N"-pentamethyldiethylenetriamine (PMDETA) were added, after which the polymerization was started by addition of 9 μL (0.06 mmol) EBiB. Precipitation of polymer in aqueous EDTA solution (0.07M) gave 147 mg polymer. $M_{n\ theo}$ = 3.5 kg/mol. SEC (DMSO): M_n = 4.5, M_w/M_n = 1.15. ^{1}H NMR (DMSO-d_6): δ 7.65 (br s, pyrimidine-H6), 7.30 (br s, NH$_2$), 5.75 (br s, pyrimidine-H5), 3.91 (br s, O-CH$_2$-CH$_2$), 3.71 (br s, CH$_2$-CH$_2$-N), 2.0-1.7 (br m, {CH$_2$-C(CH_3)}, CH$_2$-CH$_2$-CH$_2$-N), 1.2-0.6 (br m, {CH$_2$-C(CH_3)}).

Poly[3-(guanin-9-yl)propyl methacrylate] (15)

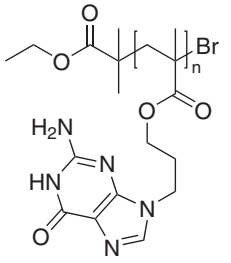

22 μL of a stock solution containing 0.3M CuBr (6.6 μmol) and 0.6M bpy (13 μmol) in DMSO-d_6 was added to an NMR-tube charged with a solution of monomer **5** (26.8 mg, 96.7 μmol) in 0.7 mL DMSO-d_6. After deoxygenating by purging with argon for 20 minutes, the polymerization was started by addition of 12 μL 0.5M EBiB stock solution (6 μmol) in DMSO-d_6, followed by immediate recording of the first ^{1}H NMR spectrum at 40°C. Follow-up spectra were recorded at different time intervals by applying steady state scans. The polymerization was quenched by precipitation of the reaction mixture in an aqueous EDTA solution (0.07 M). Centrifuging the precipitated product yielded 10 mg of polymer. $M_{n\ theo}$ = 3.2 kg/mol, SEC (DMSO): M_n = 6.5 kg/mol, M_w/M_n = 1.15. ^{1}H

NMR (DMSO-d_6): δ 10.6 (br s, purine-N<u>H</u>), 8.15 (br s, purine-<u>H</u>8), 6.45 (br s, purine-N<u>H</u>$_2$), 4.05-3.86 (br s, O-C<u>H</u>$_2$-CH$_2$ + CH$_2$-C<u>H</u>$_2$-N$_{purine}$), 2.09 (br s, O-CH$_2$-C<u>H</u>$_2$-CH$_2$-N$_{purine}$), 1.89-1.55 (br s, C<u>H</u>$_2$-C(CH$_3$)}), 1.10-0.55 (br m, CH$_2$-C(C<u>H</u>$_3$)}).

2.6 References

1. C. A. Mirkin. *Inorg. Chem.* **2000**, *39*, 2258-2272.
2. Z. J. Gartner and D. R. Liu. *J. Am. Chem. Soc.* **2001**, *123*, 6961-6963.
3. N. C. Seeman. *Biochemistry* **2003**, *42*, 7259-7269.
4. N. C. Seeman. *Chem. Biol.* **2003**, *10*, 1151-1159.
5. J. M. Nam, S. I. Stoeva and C. A. Mirkin. *J. Am. Chem. Soc.* **2004**, *126*, 5932-5933.
6. M. Akashi, H. Takada, Y. Inaki and K. Takemoto. *J. Polym. Sci., Part A: Polym. Chem.* **1979**, *17*, 747-757.
7. K. Takemoto and Y. Inaki. *Adv. Polym. Sci.* **1981**, *41*, 1-51.
8. Y. Inaki, K. Ebisutani and K. Takemoto. *J. Polym. Sci., Part A: Polym. Chem.* **1986**, *24*, 3249-3262.
9. Y. Inaki. *Prog. Polym. Sci.* **1992**, *17*, 515-570.
10. R. P. Sijbesma, F. H. Beijer, L. Brunsveld, B. J. B. Folmer, J. Hirschberg, R. F. M. Lange, J. K. L. Lowe and E. W. Meijer. *Science* **1997**, *278*, 1601-1604.
11. L. Brunsveld, B. J. B. Folmer, E. W. Meijer and R. P. Sijbesma. *Chem. Rev.* **2001**, *101*, 4071-4097.
12. S. J. Rowan, P. Suwanmala and S. Sivakova. *J. Polym. Sci., Part A: Polym. Chem.* **2003**, *41*, 3589-3596.
13. S. Sivakova and S. J. Rowan. *Chem. Soc. Rev.* **2005**, *34*, 9-21.
14. E. A. Fogleman, W. C. Yount, J. Xu and S. L. Craig. *Angew. Chem., Int. Ed.* **2002**, *41*, 4026-4028.
15. J. Xu, E. A. Fogleman and S. L. Craig. *Macromolecules* **2004**, *37*, 1863-1870.
16. Y. Wang, B. A. Armitage and G. C. Berry. *Macromolecules* **2005**, *38*, 5846-5848.
17. R. G. Davies, V. C. Gibson, M. B. Hursthouse, M. E. Light, E. L. Marshall, M. North, D. A. Robson, I. Thompson, A. J. P. White, D. J. Williams and P. J. Williams. *J. Chem. Soc., Perkin Trans. 1* **2001**, 3365-3381.
18. H. S. Bazzi and H. F. Sleiman. *Macromolecules* **2002**, *35*, 9617-9620.
19. A. Khan, D. M. Haddleton, M. J. Hannon, D. Kukulj and A. Marsh. *Macromolecules* **1999**, *32*, 6560-6564.
20. A. Marsh, A. Khan, D. M. Haddleton and M. J. Hannon. *Macromolecules* **1999**, *32*, 8725-8731.
21. J.-F. Lutz, A. F. Thuenemann and K. Rurack. *Macromolecules* **2005**, *38*, 8124-8126.
22. T. Glauser, M. Ranger, B. Kalra, W. Gao, J. Hedrick and R. A. Gross. *Polym. Prepr. (Am. Chem. Soc., Div. Polym. Chem.)* **2003**, *44*, 624-625.
23. H. J. Spijker, A. T. J. Dirks and J. C. M. van Hest. *Polymer* **2005**, *46*, 8528-8535.
24. H. J. Spijker, A. J. Dirks and J. C. M. Van Hest. *J. Polym. Sci., Part A: Polym. Chem.* **2006**, *44*, 4242-4250.
25. C. Dubosclardgottardi, P. Caubere and Y. Fort. *Tetrahedron* **1995**, *51*, 2561-2572.
26. H. Vorbrüggen, K. Krolikiewicz and B. Bennua. *Chem. Ber.* **1981**, *114*, 1234-1255.
27. O. F. Schall and G. W. Gokel. *J. Am. Chem. Soc.* **1994**, *116*, 6089-6100.
28. H. Vorbrüggen. *Acc. Chem. Res.* **1995**, *28*, 509-520.
29. J. Kjellberg and G. Johansson. *Tetrahedron* **1986**, *42*, 6541-6544.
30. P. Garner and S. Ramakanth. *J. Org. Chem.* **1988**, *53*, 1294-1298.
31. T. F. Jenny, K. C. Schneider and S. A. Benner. *Nucleosides Nucleotides* **1992**, *11*, 1257-1261.
32. F. P. Clausen and J. Juhlchristensen. *Org. Prep. Proced. Int.* **1993**, *25*, 373-401.
33. H. Waldmann and A. Reidel. *Angew. Chem., Int. Ed.* **1997**, *36*, 647-649.
34. S. Flohr, V. Jungmann and H. Waldmann. *Chem., Eur. J.* **1999**, *5*, 669-681.
35. D. Kadereit and H. Waldmann. *Chem. Rev.* **2001**, *101*, 3367-3396.
36. L. Ayres, M. R. J. Vos, P. Adams, I. O. Shklyarevskiy and J. C. M. van Hest. *Macromolecules* **2003**, *36*, 5967-5973.

37. G. L. Eichhorn, P. Clark and E. D. Becker. *Biochemistry* **1966**, *5*, 245-253.
38. I. Samasundaram, M. K. Kommiya and M. Palaniandavar. *J. Chem. Soc., Dalton Trans*. **1991**, 2083-2089.
39. A. K. Nanda and K. Matyjaszewski. *Macromolecules* **2003**, *36*, 1487-1493.
40. R. N. Keller and H. D. Wycoff. *Inorganic Syntheses* **1946**, *2*, 1-4.

Chapter 3

Unusual rate enhancement in the thymine assisted ATRP process of adenine monomers

3 Unusual rate enhancement in the thymine assisted ATRP process of adenine monomers

3.1 Introduction

Template polymerization is crucial to Nature, as it forms the basis for correct DNA replication, transcription and protein synthesis. During these processes single polynucleobase strands are used as polymer template for the production of new, biopolymer chains with an unsurpassed level of control over composition and degree of polymerization. The specific recognition between the two base pairs adenine – thymine (or uracil) and guanine – cytosine, also known as Watson-Crick base pairing, is one of the main elements that enables the occurrence of this template process.

Natural template polymerization has inspired many polymer chemists to investigate this concept for use in synthetic polymer chemistry. Several different interactions between polymer chain and monomer, such as electrostatic[1], dipole-dipole interactions or hydrogen bonding have been described[2, 3]. The latter is by far the most versatile and also the most investigated system. Pioneering work was performed by Challa et al.[4-10] and others[11, 12] who investigated the use of hydrogen bonding interactions between acrylic acid and vinyl pyrrolidone, and observed, among other things, control over tacticity and polymer chain length by the presence of a template. Takemoto and Inaki[13, 14] investigated the effect of the presence of a nucleobase-containing polymer on the rate of polymerization of the complementary nucleobase-functional monomer.

In general, for radical template polymerizations there are two mechanisms described for template polymerizations: type I (zip mechanism) and type II (pickup mechanism)[15]. In the first there is a strong interaction between monomer and template. Therefore, monomer is pre organized on the template and polymerization takes place on the template. The second mechanism has a weaker interaction between monomer and template and therefore polymerization will start in solution. When the oligomer has a certain critical length, complex formation with the template will occur as a result of cooperative interactions and further propagation takes place on the template by picking up monomers from solution. It seems the difference between mechanism type I and II is not very distinct.

If the critical length for the oligomer to be absorbed on the template is small, then mechanism II is close to type I. on the other hand if the critical length is long the template mechanism will be close to type II.

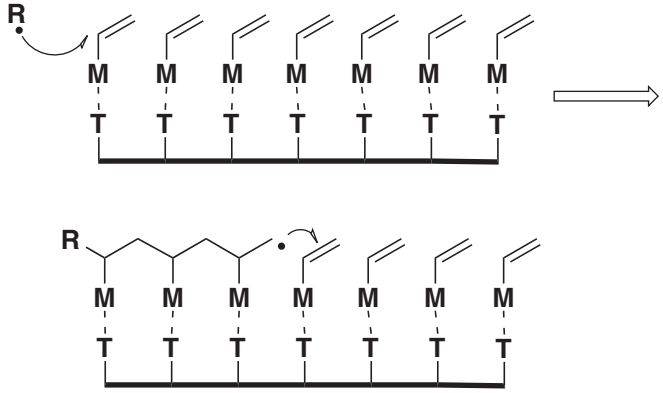

Figure 1. Schematic representation of type I template polymerization. Monomer is bound to template and polymerization propagation takes place on the template.

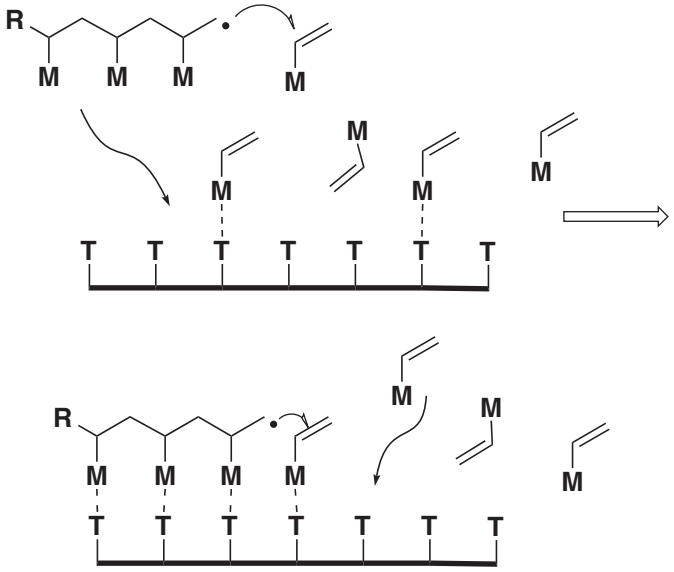

Figure 2. Schematic representation of type II template polymerization. Initial polymerization takes place in solution until a critical length is obtained after which propagation continues on the template.

The type of mechanism is usually determined from kinetic studies. Typically, the relative rate of template polymerization is compared with blank polymerizations under the same conditions but without template present. In the proposed scheme the maximum of relative polymerization rate is at [T]/[M] = 1, assuming a very large association constant resulting in a 1:1 interaction between template and monomer, for type I mechanism and decreases thereafter. For type II mechanism, the rate enhancement is generally caused by a

retardation of the termination reaction. Therefore, the maximum rate of polymerization is attained at the critical concentration when every growing oligomer is absorbed at the template.

With the development of controlled radical polymerization[16-19] such as atom transfer radical polymerization (ATRP), researchers are nowadays able to prepare polymers with low polydispersity and with control over architecture, using a large variety of monomers. Haddleton and Gross[20-22] have shown ATRP to be tolerant towards nucleobase functionality in monomers, demonstrating the versatility and robustness of this controlled polymerization technique.

These results inspired us to use ATRP for the detailed investigation of the effects of nucleobases on the polymerization of complementary nucleobase monomers. In this chapter we describe our studies with respect to the presence of both monomeric and polymeric thymine templates on the ATRP process of adenine methacrylate by determining the kinetics of the polymerization via ^{1}H NMR spectroscopy.

3.2 Preparation of thymine-functional template

To investigate the interaction of adenine with the complementary nucleobase thymine during polymerization, a poly ethylene glycol (PEG) thymine block copolymer was prepared (scheme 1), to ensure solubility of the complex to be possibly formed. Poly(ethylene glycol) methyl ether was first treated with 2-bromoisobutyryl bromide in the presence of Et_3N to obtain PEG macro initiator **1**. Successively, ATRP of **2** using initiator **1** and the CuCl/2 bpy catalyst was performed. At a conversion of 71 % the reaction was quenched using a procedure described by Sawamoto et al.[23] by addition of 1-phenyl-1-(trimethylsilyloxy)ethylene, resulting in block copolymer **3**. The quenching step after the polymerization was necessary to remove the bromide end group and to prevent initiation from the thymine block copolymer during the template polymerization experiments of adenine.

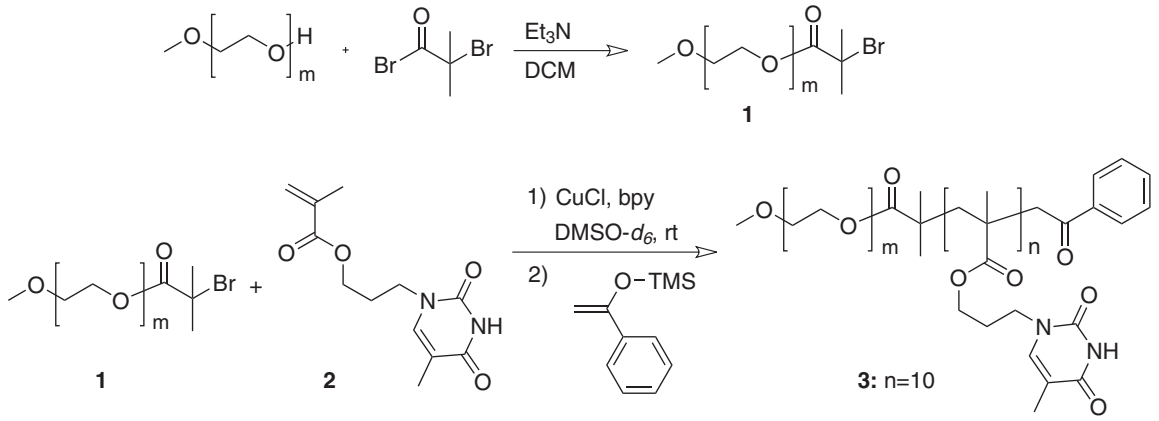

scheme 1. Synthesis of PEG macro initiator **1** and PEG-*b*-T10 block copolymer **3.**

As can be seen in figure 3A, the quenching step proceeded effectively since monomer conversion stopped after addition of 1-phenyl-1-(trimethylsilyloxy)ethylene. Despite the deviation from first order kinetics the desired PEG-thymine block copolymer was obtained with a relatively low PDI (1.30) and the M_n (4.9 kg/mol) obtained by GPC (figure 3B) was in agreement with the theoretical molecular weight (4.5 kg/mol), and with a DP of 10 thymine units, based on NMR calculations.

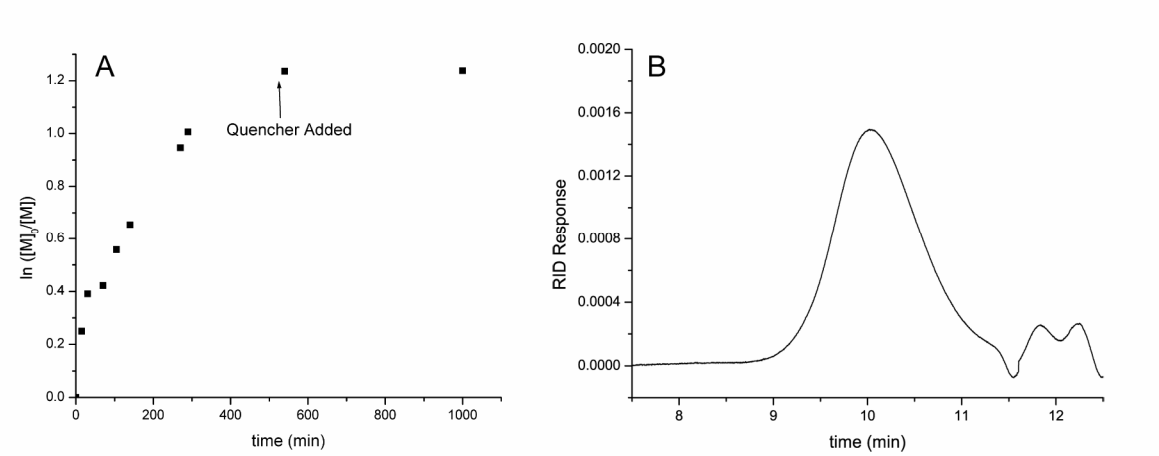

Figure 3. **A**) plot of ln ($[M]_0/[M]_t$) vs time of the polymerization of **2** (0.415 M) with PEG initiator **1** (0.028 M), CuCl (0.028 M), bpy (0.056 M) and, after 540 min quencher (0.284 M). **B**) GPC trace of PEG-*b*-T10 (**3**) in DMSO at 70 °C after work up.

3.3 ATRP of nucleobase monomers 2 and 4 in the presence of thymine moieties

Both adenine and thymine monomers were polymerized using ATRP in the presence of the PEG-*b*-T10 block copolymer template **3** in a 1:1 nucleobase ratio. The ratio was based on molar equivalents of monomer concentration and thymine repeating units present in the template. DMSO-d_6 was chosen as a solvent since template and monomer were well soluble in this solvent. In addition Inaki[24] already observed a template effect using DMSO/ethylene glycol mixtures.

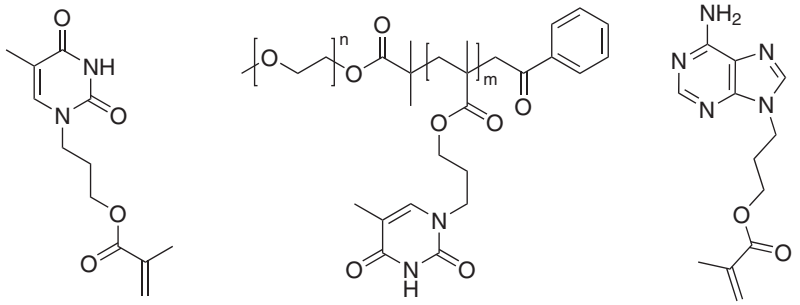

Figure 4. Thymine template **3** used for the polymerization of adenine monomer **4** and thymine monomer **2**.

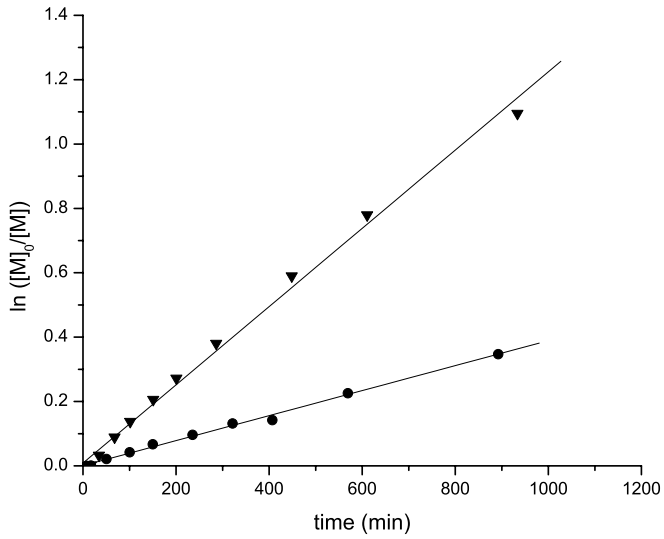

Figure 5. Kinetic plots for ATRP of adenine monomer **4** (●, **4** = 0.13 M, CuCl = 0.012 M, bpy = 0.024 M, EBiB = 0.014 M) and **4** in the presence of **3** (▼, **4** = 0.13 M, CuCl = 0.012 M, bpy = 0.024 M, EBiB = 0.014 M, **3** = 0.014 M with a ratio thymine: adenine units = 1.04.

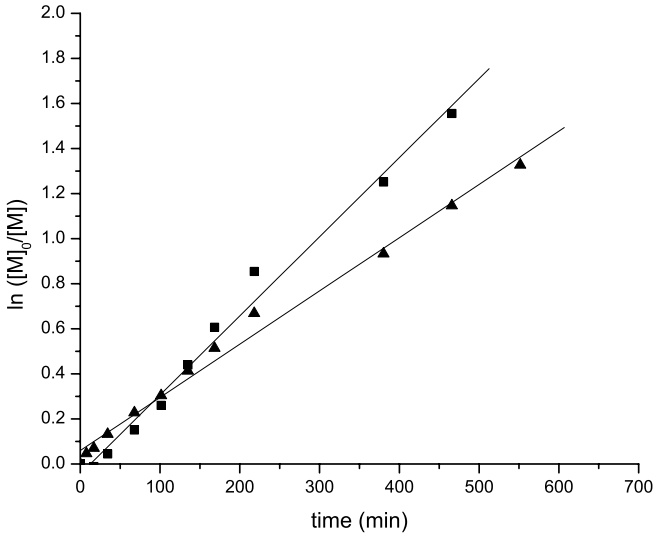

Figure 6. Kinetic plots for the ATRP of thymine monomer **2** (■, **2** = 0.13 M, CuCl = 0.012 M, bpy = 0.024 M, EBiB = 0.014 M) and **2** in the presence of **3** (▲, **2** = 0.13 M, CuCl = 0.012 M, bpy = 0.024 M, EBiB = 0.014 M, **3** = 0.014 M) with a ratio of thymine: thymine units = 0.98.

Both polymerizations of **4** and **2** (figure 5 and figure 6 respectively) proceeded via first order kinetics, indicating control over the polymerization while the block copolymer template was present. As can be seen in figure 5 the polymerization of adenine monomer was considerably accelerated by the presence of complementary thymine block copolymer **3**, whereas the polymerization rate of thymine monomer (figure 6) was not significantly affected by addition of **3**. These results suggest the occurrence of a specific adenine - thymine interaction, and even could point in the direction of a template polymerization process.

In order to obtain more information about this acceleration phenomenon, the effect of the molar ratio between adenine monomer **4** and thymine functionalized polymer **3** on the polymerization rate was subsequently investigated. The concentration of **3** and initiator (EBiB) was kept constant while the amount of adenine monomer **4** was varied. The initial apparent rate constants for the polymerization of the adenine monomer are depicted in figure 7 and compiled in table 1.

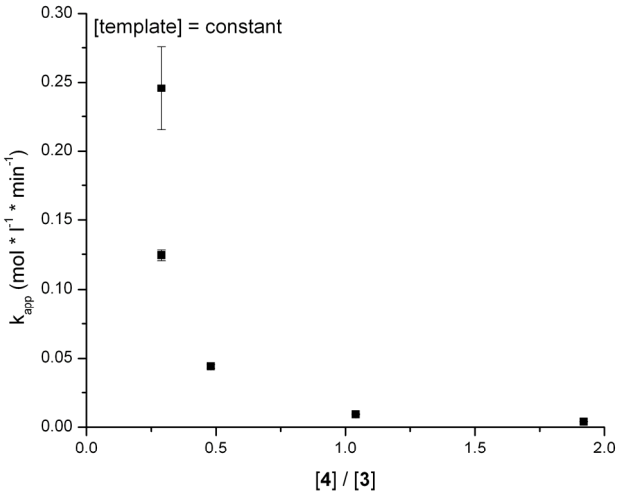

Figure 7. Apparent rate constants of the ATRP experiments at different monomer (**4**) to template (**3**) ratios.

Table 1. Apparent rate constants for the polymerization of monomers **2** and **4** with different additives at different ratios

	Monomer	additive	ratio (monomer : additive)	k_{app} *10^{-3} (mol*L^{-1}*min^{-1})
1	**4**	-	-	2.96
2	**4**	PEG-*b*-T10 (**3**)	1.9 : 1.0	3.99
3	**4**	PEG-*b*-T10 (**3**)	1.0 : 1.0	9.30
4	**4**	PEG-*b*-T10 (**3**)	0.5 : 1.0	44.3
5	**4**	PEG-*b*-T10 (**3**)	0.3 : 1.0	124
6	**4**	PEG-*b*-T10 (**3**)	0.3 : 1.0	246
7	**4**	succinimide	1.0 : 1.0	19.5
8	**4**	Thy-C6 (**5**)	1.0 : 1.0	35.8
9	**4**	**2**	1.0 : 1.0	29.6
10	**2**	**4**	1.0 : 1.0	30.4
11	**2**	-	-	26.7
12	**2**	PEG-*b*-T10 (**3**)	1.0 : 1.0	17.7

As can be seen in table 1 the rate constant increased upon addition of template polymer with a factor of 3 when a 1 to 1 ratio (entry 1 and 3) was used. Compared to this value the rate decreased (entry 2) when an adenine / thymine ratio of 2:1 was used and markedly increased by a factor of 100 when an excess of template was added (entry 5 and 6). The error obtained form measuring kinetics with ^{1}H NMR and the large polymerization rate are most likely the reason for the difference between entry 5 and 6.

To further explore this phenomenon and to elucidate whether this rate enhancement was due to template polymerization, we studied the effect of addition of single thymine containing molecules on the ATRP of **3**. In order to maintain solubility upon polymerization and to have a structure similar to the thymine monomer, 1-hexyl-thymine instead of thymine was used, which was readily synthesized via the route depicted in scheme 2[25].

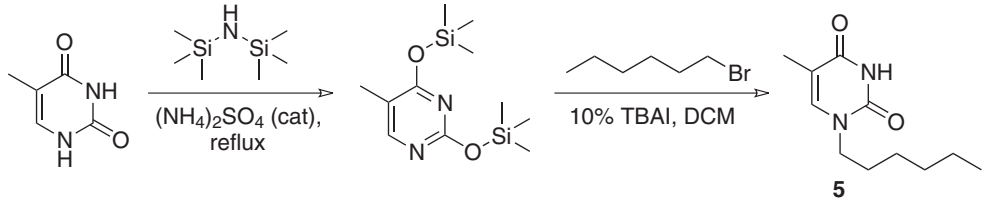

scheme 2. Synthesis of 1-hexyl-thymine **5.**

When monomer **4** was polymerized in the presence of an equimolar amount of 1-hexyl-thymine **5** first order kinetics were observed as can be seen in figure 8. Also the polymerization rate was much faster (k_{app} = 35.8*10^{-3}) compared to the polymerization without thymine units present (k_{app} = 2.96*10^{-3}), or even in the presence of polymer template.

Besides thymine derivative **5**, succinimide was used in a template polymerization experiment, since this molecule should also be able to form hydrogen bonds with the adenine monomer. In this case too a higher polymerization rate was observed (k_{app} = 19.5*10^{-3}). An overview of the template polymerization results is depicted in figure 8.

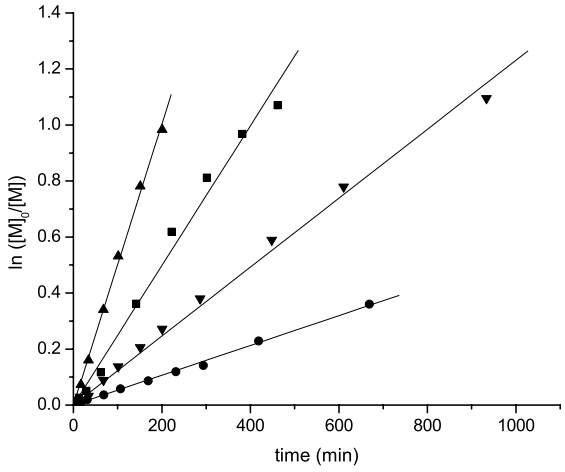

Figure 8. Kinetic plot of adenine polymerization in the presence of different additives ● (**4** = 0.13 M, CuCl = 0.012 M, bpy = 0.024 M, EBiB = 0.014 M), ▼ (**4** = 0.13 M, CuCl = 0.012 M, bpy = 0.024 M, EBiB = 0.014 M, **3** = 0.014 M), ■ (**4** = 0.11 M, CuCl = 0.0096 M, bpy = 0.021 M, EBiB = 0.011 M, succinimide = 0.11 M), ▲ (**4** = 0.13 M, CuCl = 0.012 M, bpy = 0.024 M, EBiB = 0.014 M, **5** = 0.13 M).

In line with the observed increase in polymerization rate of adenine monomer upon addition of complementary moieties, is the copolymerization of monomers **4** and **2**. Remarkable is the fact that both monomers have a similar polymerization rate (adenine k_{app}=29.6*10-3, thymine k_{app}=30.4*10-3 L*mol^{-1}*min^{-1}) as can be seen in figure 9.

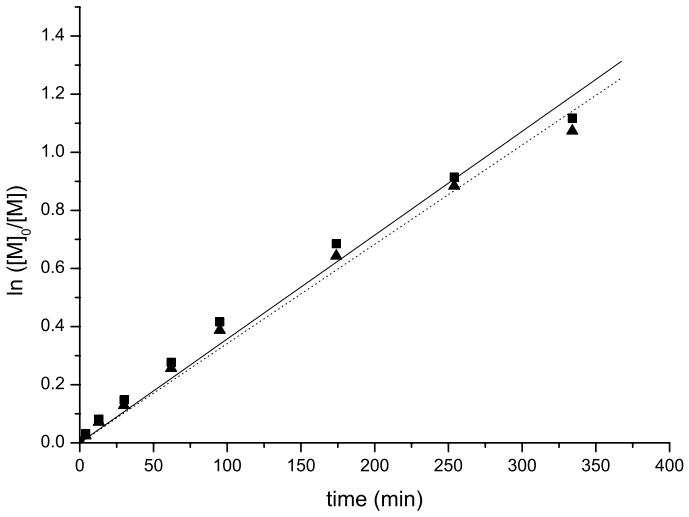

Figure 9. Kinetic plots of copolymerization of monomer **2**(■) and **4**(▲) using EBiB as initiator (**4** = 0.11 M, **2** = 0.11 M, CuCl = 0.011 M, bpy = 0.022 M).

Haddleton et al. have investigated the effects of DMSO on copper mediated living radical polymerizations and they have shown with ^{1}H NMR and UV experiments the influence of DMSO on the copper catalyst[26]. Since all of the template experiments were performed in DMSO the observed increase in reaction rate could not be solely assigned to DMSO interactions with the copper catalyst. From literature and ATRP experiments with all four nucleobases conducted in chapter 2 it was known that nucleic acids could bind to copper (II)[27, 28] and could therefore have an influence on the ATRP catalyst. To further elucidate whether complex formation of adenine or thymine moieties with copper chloride could count for the increase in polymerization rate UV-vis experiments were conducted.

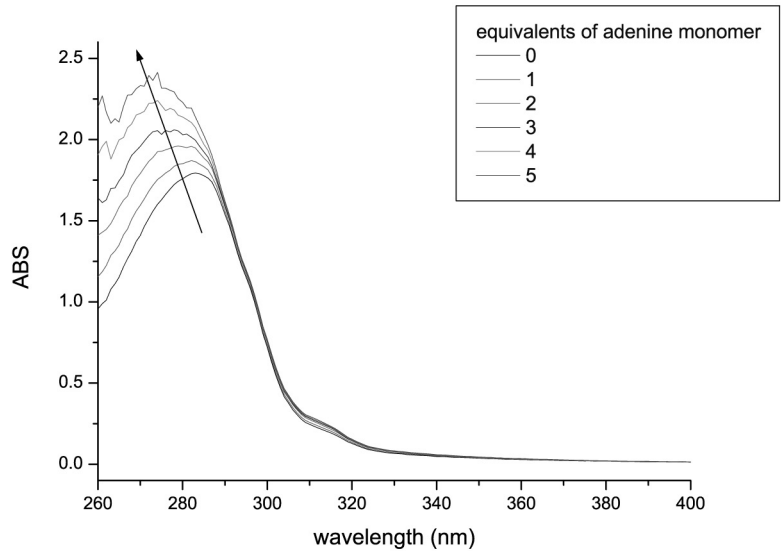

Figure 10. Addition of 0 - 5 equivalents of adenine monomer **4** to a solution of bpy and CuCl in DMSO.

As can be seen in figure 10 the absorption maximum shifted from 285 nm to 275 nm upon increasing the amount of adenine monomer. Since no new peak was observed and only a shift occurred upon addition of adenine monomer it is assumed that under the conditions the UV spectra were measured adenine monomer is not coordinating to copper, creating a new complex.

3.4 Discussion

All ATRP experiments were performed in DMSO for several reasons. Nucleobase monomers and polymers were well soluble in this solvent, which therefore enabled kinetics studies that were not hampered by precipitation or aggregation. Because these experiments were performed in DMSO-d_6, ^{1}H-NMR spectroscopy could be used for the determination of the kinetics. A major disadvantage of the use of a polar solvent such as DMSO is that no strong hydrogen bonding interactions between adenine and thymine were expected. In addition it has been shown that polar solvents in general have a rate enhancing effect on ATRP[29, 26]. Those rate enhancements were explained by the existence of a monomeric copper species. Data from literature[30, 31] also shows that DMSO can coordinate to copper, changing the nature of the catalyst. Because Takemoto and Inaki[32, 24] showed that a template effect still

could occur in polar solvents as a result of complementary nucleobase interactions, we decided to start our investigations with DMSO solutions. Also in our case the presence of a specific interaction could be interpreted from the fact that thymine functionalized polymer accelerates the polymerization of adenine monomer, while thymine monomer is not accelerated by the same polymer template (figure 5 and 6).

To further investigate these results the ratio between monomer and polymer template was changed. In general, during template polymerizations the rate of polymerization depends on the presence of template polymer and on the strength of the interaction between template and monomer. As shown in figure 11, the $k_{p,app}$ should have an optimum around 1 to 1 binding of monomer to templating moiety[6, 7, 2, 3].

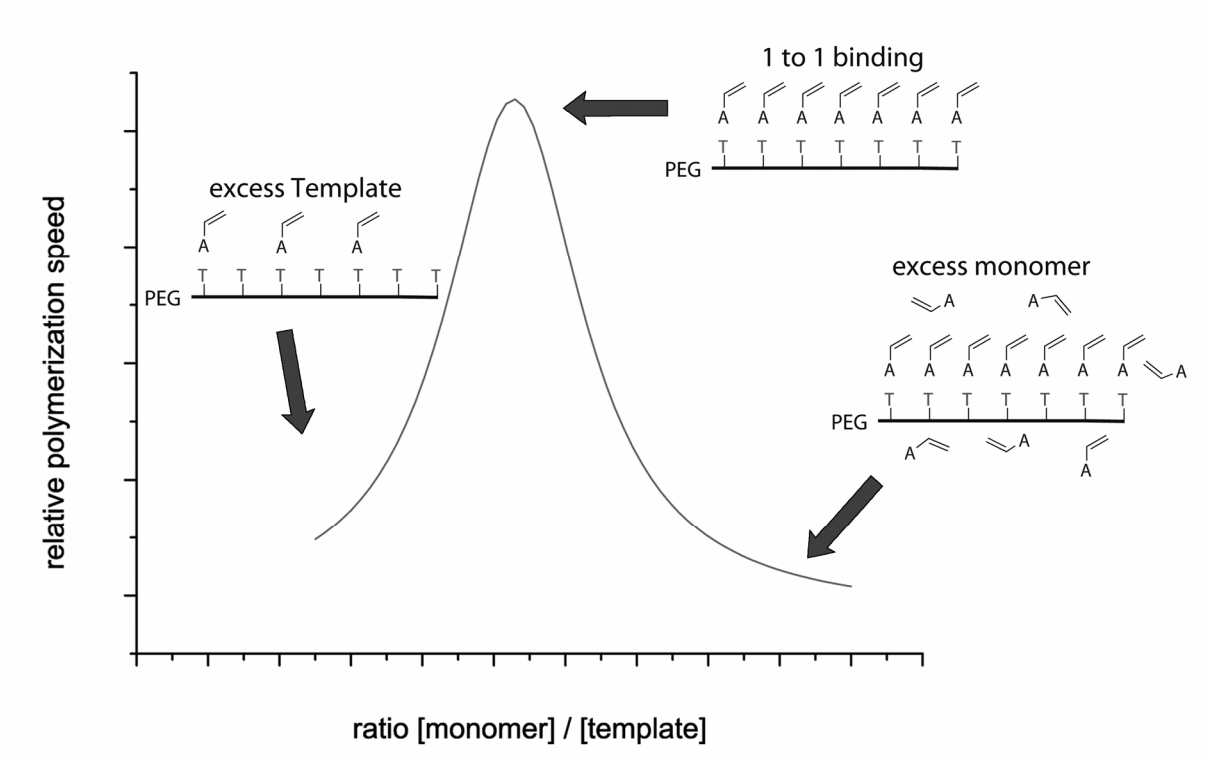

Figure 11. Schematic representation of a possible relative polymerization speed at different monomer to template ratios.

If the optimal amount of monomer is absorbed onto the template one can imagine the polymerization rate will be enhanced due to the close proximity of monomer and the growing polymer chain. An excess of template would reduce the relative amount of monomer bound to each polymer template. As a consequence, monomers are not in close proximity of each other, therefore no increased polymerization rate is expected.

An excess of monomer means a significant amount of monomer will polymerize freely in solution and therefore has no increased polymerization speed. The larger the excess the lower the overall polymerization rate will be.

In our case, when the amount of template was increased, the polymerization rate increased even more. Surprisingly, the polymerization speed of adenine monomer increased by a factor of 100 when a large excess of thymine functionalized polymer was used (table 1, entry 5 and 6). Therefore a different mechanism must be in effect during the polymerization of adenine monomer with complementary thymine polymer present.

To investigate further what effect was responsible for the polymerization rate increase adenine monomer was polymerized in the presence of 1-hexyl-thymine moiety **6**. Also in this case a rate enhancement, even greater than with polymer **5** was observed. In addition, succinimide, which has the same hydrogen bonding capabilities as thymine, but is less specific for adenine, shows also an increase in the polymerization rate of adenine, albeit smaller than for thymine. Succinimide has been used before to enable the polymerization of adenine monomer via ROMP[33]. Remarkable is the effect that the thymine monomer **2** is not affected by addition of complementary moieties (table 2 entry 10, 11 and 12), while ATRP of the adenine monomer is accelerated.

The most plausible explanation for all the phenomena observed is that the rate acceleration is a result of a specific interaction between adenine and thymine moieties. The exact type of interaction is until now rather elusive. Although hydrogen bonding between the complementary nucleobases, or between succinimide and adenine would be a logical assumption, the use of DMSO-d_6 as a solvent hampers the identification in the ^{1}H NMR and FTIR spectra of the occurrence of hydrogen bonding interaction between adenine and thymine. A possible reason why single nucleobase interactions result in acceleration of ATRP of adenine methacrylate **3** can be found when one compares the rates of polymerization of **2** and **3** in absence of any polymeric template. From these experiments it is clear that thymine polymerization proceeds much faster than adenine polymerization. The adenine moiety therefore slows down the ATRP process. Adenine seems to interact with the ATRP copper complex, thereby partly deactivating the catalyst or creating a different, less active catalytic copper species. Unfortunately, UV-vis experiments did not provide any clear evidence for this interaction and additionally, in our case the ^{1}H NMR spectra did not evidently indicate complex formation of adenine with copper[28].

If on the other hand thymine would influence or activate the copper catalyst, deviations from first order kinetics would be expected during the polymerization of thymine monomer, because monomeric thymine is much better at increasing the polymerization rate compared to polymeric thymine. Therefore, during ATRP of thymine the acceleration effect should diminish. Since this is not the case the explanation that adenine affects the catalyst is more plausible. By adding thymine either in polymeric or monomeric form, or by adding succinimide, which is also complementary to adenine, to the polymerization, adenine interacts with these complementary species and therefore less with the copper catalyst, generating a more active copper catalyst species. As a result the rate of polymerization is increased.

3.5 Conclusions

Adenine and thymine methacrylate monomers can be synthesized and polymerized in a controlled fashion using ATRP in DMSO-d_6 as a solvent. When a thymine functionalized block copolymer was added as a template to the polymerization of adenine monomer a significant rate enhancement was observed. In addition this rate enhancement proved to be specific for the adenine – thymine base pair because the polymerization rate of thymine monomer was not amplified. Further elucidation of the polymerization rate enhancement by changing the adenine to thymine ratios showed that if an excess of thymine block copolymer was added the rate enhancement was increased up to 100 times. This interesting phenomenon was not in agreement with any of the known template polymerization studies or other polymerizations of functional monomers in DMSO found in literature. Therefore complementary monomeric moieties were also included during polymerization and surprisingly showed an even greater rate enhancement compared to polymeric thymine. These findings showed that in DMSO different catalytic species were formed that influence the rate of adenine methacrylate polymerization significantly.

3.6 Experimental

Materials

All reactions were performed under a nitrogen atmosphere, unless otherwise stated. DMF was dried over anhydrous $MgSO_4$, followed by distillation under reduced pressure and storage under an argon atmosphere. Dichloromethane (DCM), heptane and ethyl acetate (EtOAc) were distilled over calcium hydride (CaH_2) and 1,4-dioxane was freshly distilled over $LiAlH_4$. Copper chloride (CuCl) was purified according to a literature procedure[34]. Silica gel column chromatography (SGCC) was performed using Acros silica gel (0.035-0.070 mm, pore diameter ca. 6 nm). TLC was carried out on Merck precoated silica gel 60 F-254 plates. Compounds were visualized using UV and permanganate staining agent. Other chemicals were used as received unless otherwise stated. The synthesis of compounds **2** and **4** are described in chapter 2 as compounds 2 and 3 respectively.

Instrumentation

^{1}H NMR spectra were recorded on a Varian INOVA400 instrument at 400 MHz and ^{13}C NMR spectra were recorded on a Bruker DPX300 instrument at 75 MHz. Chemical shifts (δ) are given in ppm relative to the internal standard (Me_4Si or DMSO-d_6). IR spectra were recorded on an ATI Matson Genesis Series FTIR spectrometer with fitted ATR cell. HRMS spectra were recorded on a VG 7070 or MAT 900 mass spectrometer. GPC measurements were performed using a Shimadzu LC-10ADvp system equipped with PL gel 5 μm guard column, a PL gel 5 μm mixed D column, differential refractive index detector (Shimadzu RID-10A) at 38°C and a UV detector (Shimadzu SPD-10AVvp). The system was operated with a flow of 0.8 mL/min at 70°C using dimethylsulfoxide (DMSO, 0.02 M LiCl) as an eluent and polyethylene glycol standards in the range 1900 to 124700 g/mol. Or at a flow of 1 mL/min at 35°C using THF as an eluent and polystyrene standards in the range of 580 to 377400 g/mol to calibrate the GPC. UV-Vix spectra were recorded on a Varian Cary 50.

α-methyl-ω-(2-bromo-2-methyl propionate)poly(ethylene glycol) (1)

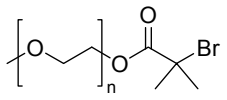

Poly(ethylene glycol) methyl ether 2000 (5.12 g, 2.56 mmol) and Et_3N (0.5304 g, 5.24 mmol) were dissolved in DCM (100 mL) and cooled to 0°C. 2-bromo-isobutyrylbromide (0.8824 g, 3.83 mmol) was added drop wise and the mixture was warmed to ambient temperature. After 18 hours an additional amount of 2-bromo-isobutyrylbromide (0.84839 g, 3.69 mmol) was added and the mixture was stirred for another 40 hours. The remaining 2-bromo-isobutyrylbromide was quenched with MeOH (10 mL). The mixture was washed with a saturated $NaHCO_3$ solution (50 mL) and water (50 mL). The organic phase was dried over anhydrous $MgSO_4$ and concentrated under reduced pressure to give a waxy yellowish solid which was further purified using column chromatography (MeOH/DCM; 1:9) after which 5.22 g (95%) product **1** was obtained as a white, waxy solid. ^{1}H NMR (300 MHz, $CDCl_3$): δ 4.31 (t, 2H, J = 4.8 Hz, CH_2-C$\underline{H}_2$-O-C(=O)), 3.63 (br m, 180H, {C$\underline{H}_2$-C$\underline{H}_2$-O} + endgroups), 3.37 (s, 3H, C$\underline{H}_3$-O), 1.93 (s, 6H, C(=O)-C(C$\underline{H}_3$)$_2$-Br); ^{13}C NMR ($CDCl_3$): δ 171.15, 71.91, 70.55, 68.72, 65.13, 59.05, 55.76, 30.91. IR (solid): ν 1731, 1102$_r$; SEC (THF) M_n = 2.8 kg/mol, PDI = 1.06.

poly(ethylene glycol)-*block*-poly[3-(thymin-1-yl)propyl methacrylate] (3)

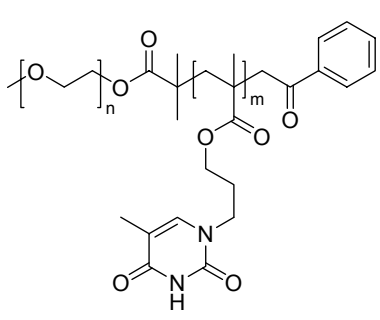

Monomer **2** (0.786 g, 3.11 mmol), CuCl (20.5 mg, 0.207 mmol) and 2,2'-bipyridine (bpy, 65.8 mg, 0.421 mmol) were placed in a Schlenk tube. After deoxygenation by three cycles of evacuation, followed by applying a dry nitrogen atmosphere, the Schlenk tube was put under an argon atmosphere. DMSO-d_6 (4.0 mL) was added, followed by addition of an argon purged solution of **1** (0.446 g, 0.207 mmol) in DMSO-d_6 (3.5 mL). The polymerization reaction was performed at ambient temperature. Samples were taken periodically in order to analyze the monomer conversion with ^{1}H NMR spectroscopy. At 540 min 1-phenyl-1-(trimethylsiloxy)-ethylene (0.410 g, 2.13 mmol) was added to quench the ATRP and end cap the polymer. The reaction mixture was precipitated in an aqueous EDTA solution (0.055 M) after which the crude product was extracted with DCM (5 times 50 mL). The separation required the addition of brine. The organic phase was dried over anhydrous $MgSO_4$ and was concentrated under reduced pressure. The product was further purified using sephadex column chromatography (LH-20, MeOH/DCM; 1:1) resulting after freeze drying in 0.771 g of the desired product as a white solid. ^{1}H-NMR (300 MHz, DMSO-d_6): δ 11.14 (br. s, NH pyrimidine), 7.55-8.00 (m, CH_2-C(=O)-C$_6\underline{H}_5$ aromatic endgroup

signals), 7.39 (br s, H^6 pyrimidine), 3.92 (br s, O-C<u>H</u>$_2$-CH$_2$), 3.69 (br s, CH$_2$-C<u>H</u>$_2$-N), 3.50 (br s, {C<u>H</u>$_2$-C<u>H</u>$_2$-O} PEG block), 3.24 (s, O-C<u>H</u>$_3$ endgroup), 2.23 (br s, CH$_2$-C<u>H</u>$_2$-CH$_2$-N), 1.6-2.0 (br m, {C<u>H</u>$_2$-C(CH$_3$)}), 0.6-1.4 (br m, {CH$_2$-C(C<u>H</u>$_3$)}); IR (solid): ν 1672, 1105; SEC (DMSO): M_n = 4.9 kg/mol, M_w = 6.5 kg/mol, PDI = 1.30.

1-hexyl-thymine (5)

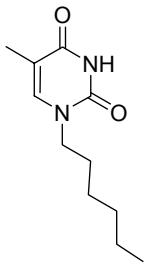

To a round bottom flask fitted with a condenser and a $CaCl_2$ tube was added 301.3 mg (2.39 mmol) thymine, 8.0 mg (0.06 mmol) $(NH_4)_2SO_4$ and 4 mL (18.96 mmol) hexamethyldisilazane. The suspension was heated under reflux for 18 h. The resulting clear reaction mixture was concentrated under reduced pressure, yielding a colorless oil. The oil was re-dissolved in dry DCM (4 mL) whereupon tetrabutylammonium iodide (TBAI, 43.9 mg, 0.12 mmol) and 1-bromohexane (335 µL, 2.39 mmol) were added. After refluxing for 4 days the mixture was concentrated under reduced pressure. The crude product was purified with column chromatography (3% MeOH in DCM) yielding a pure white solid (90 mg, 17.9 %). mp = 129.2 °C; R_f (3% MeOH in DCM) = 0.16; ^{1}H NMR (300 MHz, $CDCl_3$) δ 8.30 (br. s, 1H, H^3 pyrimidine), 6.94 (q, 1H, *J* = 1.2 Hz, H^6 pyrimidine), 3.67 (t, 2H, *J* = 7.2 Hz, N-C<u>H</u>$_2$-CH$_2$), 1.92 (m, 3H, *J* = 1.2 Hz, C^5-CH$_3$ pyrimidine), 1.69 (m, 2H, *J* = 6.9 Hz, N-CH$_2$-C<u>H</u>$_2$-CH$_2$), 1.31 (m, 6H, -CH$_2$-C<u>H</u>$_2$-C<u>H</u>$_2$-C<u>H</u>$_2$-CH$_3$), 0.88 (m, 3H, 6.60 Hz, CH$_2$-CH$_3$); ^{13}C NMR ($CDCl_3$) δ 163.85, 150.57, 140.29, 110.51, 48.82, 31.66, 29.39, 26.43, 22.82, 14.35, 12.72. IR (solid): ν 1687, 1651.

ATRP of adenine monomer 4 (general procedure for polymerization in an NMR tube)

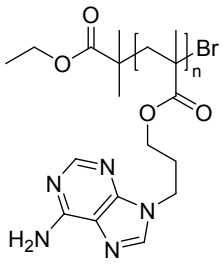

Monomer **4** (17.0 mg, 0.065 mmol) was added to an NMR tube which was placed in a Schlenk tube. Deoxygenation was performed by three cycles of evacuation, and refilling with dry nitrogen. The monomer was dissolved in 0.4 mL DMSO-d_6, followed by addition of 0.1 mL of a catalyst stock solution (4.7 mg (0.047 mmol) CuCl and 15.1 mg (0.096 mmol) bpy dissolved in 0.8 mL DMSO-d_6). The mixture was purged with argon for 5 minutes, after which the polymerization was started by addition of ethyl α-bromo isobutyrate (EBIB) (1 µL, 0.007 mmol), followed by immediate recording of the first ^{1}H NMR spectrum at 30°C. Follow up spectra were recorded at different time intervals by applying steady state scans.

ATRP of thymine monomer 2

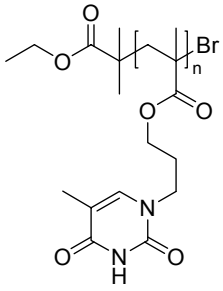

Monomer **2** was polymerized according to the general procedure using **2** (16.6 mg, 0.0658 mmol), 0.4 mL DMSO-d_6, 0.1 mL stock solution (4.6 mg (0.046 mmol) CuCl and 15.0mg (0.096 mmol) bpy in 0.8 mL DMSO-d_6) and 1.0 µl (6.8 µmol) EBiB.

ATRP of 2 in the presence of 3

Monomer **2** was polymerized according to the general procedure using **2** (16.8 mg, 0.0666 mmol), **3** (32.0 mg, 0.0072 mmol), 0.4 mL DMSO-d_6, 0.1 mL stock solution (4.6 mg (0.046 mmol) CuCl and 15.1 mg (0.0967 mmol) bpy in 0.8 mL DMSO-d_6) and 1.0 µl (6.8 µmol) EBiB.

ATRP of 4 in the presence of 3

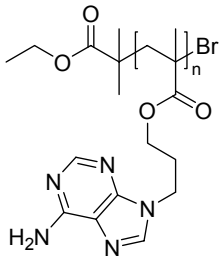

Monomer **4** was polymerized according to the general procedure using **4** (17.0 mg, 0.0651 mmol), **5** (32.0 mg, 0.0072 mmol), 0.4 mL DMSO-d_6, 0.1 mL stock solution (4.7 mg (0.047 mmol) CuCl and 15.1 mg (0.0967 mmol) bpy in 0.8 mL DMSO-d_6) and 1.0 µl (6.8 µmol) EBiB.

ATRP of 4 in the presence of 5

Monomer **4** was polymerized according to the general procedure using **4** (17.2 mg, 0.0658 mmol), **5** (13.8 mg, 0.0657 mmol), 0.4 mL DMSO-d_6, 0.1 mL stock solution (4.6 mg (0.046 mmol) CuCl and 14.7 mg (0.0941 mmol) bpy in 0.8 mL DMSO-d_6) and 1.0 µl (6.8 µmol) EBiB.

ATRP of 4 in the presence of succinimide

Monomer **4** was polymerized according to the general procedure using **4** (17.6 mg, 0.0674 mmol), succinimide (6.7 mg, 0.0676 mmol), 0.5 mL DMSO-d_6, 0.1 mL stock solution (4.6 mg (0.046 mmol) CuCl and 15.7 mg (0.0986 mmol) bpy in 0.8 mL DMSO-d_6) and 1.0 µl (6.8 µmol) EBiB.

Copolymerization of 2 and 4

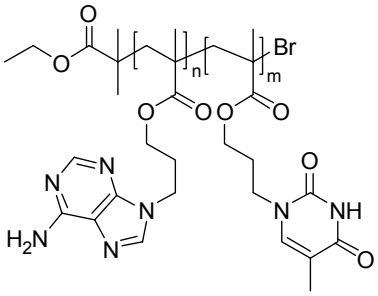

Monomer **2** and **4** were polymerized according to the general procedure using **2** (17.0 mg, 0.0674 mmol), **4** (17.5 mg, 0.0670 mmol), 0.5 mL DMSO-d_6, 0.1 mL stock solution (4.1 mg (0.041 mmol) CuCl and 13.4 mg (0.0858 mmol) bpy in 0.68 mL DMSO-d_6) and 1.0 µl (6.8 µmol) EBiB.

Titration of CuCl /2 bpy with adenine monomer 4.

A solution containing bpy ($10*10^{-5}$ mol/L) and CuCl ($5*10^{-5}$ mol/L) in HPLC grade DMSO was prepared (solution A) and a solution of **4** in HPLC grade DMSO (0.010 mol/L) (solution B) was prepared. The titration was performed in a batch wise fashion by addition of 1 µL solution B to 1 mL of solution A, followed by mixing and recording of the UV-Vis spectrum after each addition.

3.7 References

1. M. G. Cascone, L. Lazzeri, N. Barbani, C. Cristallini and G. Polacco. *Polym. Int.* **1996**, *41*, 17-21.
2. S. Polowinski. *Template polymerization*, ed.; ChemTec Publishing: Toronto-Scarborough, 1997; Vol.
3. S. Polowinski. *Prog. Polym. Sci.* **2002**, *27*, 537-577.
4. T. Bartels, Y. Y. Tan and G. Challa. *J. Polym. Sci., Part A: Polym. Chem.* **1977**, *15*, 341-351.
5. H. T. Van de Grampel, Y. Y. Tan and G. Challa. *Makromol. Chem., Macromol. Symp.* **1988**, *20*, 83-89.
6. H. T. Van de Grampel, Y. Y. Tan and G. Challa. *Macromolecules* **1990**, *23*, 5209-5216.
7. H. T. Van de Grampel, Y. Y. Tan and G. Challa. *Macromolecules* **1991**, *24*, 3767-3772.
8. H. T. Van de Grampel, Y. Y. Tan and G. Challa. *Macromolecules* **1991**, *24*, 3773-3778.
9. H. T. Van de Grampel, Y. Y. Tan and G. Challa. *Macromolecules* **1992**, *25*, 1041-1048.
10. H. T. Van de Grampel, G. Tuin, Y. Y. Tan and G. Challa. *Macromolecules* **1992**, *25*, 1049-1056.
11. V. S. Trubetskoy, V. G. Budker, L. J. Hanson, P. M. Slattum, J. A. Wolff and J. E. Hagstrom. *Nucleic Acids Res.* **1998**, *26*, 4178-4185.
12. I. Rainaldi, C. Cristallini, G. Ciardelli and P. Giusti. *Polym. Int.* **2000**, *49*, 63-73.
13. K. Takemoto and Y. Inaki. *Adv. Polym. Sci.* **1981**, *41*, 1-51.
14. Y. Inaki. *Prog. Polym. Sci.* **1992**, *17*, 515-570.
15. Y. Y. Tan and G. Challa. *Makromol. Chem., Macromol. Symp.* **1987**, *10/11*, 215-233.
16. J. S. Wang and K. Matyjaszewski. *Macromolecules* **1995**, *28*, 7901-7910.
17. J. S. Wang and K. Matyjaszewski. *J. Am. Chem. Soc.* **1995**, *117*, 5614-5615.
18. M. Kamigaito, T. Ando and M. Sawamoto. *Chem. Rev.* **2001**, *101*, 3689-3745.
19. K. Matyjaszewski and J. H. Xia. *Chem. Rev.* **2001**, *101*, 2921-2990.
20. A. Khan, D. M. Haddleton, M. J. Hannon, D. Kukulj and A. Marsh. *Macromolecules* **1999**, *32*, 6560-6564.
21. A. Marsh, A. Khan, D. M. Haddleton and M. J. Hannon. *Macromolecules* **1999**, *32*, 8725-8731.
22. T. Glauser, M. Ranger, B. Kalra, W. Gao, J. Hedrick and R. A. Gross. *Polym. Prepr. (Am. Chem. Soc., Div. Polym. Chem.)* **2003**, *44*, 624-625.
23. K. Tokuchi, T. Ando, M. Kamigaito and M. Sawamoto. *J. Polym. Sci., Part A: Polym. Chem.* **2000**, *38*, 4735-4748.
24. Y. Inaki, K. Ebisutani and K. Takemoto. *J. Polym. Sci., Part A: Polym. Chem.* **1986**, *24*, 3249-3262.
25. H. Vorbrüggen. *Acc. Chem. Res.* **1995**, *28*, 509-520.
26. S. Monge, V. Darcos and D. M. Haddleton. *J. Polym. Sci., Part A: Polym. Chem.* **2004**, *42*, 6299-6308.
27. G. L. Eichhorn, P. Clark and E. D. Becker. *Biochemistry* **1966**, *5*, 245-253.
28. N. A. Berger and G. L. Eichhorn. *Biochemistry* **1971**, *10*, 1847-1857.
29. K. Matyjaszewski, Y. Nakagawa and C. B. Jasieczek. *Macromolecules* **1998**, *31*, 1535-1541.
30. R. D. Willett, G. Pon and C. Nagy. *Inorg. Chem.* **2001**, *40*, 4342-4352.
31. C. Y. Su, S. Liao, M. Wanner, J. Fiedler, C. Zhang, B. S. Kang and W. Kaim. *Dalton Trans.* **2003**, 189-202.
32. M. Akashi, H. Takada, Y. Inaki and K. Takemoto. *J. Polym. Sci., Part A: Polym. Chem.* **1979**, *17*, 747-757.
33. H. S. Bazzi and H. F. Sleiman. *Macromolecules* **2002**, *35*, 9617-9620.
34. R. N. Keller and H. D. Wycoff. *Inorganic Syntheses* **1946**, *2*, 1-4.

Chapter 4

Synthesis and assembly behavior of nucleobase functionalized block copolymers

4 Synthesis and assembly behavior of nucleobase functionalized block copolymers

4.1 Introduction

The use of oligonucleobase moieties in materials science has experienced a growing interest in recent years. Several researchers have elegantly shown the application of oligonucleotides as versatile building blocks for the synthesis of e.g. controlled nanoscaled structures[1, 2] and molecular machines[3, 4]. Also in polymer science, oligonucleobases have become topic of investigation. Nucleobase functionalized polymers have been applied in various applications like template polymerizations (chapter 3)[5-7] and supramolecular materials, in which the non-covalent anchors are based on oligonucleotides[8, 9]. Lutz et al[10] have found that incorporation of complementary nucleobase functionality into synthetic copolymers leads to materials which can exhibit a DNA like melting behavior. In addition, Rowan et al have prepared thermo responsive supramolecular polymer materials, in which the non-covalent interactions are based on single nucleobase moieties[11-13]. The recent advances in controlled (radical) polymerization techniques such as ATRP[14-19] have further increased the activities in the polymer chemistry field. These methods allow the formation of well-defined polymer architectures in which a large variety of biological functionalities, amongst which nucleobases, can be included[20, 21].

It is well known that amphiphilic block copolymers have the ability to assemble into multiple morphologies in solution. Depending on a number of parameters, such as the ratio of the hydrophilic and hydrophobic blocks, the morphology can vary from spherical micelles, rods, and vesicles to large compound micelles (LCMs)[22]. Even more structural control is possible when block copolymers are used that are built up out of a synthetic and a biomolecular part. Another method was developed by Rotello and coworkers, who prepared plug and play polymers that facilitated recognition through hydrogen-bonding interactions to change the morphology of the polymers[23, 24] or even direct self assembly of patterned surfaces[25]. Several examples in which peptide sequences are incorporated into polymer chains have shown to control the material properties and enable self assembly into well defined nanoscaled architectures[26-28]. Besides proteins, this could also apply to nucleobase block copolymers. In previous investigations it already has been demonstrated that

incorporation of small oligo nucleotide strands has a vast potential to influence the aggregation of block copolymers[19]. Often the incorporation of these bio-functional moieties into the polymer chain facilitates some form of aggregation. Either, the aggregation of the biological functionality is enhanced by the polymer chain, or aggregation of the polymer chains is increased via specific interactions between the biological functionalities. In addition, the nano-compartmentalization by block copolymer micelles or vesicles containing biomolecular functionality may provide interesting properties that could lead to applications such as controlled drug or gene delivery[29].

As a continuation of the work described in chapter 3[7] we were interested in the effect of complementary nucleobase functionality on the aggregation behavior of amphiphilic block copolymers. For this purpose we have synthesized a series of well-defined poly(ethylene glycol)-poly(adenine) and poly(ethylene glycol)-poly(thymine) block copolymers via ATRP and have studied the aggregation phenomena of both the separate block copolymers and a mixture of polymers with complementary nucleobases. Although it was expected that the additional non-covalent interaction would lead to an enhanced ability of the block copolymer mixture to assemble, surprisingly the reverse is shown to be the case.

4.2 Synthesis of block copolymers

Thymine and adenine monomers **1** and **2**, and PEG initiator **3** were synthesized using a previously described procedure7. Both monomers were polymerized via ATRP to two different average degrees of polymerization in the range of 10 to 30 using a procedure described in chapter 3. At the conversion where the desired DP was reached, the polymers were end capped by quenching the ATRP reaction with a tenfold excess of 1-phenyl-1-(trimethylsiloxy)-ethylene (scheme 1)[30].

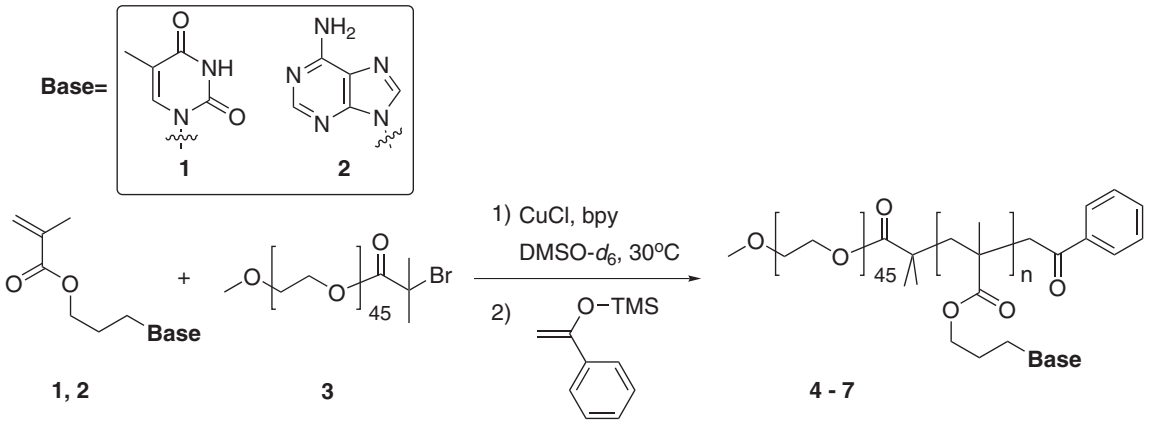

scheme 1. Preparation of PEG block copolymers with thymine and adenine monomers **1** and **2,** followed by end capping of the polymerization using a silyl enol ether.

The polymerizations were monitored with ^{1}H-NMR spectroscopy in order to follow the monomer conversion and subsequently determine the kinetics. For the ATRP experiments of monomer **1** the relative monomer concentration was determined by the ratio between the acrylic proton signal at δ 5.98 ppm and the pyrimidine-NH signal at δ 11.16 ppm in the ^{1}H NMR spectrum. In case of monomer **2** the ratio between the ^{1}H NMR signals at δ 5.90 ppm and δ 8.13 ppm was used.

As can be seen in figure 1 and 2 the kinetic plots of the polymerizations show good first order kinetics, indicating control over the polymerization. These findings were confirmed by the reasonably low polydispersity indices found by SEC. In addition, the quenching step by addition of 1-phenyl-1-(trimethylsiloxy)-ethylene proceeded effectively. The final degrees of polymerization were determined after work up by ^{1}H-NMR spectroscopy.

Table 1. Molecular weight data of adenine and thymine block copolymers

copolymer	nucleobase monomer	$M_{n\ theo}$ kg/mol	DP[a]	M_n[a] kg/mol	M_n[b] kg/mol	M_w/M_n[b]
4, PEG-*b*-T10	1	5.1	14.3	5.8	5.8	1.20
5, PEG-*b*-T20	1	7.4	21.3	7.5	8.8	1.20
6, PEG-*b*-A10	2	4.8	11.2	5.1	5.5	1.22
7, PEG-*b*-A30	2	8.6	30.3	10.1	6.8	1.21

a) Calculated by using the integration ratio of the PEG blocks at 3.51 ppm (-O-CH_2-CH_2-) and the O-CH_2- of the nucleobase block at 3.60 ppm in the ^{1}H NMR spectra. b) Determined by SEC using DMSO as eluent.

For PEG-*b*-T10, PEG-*b*-T20 and PEG-*b*-A10 the DPs coincided with the values determined by the conversion measurements. In case of PEG-*b*-A30 a discrepancy was observed and the final DP of 30 was considerably higher than expected. This is probably due to the slightly higher conversion and the more strenuous work up procedure, due to the lower solubility of the block copolymer, which probably resulted in a relative loss of the lower molecular weight fraction.

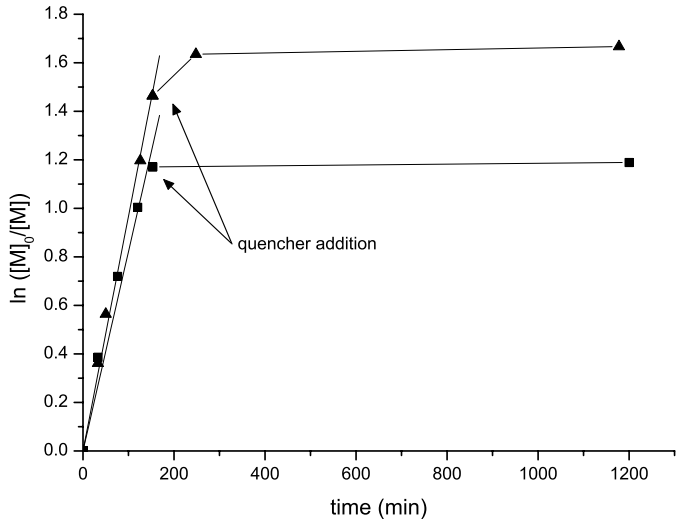

Figure 1. Kinetic data for the polymerization of thymine monomer **1** with PEG macro initiator **3** at different monomer to initiator ratios: PEG-*b*-T10 ▲ (**1** = 0.46 M, **3** = 0.032 M, CuCl = 0.034 M, bpy = 0.068 M) and PEG-*b*-T20 ■ (**1** = 0.41 M, **3** = 0.014 M, CuCl = 0.014 M, bpy = 0.029 M). The arrows indicate the moment of addition of the silyl enol quencher.

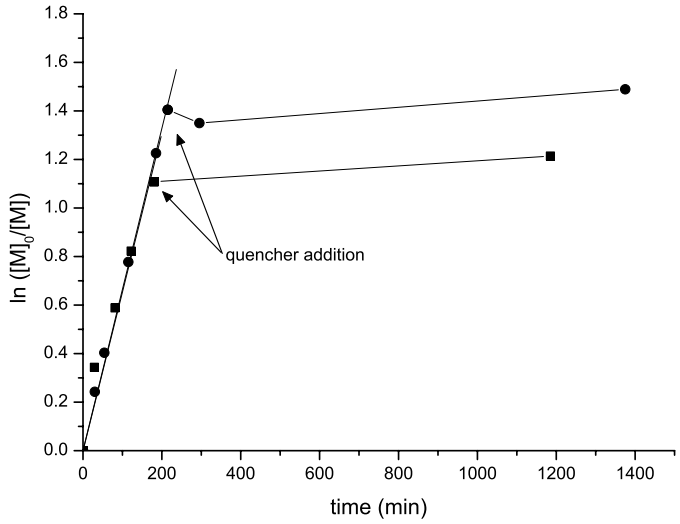

Figure 2. Kinetic data for the polymerization of adenine monomer **2** with PEG macro initiator **3** at different monomer to initiator ratios: PEG-*b*-A10 ■ (**2** = 0.32 M, **3** = 0.023 M, CuCl = 0.033 M, bpy = 0.070 M) and PEG-*b*-A30 ● (**2** = 0.34 M, **3** = 0.011 M, CuCl = 0.022 M, bpy = 0.048 M). The arrows indicate the moment of addition of the silyl enol quencher.

4.3 Aggregation studies

The assembly behavior of the PEG-*b*-T10 and PEG-*b*-A10 block copolymers was investigated with a variety of techniques. Furthermore, the effect of interaction between complementary nucleobases on aggregation was studied on equimolar mixtures of block copolymers PEG-*b*-T10 (**4**) and PEG-*b*-A10 (**6**). Initially the longer block copolymers PEG-*b*-T20 (**5**) and PEG-*b*-A30 (**7**) were also investigated. However, aggregation measurements were hampered by solubility problems. Because these problems already occurred after a surprisingly small increase in DP, an effective investigation of the effect of DP on assembly was therefore not possible.

4.3.1 Critical aggregation concentration (CAC) determination

The critical aggregation concentration of the different block copolymers was determined via fluorescence spectroscopy using the probe 1,6-diphenyl-1,3,5-hexatriene (DPH), of which it is known that it fluoresces in a hydrophobic environment and that the fluorescence is quenched in an aqueous environment. Upon formation of polymeric aggregates, a more hydrophobic environment is created, which leads to a strong increase in

fluorescence intensity of the DPH probe at 430 nm. A typical CAC determination curve is depicted in figure 3, for PEG-*b*-A10.

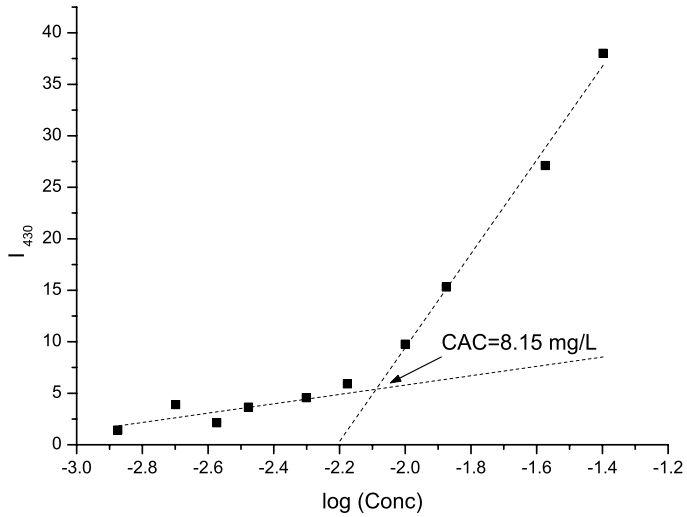

Figure 3. Plot of the fluorescence intensity of DPH at 430 nm versus log concentration (mg/mL) of PEG-*b*-A10 in water.

From the intersection point between the two regression-lines, the CAC could be calculated. An overview of the CAC values for the block copolymers and their mixture is depicted in table 2. As expected, both polymers have a similar CAC of 8 mg/L since both polymers have a similar DP. In addition no difference between the adenine and thymine side groups could be observed with respect to effect on aggregation. Interestingly, when a mixture of the adenine and thymine block copolymers was investigated, a significant increase in CAC to 12 mg/L compared to both the CAC values of PEG-*b*-T10 and PEG-*b*-A10 was observed.

4.3.2 Cryo Scanning Electron Microscopy studies

The morphology of the block copolymer assemblies was further studied with Cryo Scanning Electron Microscopy (CryoSEM). Depicted in figure 4 are typical examples of the observed particles of the polymer solutions with concentrations above the CAC.

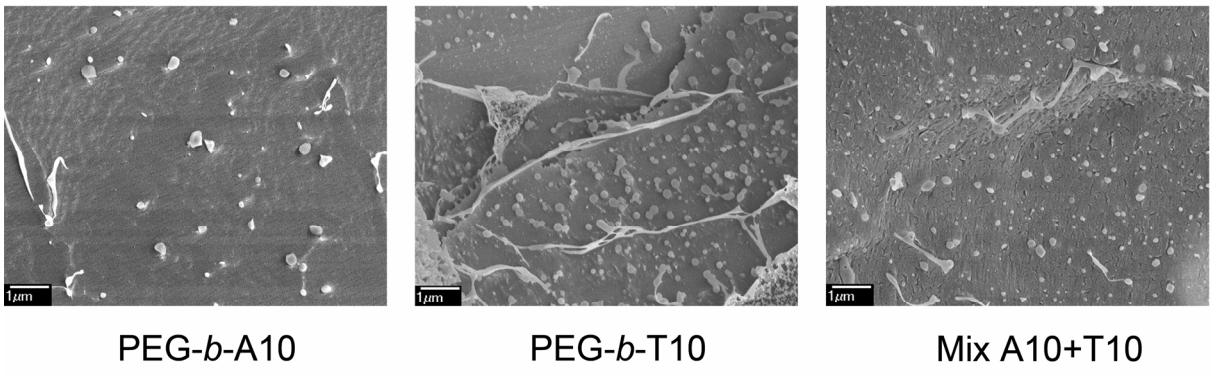

Figure 4. cryo SEM pictures of different polymer samples at 1 mg/mL

For both PEG-*b*-T10 and PEG-*b*-A10 and an equimolar mixture spherical aggregates were observed, with diameters of about 100-300 nm. The rather broad size distribution is attributed to the fact that with cryoSEM samples have frozen water as a matrix. Therefore, it is difficult to see if the observed particles are completely free or partially surrounded by matrix, in which case you only see part of the actual aggregate. As a consequence, cryoSEM is not an ideal technique to measure accurate particle sizes.

4.3.3 Particle size measurements

The CAC and cryoSEM measurements suggested that aggregation of the block copolymers occurred and that spherical particles were formed. To further investigate aggregate formation, dynamic light scattering (DLS) measurements were performed on the various polymer solutions within a concentration range of 0.03 to 2 g/L which is well above the observed CAC (8 mg/L). The lower molecular weight adenine and thymine block copolymers (PEG-*b*-T10 and PEG-*b*-A10) were well soluble in water and other solvents. DLS studies in water at 25°C under three different angles showed the presence of spherical particles for polymer PEG-*b*-T10 (**4**) and PEG-*b*-A10 (**6**). Successively a CONTIN analysis was performed to investigate the size distribution of the aggregates. With this technique, the probabilities for a series of relaxation decays (Γ) are obtained. Assuming the measured particles are spherical, the hydrodynamic radius of a particle can be calculated, and a probability plot can be made from these data for a certain particle size.

As can be seen in figure 5, both polymer **4** (PEG-*b*-T10) and **6** (PEG-*b*-A10) revealed a bimodal particle distribution after CONTIN analysis of the DLS data. In both block copolymer solutions aggregates were observed with an average size of about 20 nm and a relative narrow peak width, whereas the second peak in the CONTIN analysis indicated the presence of aggregates with an average sizes of 150 and 208 nm at a measurement angle of 90 degrees, for block copolymer **4** and **6** respectively. The ratio, averaged over three measured angles, of the smaller aggregates versus larger aggregates was 2.3 to 1 for block copolymer **4** and 2.6 to 1 for block copolymer **6**. There was a difference between the observed aggregate sizes of the larger structures at different angles. These findings could indicate that these aggregates were not fully spherical and were therefore less well defined.

To exclude the possibility of kinetic entrapment of polymer aggregates, the polymer solutions were annealed by heating to 85°C followed by slowly cooling to ambient temperature. The CONTIN analysis after the heat cycle (data not shown) also revealed the same bimodal particle distribution and no significant changes in particle sizes were observed.

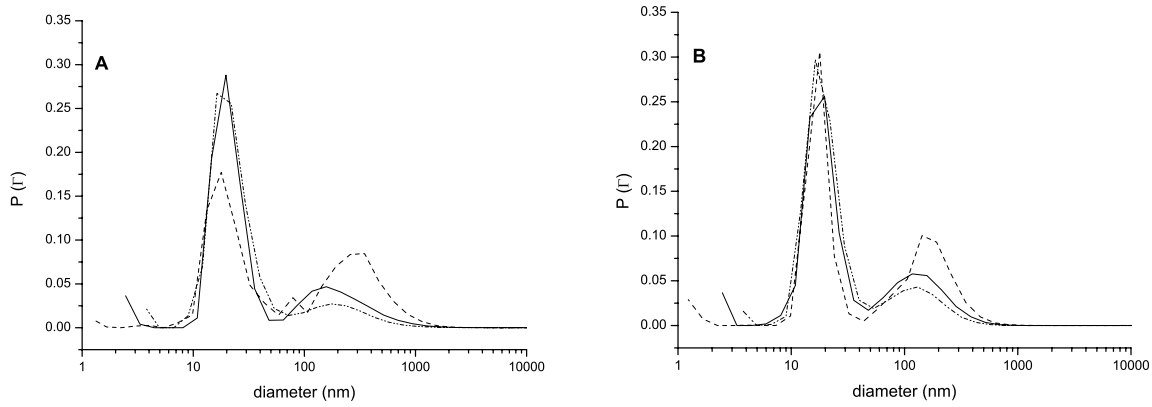

Figure 5. CONTIN analysis of (**A**) PEG-*b*-A10 and (**B**) PEG-*b*-T10, depicted as a plot of the normalized weighted probability of Γ versus particle size, measured at different angles (60°(dash), 90°(solid) and 120°(dash dot dot)) with a polymer concentration of 2 mg/mL.

Depicted in figure 6 is the CONTIN analysis of the mixture of block copolymers **4** and **6** in a 1 to 1 equimolar ratio. A change in aggregate size distribution, compared to the individual block copolymers (figure 5 A and B) could be observed. The smaller aggregates of the individual polymers around 20 nm disappeared and a broad distribution with an

average particle size of 73 nm (90°) appeared. In addition, the observed diameters were similar at all angles measured, indicating that the particles formed were spherical.

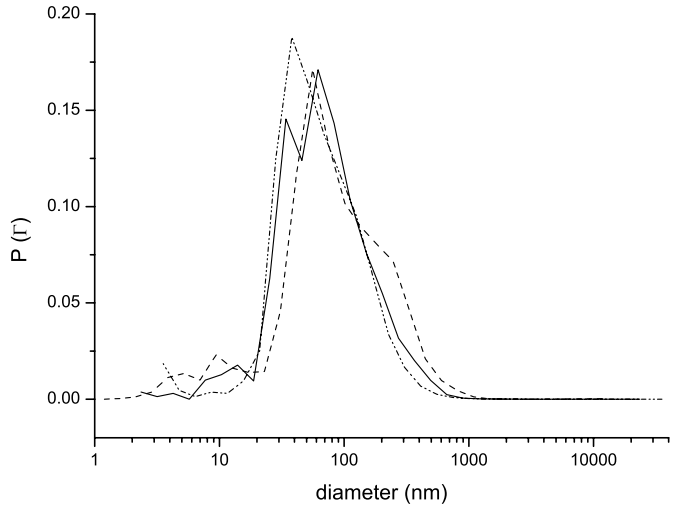

Figure 6. CONTIN analysis of the mixture of PEG-*b*-T10 and PEG-*b*-A10 depicted as a plot of the normalized weighted probability of Γ versus particle size, measured at different angles (60°(dash), 90°(solid) and 120°(dash dot dot)) with a total polymer concentration of 2 mg /mL.

Table 2. Size measurements and critical aggregation concentration values.

Copolymer	CAC[a] (mg/L)	Diameter[b] (nm)	
4, PEG-b-T10	8.0	19±10	150±145
6, PEG-b-A10	8.2	20±10	208±187
4 + 6, Mix A10+T10	11.6	73±54	-

a) aggregation concentration determined by fluorescence of DPH in water polymer mixtures. b) particle diameters obtained from Gaussian fit of CONTIN analysis at 90°.

4.3.4 UV-Vis experiments

Base pairing interactions between adenine and thymine often involve both π-π and hydrogen bonding interactions and from literature it is known that these interactions can cause distinct changes in the UV-vis spectrum of nucleobase functionalized materials[31, 10].

Therefore, spectrophotometric measurements were carried out on all three polymer solutions. Depicted in figure 7 are the temperature dependence absorption spectra of PEG-*b*-A10 (50 mg/L, [Adenine]=1.1*10^{-4} mol/L) and PEG-*b*-T10 (50 mg/L, [Thymine]=1.1*10^{-4} mol/L) solutions. In case of PEG-*b*-A10 the self association of the adenine units showed

negligible spectral changes upon increasing temperature, although at higher temperatures some scattering was observed. Scattering could be explained by precipitation of PEG-*b*-A10, which was indeed confirmed by turbidity measurements (figure 8 (right)). Both PEG-*b*-T10 and the polymer mixture did not become turbid upon increasing temperature.

The absorption maximum at 271 nm of PEG-*b*-T10 decreased upon increasing temperature. The exact nature of this observation is still unclear. However, upon mixing these polymer solutions in an equimolar ratio ([Thymine]=[Adenine]=5.4*10^{-5} mol/L), an increase and shift in absorption maxima from 264 to 266 nm could be observed.

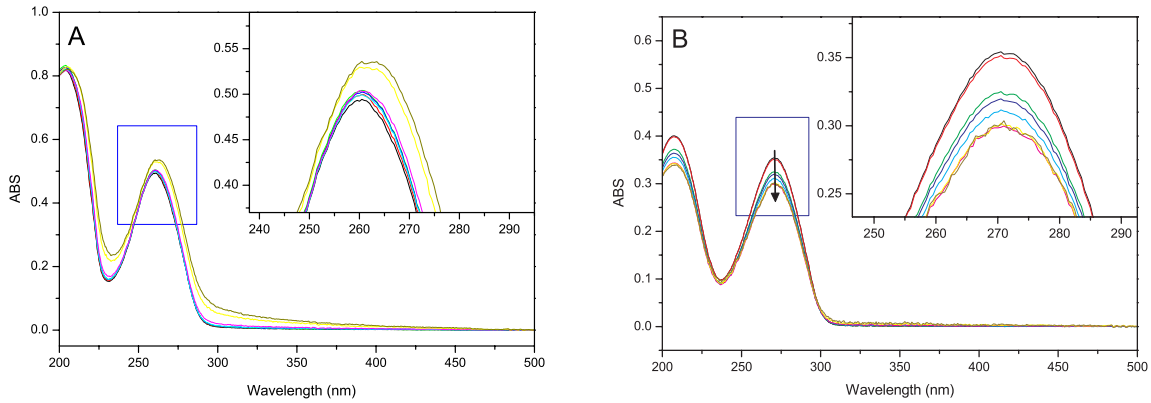

Figure 7. UV-vis absorption spectra of A) 50 mg/L (PEG-*b*-A10 and B) 50 mg/L PEG-*b*-T10 in the temperature range 25-80°C. The arrow indicates the change observed by increasing temperatures.

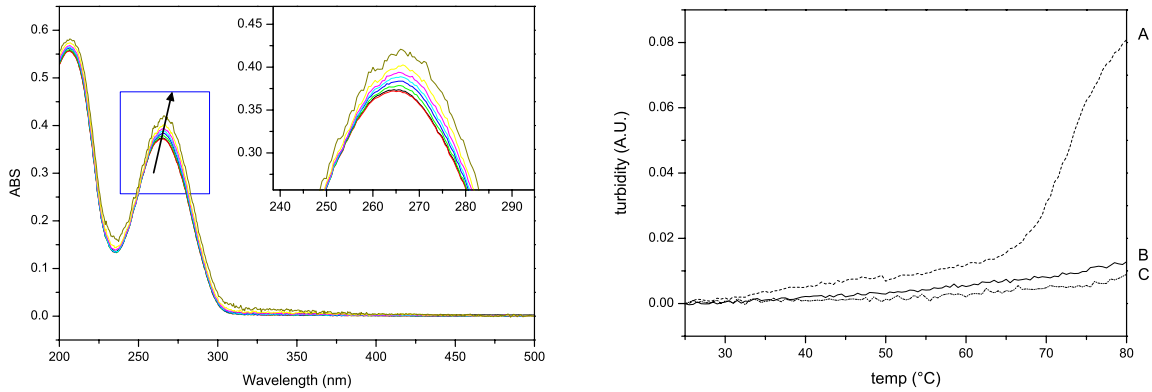

Figure 8. Left, UV-vis absorption spectra of equimolar mixture of PEG-*b*-A10 and PEG-*b*-T10 in the temperature range 25-80°C. The arrow indicates the change in absorption maxima (264 (25°C) to 266 nm (80°C)) by increasing temperatures. Right, turbidity observed at 450 nm of (**A**) PEG-*b*-A10 (50 mg/L) (**B**) PEG-*b*-T10 (50 mg/L) and (**C**) equimolar mixture of PEG-*b*-A10 and PEG-*b*-T10 at increasing temperature.

4.4 Discussion

The assembly of amphiphilic block copolymers is a well-documented phenomenon. In case of traditional synthetic block polymers, aggregation is mostly governed by the hydrophobic to hydrophilic ratio. With the block copolymers described in this chapter, a possible additional feature could play a role in the assembly process, namely the complementary interaction between adenine and thymine units. In order to be able to investigate whether this effect could be observed, four different block copolymers were successfully synthesized, varying in DP and type of nucleobase. Unfortunately, for the longer block copolymers **5** and **7,** the hydrophobic part of the block copolymer dominated, hence the solubility in water was very low, which hampered aggregate measurements. Consequently, polymer **5** and **7** were not subjected to further studies.

The shorter polymers **4** (PEG-*b*-T10) and **6** (PEG-*b*-A10) are much better soluble in water and were therefore used for further study with respect to their aggregation behavior. CAC, CryoSEM and DLS measurements revealed the presence of polymer aggregates in water. CONTIN analysis of the DLS data of the two separate block copolymers revealed a bimodal distribution. Since heat treatment did not change this distribution, the presence of kinetically entrapped structures can be excluded. Both polymers have one aggregate with a diameter around 20 nm, which is indicative of micelle formation. The second aggregate is much larger with a much broader size distribution. The most plausible explanation for the larger aggregates is the formation of large compound micelles (LCM's). Both block copolymers have furthermore similar CAC values. Therefore, the primary driving force for aggregation for the separate block copolymers must be the hydrophobic nature of the poly(methacrylate) back bone, since no obvious effect of the presence of nucleobase functionalities can be observed. Remarkably, mixing of the block copolymers **4** and **6** increases the molecular solubility of the polymers, since a higher CAC is observed. With DLS particles with an average size of 73 nm are found and CONTIN analysis shows this to be a broad but monomodal size distribution. These findings are indicative for complete mixing of the two polymers into one type of particle. Furthermore, if polymers **4** and **6** would not mix into a new type of particle, one would expect the CONTIN analysis of the mixture also to reveal a bimodal distribution. Therefore, these observations indicate that interaction occurs between complementary block copolymers via the nucleobase moieties.

UV-vis measurements support these findings, since upon heating the polymer mixture a change in the UV absorption band maxima, indicative for the breaking up of base-pair interactions, can be observed[31, 10]. In addition the separate block polymer solutions show a different behavior upon heating. Although PEG-*b*-A10 showed no temperature effects, the decrease in absorption maxima of PEG-*b*-T10 with increasing temperature was indicative of self association. The exact nature of this behavior remains elusive. Besides hydrogen bonding interactions also π-π stacking interactions can play a crucial role on the aggregation behavior of these block copolymers.

On the basis of these findings it can be stated that interactions between the nucleobase moieties thymine and adenine shift the hydrophobic to hydrophilic balance of the block copolymers in the direction of increased hydrophilicity. This can be explained by an improved shielding of the hydrophobic elements via the formation of small, water-soluble polymer assemblies. This results in a diminished hydrophobicity and therefore a shift of the CAC to higher values.

4.5 Conclusions

Four nucleobase-functionalized block copolymers were synthesized in a controlled fashion using ATRP from a PEG-based macro initiator of either thymine or adenine nucleobase functional methacrylates. The two shorter block copolymers formed aggregates in water and the CAC was determined using fluorescence spectroscopy. The separate block copolymers showed an identical aggregation behavior, which indicates that the assembly was mainly governed by the hydrophobic to hydrophilic balance. Upon mixing of the block copolymers, an increase in CAC compared to both separate block copolymers was observed, as well as a different particle size distribution. Additionally UV-vis experiments indicated base-paring interactions occurred upon mixing. These observations suggest that besides the amphiphilic character, an additional parameter plays a crucial role in the block copolymer assembly, namely the interaction between the complementary thymine and adenine moieties, which results in an increased solubility of the block copolymers by an improved shielding of the hydrophobic blocks.

4.6 Experimental

Materials
All reactions were performed under a nitrogen atmosphere, unless otherwise stated. Copper chloride (CuCl) was purified according to a literature procedure[32]. The synthesis of monomers 3-(thymin-1-yl)propyl methacrylate (**1**) and 3-(adenin-9-yl)propyl methacrylate (**2**) is described in chapter 2 and the synthesis of PEG initiator α-(2-bromo-2-methyl propionate)-ω-methylpoly(ethylene glycol) (**3)** is described in chapter 3[7]. Other chemicals were used as received unless otherwise stated.

Instrumentation
^{1}H NMR spectra were recorded on a Varian inova400 instrument at 400 MHz and ^{13}C NMR spectra were recorded on a Bruker DPX300 instrument at 75 MHz. Chemical shifts (δ) are given in ppm relative to the internal standard (Me_4Si or DMSO-d_6). IR spectra were recorded on an ATI Matson Genesis Series FTIR spectrometer with fitted ATR cell. SEC measurements were performed on a Shimadzu HPLC system equipped with PL gel 5 μm guard column and a PL gel 5 μm mixed D column and differential refractive index (38°C) and UV detection (280 nm). The system was operated with a flow of 0.8 mL·min^{-1} at 70°C using dimethylsulfoxide (DMSO, 0.02 M LiCl) as an eluent. Polyethylene glycol standards in the range of 1900 to 124700 Da were used to calibrate the SEC.

Turbidity measurements
Temperature turbidity correlation curves were measured on a Jasco J-810 spectropolarimeter, with a programmable Peltier temperature control cell. Samples were dissolved in milliQ water to a concentration of 50 mg/L and were placed in a 1 cm quartz cuvette. All samples were analyzed at a fixed wavelength of 450 nm at different temperatures.

Cryo SEM studies
CryoSEM was performed on JEOL JSM T300 apparatus operating at 30 kV. Typically, a sample of block copolymer in water (1.0 mg/mL) was rapidly freezed using nitrogen slush. The sample was freeze-fractured using a standard procedure and transferred into the apparatus. After 5 minutes of sublimation the sample was inserted into the sample chamber.

UV-Vis measurements
Spectra were recorded on a Varian Cary 50 Conc UV-Visible spectrophotometer equipped with a RM6 Lauda temperature controller. Samples were dissolved in milliQ water to a concentration of 50 mg/L and were placed in a 1 cm quartz cuvette. Spectra were measured at different temperatures.

Light scattering measurements
Dynamic light scattering measurements were performed using an ALV-5000 Multiple Tau Digital Correlator, ALV-125 Goniometer and an ALV-800 Transputerboard for CONTIN analysis. A Lexel - 85 Argon Ion Laser operated at a wavelength of 514.5 nm and an output power of 200 mW was used as light source. The hydrodynamic radius of the aggregates was calculated using the Stokes- Einstein equation, $r=k_BT/6\pi\eta D$, where k_B is the Boltzmann constant, T is the absolute temperature, η is the solvent viscosity and D is the diffusion constant. Samples were measured at three different angles (60, 90 and 120°) with a concentration of 1 mg/mL in milliQ water. Average particle sizes were obtained from a Gaussian fit of CONTIN data.

Determination of the critical aggregation concentration
Fluorimetric determination of the critical aggregation concentration was performed using a modified procedure of Chattopadhyay[33]. Fluorescence measurements were performed with a Perkin Elmer luminescence spectrometer LS 50 B using a 1 cm path-length quartz cuvette. The excitation wavelength was 358 nm and the emission wavelength was 430 nm. 1 μL of 5 mM 1,6-diphenyl-1,3,5-hexatriene (DPH) in THF was added to 1.5 mL of various aqueous polymer solutions in the concentration range from 0 to 0.10 mg/mL. For the polymer mixtures, the same total polymer concentrations were used. Tubes were vortexed and incubated for at least 30 min at room temperature in the dark. A background sample containing only DPH and water was prepared and the measured intensity was subtracted.

Polymerization of thymine monomer 1 using PEG initiator 3; PEG-*b*-T10 (4) general procedure.

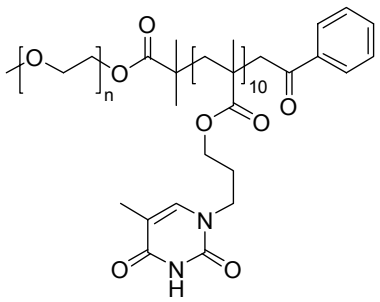

3-(thymin-1-yl)propyl methacrylate (**1**) (475.0 mg, 1.88 mmol), CuCl (13.7 mg, 0.138 mmol) and 2,2'-bipyridyl (bpy) (43.3 mg, 0.277 mmol) were placed in a Schlenk tube, followed by three vacuum – argon refill cycles. DMSO-d_6 (2.17 mL) was added and the mixture was argon purged for 10 minutes, followed by heating to 30°C. The polymerization was started by addition of 1.88 mL of an argon purged stock solution of PEG-based macro-initiator **3** (297.7 mg, 0.138 mmol) in DMSO-d_6 (2.02 mL). Samples were taken periodically in order to analyze the monomer conversion with ^{1}H-NMR spectroscopy. At 76% conversion 1-phenyl-1-(trimethylsiloxy)-ethylene (295.7 mg, 1.537 mmol) was added to quench the ATRP and end cap the polymer. The reaction mixture was poured into an aqueous EDTA solution (0.055 M), after which the crude product was extracted with dichloromethane (DCM) (3 times 50 mL). After addition of brine to the aqueous phase another three extractions with DCM were performed. The combined organic phases were dried over anhydrous $MgSO_4$, filtered and concentrated under reduced pressure. The crude product was further purified using sephadex column chromatography (LH-20, MeOH/DCM; 1:1) resulting in 511 mg of product as a pure white solid after freeze drying. ^{1}H NMR (DMSO-d_6): δ 11.16 (br s, pyrimidine-NH), 7.93 (br m, -C$_6$H$_5$), 7.63 (br s, -C$_6$H$_5$), 7.44 (br s, pyrimidine-H6), 3.92 (br s, O-CH_2-CH$_2$), 3.69 (br s, CH$_2$-CH_2-N), 3.50 (br s, {CH_2-CH_2-O}), 3.24 (s, O-CH_3 endgroup), 1.88 (br s, CH$_2$-CH_2-CH$_2$-N), 1.80-1.30 (br m, {CH_2-C(CH$_3$)}, pyrimidine-CH$_3$), 1.10-0.65 (br m, {CH$_2$-C(CH_3)}). FTIR (solid): ν 3502, 3183, 2886, 1675, 1468, 1342, 1276, 1221, 1143, 1105. SEC (DMSO): M_n = 5.8 kg/mol, M_w/M_n = 1.20, M_n (^{1}H NMR) = 5.8 kg/mol, DP (^{1}H NMR) =14.3.

Polymerization of thymine monomer 1 using PEG initiator 3; PEG-*b*-T20 (5).

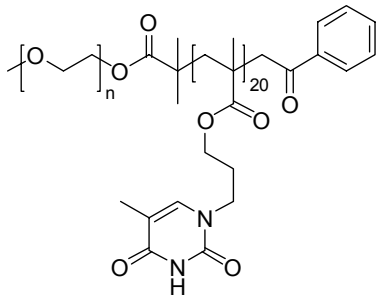

Monomer **1** was polymerized at 30°C according to the general procedure using 3-(thymin-1-yl)propyl methacrylate (**1**) (491.6 mg, 1.95 mmol), CuCl (6.7 mg, 0.068 mmol) and bpy (21.3 mg, 0.136 mmol) in 4.03 mL DMSO-d_6. The polymerization was started by addition of 0.75 mL of a stock solution containing **3** (190 mg, 0.088 mmol) in 1.0 mL DMSO-d_6. At 69% conversion 1-phenyl-1-(trimethylsiloxy)-ethylene (268 mg 1.39 mmol) was added. Yield of **5** after work up was 530 mg. ^{1}H NMR (DMSO-d_6): δ 11.16 (br s, pyrimidine-NH), 8.00-7.55 (m, CH$_2$-C(=O)-C$_6$H$_5$), 7.44 (br s, pyrimidine-H6), 3.92 (br s, O-CH_2-CH$_2$), 3.69 (br s, CH$_2$-CH_2-N), 3.51 (br s, {CH_2-CH_2-O}), 3.24 (s, O-CH_3 endgroup), 1.88 (br s, CH$_2$-CH_2-CH$_2$-N), 1.80-1.30 (br m {CH_2-C(CH$_3$)}, pyrimidine-CH_3) 1.10-0.65 (br m, {CH$_2$-C(CH_3)}). FTIR (solid): ν 3170, 2969, 2898, 1678, 1467, 1450, 1407, 1358, 1222, 1144, 1105. SEC (DMSO): M_n = 8.8 kg/mol, M_w/M_n = 1.20, M_n (^{1}H NMR) = 7.5 kg/mol, DP (^{1}H NMR) = 21.3.

Polymerization of adenine monomer 2 using PEG initiator 3; PEG-*b*-A10 (6).

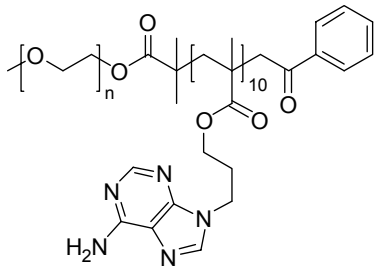

Monomer **2** was polymerized at 30°C according to the general procedure using 3-(adenin-9-yl)propyl methacrylate (**2**) (340.0 mg, 1.30 mmol), CuCl (9.4 mg, 0.095 mmol) and bpy (29.1 mg, 0.186 mmol) in 3.02 mL DMSO-d_6. The polymerization was started by addition of 1.0 mL of a stock solution containing **3** (390 mg, 0.181 mmol) in 2.0 mL DMSO-d_6. At 66% conversion 1-phenyl-1-(trimethylsiloxy)-ethylene (268 mg 1.39 mmol) was added. Extraction with DCM gave an emulsion which was centrifuged to facilitate separation. The crude product was further purified by chromatography using a Sephadex LH20 column (MeOH/DCM 1/1). Yield of **6** after work up was 330 mg of pure white polymer. ^{1}H NMR (DMSO-d_6): δ 8.15 (br s, purine-H), 8.10 (br s, purine-H), 7.30 (br purine-NH$_2$), 4.21 (br s, O-CH_2-CH$_2$), 3.90 (br s, CH_2-CH$_2$-N$_{purine}$), 3.50 (br s, {O-CH_2-CH_2}), 3.23 (s, -O-CH_3 PEG-endgroup), 2.12 (br s, O-CH$_2$-CH_2-CH$_2$-N$_{purine}$), 1.89-1.55 (br s, {CH_2-C(CH$_3$)}), 1.00-0.70 (br m, {CH$_2$-C(CH_3)}). FTIR (solid): ν 3320, 3170, 2967, 2885, 1722, 1640, 1597, 1468, 1450, 1414. SEC (DMSO, RID): M_n = 5.5 kg/mol, M_w/M_n = 1.22, M_n (^{1}H NMR) = 5.1 kg/mol, DP (^{1}H NMR) = 11.2.

Polymerization of adenine monomer 2 using PEG initiator 3; PEG-*b*-A30 (7).

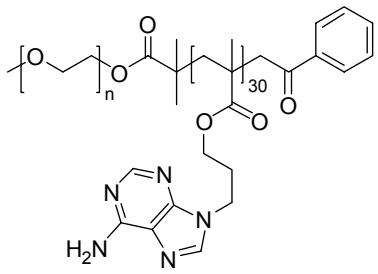

Monomer **2** was polymerized at 35°C according to the general procedure using 3-(adenin-9-yl)propyl methacrylate (**2**) (530.0 mg, 2.03 mmol), CuCl (13.1 mg, 0.132 mmol) and bpy (43.8 mg, 0.280 mmol) in 5.20 mL DMSO-d_6. The polymerization was started by addition of 0.7 mL of a stock solution containing **3** (390 mg, 0.181 mmol) in 2.0 mL DMSO-d_6. At 75% conversion 1-phenyl-1-(trimethylsiloxy)-ethylene (268 mg 1.39 mmol) was added. Extraction with DCM gave an emulsion which was centrifuged to facilitate separation. Yield of **7** after work up was 432 mg. ^{1}H-NMR (DMSO-d_6): δ 8.15 (br s, purine-*H*), 8.10 (br s, purine-*H*), 7.30 (br s, purine-NH_2), 4.21 (br s O-C$\underline{H_2}$-CH$_2$), 3.90 (br s, C$\underline{H_2}$-CH$_2$-N$_{purine}$), 3.50 (br s, {O-C$\underline{H_2}$-C$\underline{H_2}$}), 3.23 (s, PEG-O-C$\underline{H_3}$ endgroup), 2.12 (br s, O-CH$_2$-C$\underline{H_2}$-CH$_2$-N$_{purine}$), 1.89-1.55 (br s, {C$\underline{H_2}$-C(CH$_3$)}), 1.00-0.70 (br m, {CH$_2$-C(C$\underline{H_3}$)}). FTIR (Solid): ν 3327, 3179, 2893, 1722, 1640, 1596, 1475, 1449, 1415. SEC (DMSO, RID): M_n = 6.8 kg/mol, PDI = 1.21, M_n (^{1}H NMR) = 10.1 kg/mol, DP=30.3.

4.7 References

1. C. A. Mirkin. *Inorg. Chem.* **2000**, *39*, 2258-2272.
2. S. J. Park, A. A. Lazarides, C. A. Mirkin and R. L. Letsinger. *Angew. Chem., Int. Edit.* **2001**, *40*, 2909-2912.
3. H. Yan, X. P. Zhang, Z. Y. Shen and N. C. Seeman. *Nature* **2002**, *415*, 62-65.
4. N. C. Seeman. *Biochemistry* **2003**, *42*, 7259-7269.
5. Y. Inaki. *Prog. Polym. Sci.* **1992**, *17*, 515-570.
6. A. Khan, D. M. Haddleton, M. J. Hannon, D. Kukulj and A. Marsh. *Macromolecules* **1999**, *32*, 6560-6564.
7. H. J. Spijker, A. T. J. Dirks and J. C. M. van Hest. *Polymer* **2005**, *46*, 8528-8535.
8. A. K. Boal, F. Ilhan, J. E. DeRouchey, T. Thurn-Albrecht, T. P. Russell and V. M. Rotello. *Nature* **2000**, *404*, 746-748.
9. J. Xu, E. A. Fogleman and S. L. Craig. *Macromolecules* **2004**, *37*, 1863-1870.
10. J.-F. Lutz, A. F. Thuenemann and K. Rurack. *Macromolecules* **2005**, *38*, 8124-8126.
11. S. J. Rowan, P. Suwanmala and S. Sivakova. *J. Polym. Sci., Part A: Polym. Chem.* **2003**, *41*, 3589-3596.
12. S. Sivakova, D. A. Bohnsack, M. E. Mackay, P. Suwanmala and S. J. Rowan. *J. Am. Chem. Soc.* **2005**, *127*, 18202-18211.
13. S. Sivakova and S. J. Rowan. *Chem. Soc. Rev.* **2005**, *34*, 9-21.
14. M. Kato, M. Kamigaito, M. Sawamoto and T. Higashimura. *Macromolecules* **1995**, *28*, 1721-1723.
15. J. S. Wang and K. Matyjaszewski. *J. Am. Chem. Soc.* **1995**, *117*, 5614-5615.
16. A. Marsh, A. Khan, D. M. Haddleton and M. J. Hannon. *Macromolecules* **1999**, *32*, 8725-8731.
17. M. Kamigaito, T. Ando and M. Sawamoto. *Chem. Rev.* **2001**, *101*, 3689-3745.
18. K. Matyjaszewski and J. H. Xia. *Chem. Rev.* **2001**, *101*, 2921-2990.
19. T. Glauser, M. Ranger, B. Kalra, W. Gao, J. Hedrick and R. A. Gross. *Polym. Prepr. (Am. Chem. Soc., Div. Polym. Chem.)* **2003**, *44*, 624-625.
20. A. Marsh, A. Khan, M. Garcia and D. M. Haddleton. *Chem. Commun.* **2000**, 2083-2084.
21. H. S. Bazzi and H. F. Sleiman. *Macromolecules* **2002**, *35*, 9617-9620.
22. J. A. Opsteen, J. Cornelissen and J. C. M. van Hest. *Pure Appl. Chem.* **2004**, *76*, 1309-1319.
23. F. Ilhan, M. Gray and V. M. Rotello. *Macromolecules* **2001**, *34*, 2597-2601.
24. K. Das, H. Nakade, J. Penelle and V. M. Rotello. *Macromolecules* **2004**, *37*, 310-314.
25. H. Xu, R. Hong, T. X. Lu, O. Uzun and V. M. Rotello. *J. Am. Chem. Soc.* **2006**, *128*, 3162-3163.
26. L. Ayres, K. Koch, P. Adams and J. C. M. van Hest. *Macromolecules* **2005**, *38*, 1699-1704.
27. J. M. Smeenk, M. B. J. Otten, J. Thies, D. A. Tirrell, H. G. Stunnenberg and J. C. M. v. Hest. *Angew. Chem., Int. Ed.* **2005**, *44*, 1968-1971.
28. G. W. M. Vandermeulen, C. Tziatzios, R. Duncan and H. A. Klok. *Macromolecules* **2005**, *38*, 761-769.
29. A. M. Funhoff, S. Monge, R. Teeuwen, G. A. Koning, N. M. E. Schuurmans-Nieuwenbroek, D. J. A. Crommelin, D. M. Haddleton, W. E. Hennink and C. F. van Nostrum. *J. Controlled Release* **2005**, *102*, 711-724.
30. K. Tokuchi, T. Ando, M. Kamigaito and M. Sawamoto. *J. Polym. Sci., Part A: Polym. Chem.* **2000**, *38*, 4735-4748.
31. W. Saenger. *Principles of Nucleic Acid Structure*, ed.; Springer-Verlag: New York, 1984; Vol.
32. R. N. Keller and H. D. Wycoff. *Inorganic Syntheses* **1946**, *2*, 1-4.
33. A. Chattopadhyay and E. London. *Anal. Biochem.* **1984**, *139*, 408-412.

Chapter 5

Nucleobase functionalized triblock copolymers

5 Nucleobase functionalized triblock copolymers

5.1 General introduction

In Nature, many complex molecular structures obtain their threedimensional functional arrangement via secondary interactions such as hydrogen bonding, dipole-dipole interactions, hydrophobic and van der Waals interactions. Inspired by these natural phenomena, Pedersen[1], Lehn[2] and Cram[3] initiated the discipline known as supramolecular chemistry, which explores these organizational principles for the construction of self assembled manmade materials. Many different molecular architectures have since then been prepared based on non-covalent interactions.

These reversible secondary interactions have also been applied in polymer chemistry. Lehn and co-workers were the first to build up a supramolecular main-chain polymer, in which the monomers are linked by triple hydrogen bonding[4], as shown in figure 1. By using non-covalent interactions, many different macromolecular structures can nowadays be made, such as reversible polymer networks[5], rodlike nanostructures[6] and helices[7].

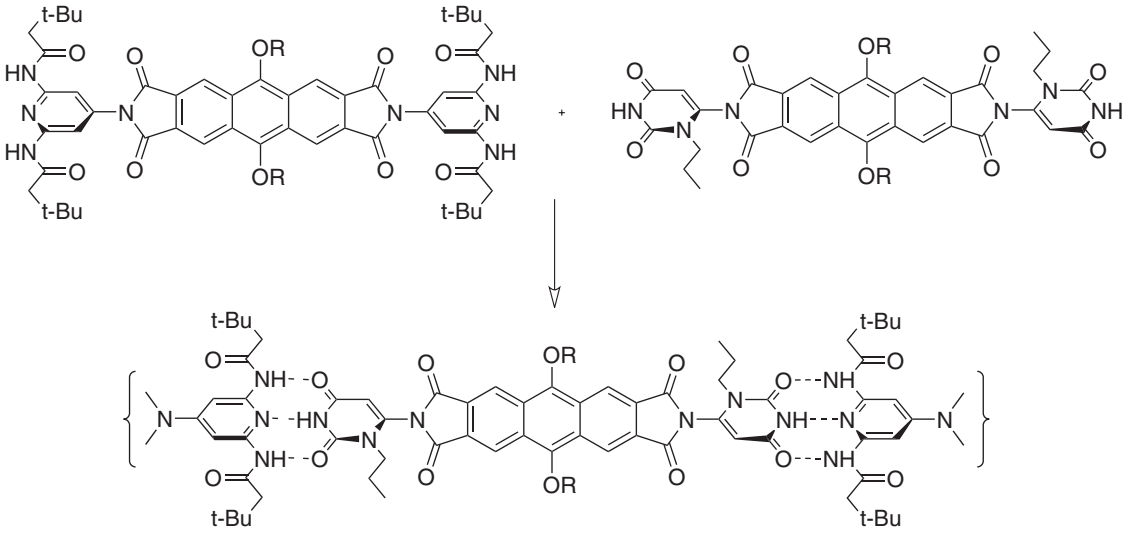

Figure 1. A liquid crystalline supramolecular polymer based on triple hydrogen bonding from rigid monomers[4].

Since supramolecular polymers are connected via completely reversible bonds, switching between single monomeric species and polymers is conveniently accomplished by varying temperature or polarity of the solvent (figure 2). The average degree of polymerization (DP) is furthermore dependent on the association constant (K_a) of the end-groups and the concentration of the solution.

Therefore, to obtain high molecular weight supramolecular polymers a high association constant between the repeating units is a prerequisite[8]. In analogy with covalent condensation polymers, the chain length of the polymer can also be affected by adding monofunctional chain stopper. This implies that monofunctional impurities also will have a strong influence on the degree of polymerization.

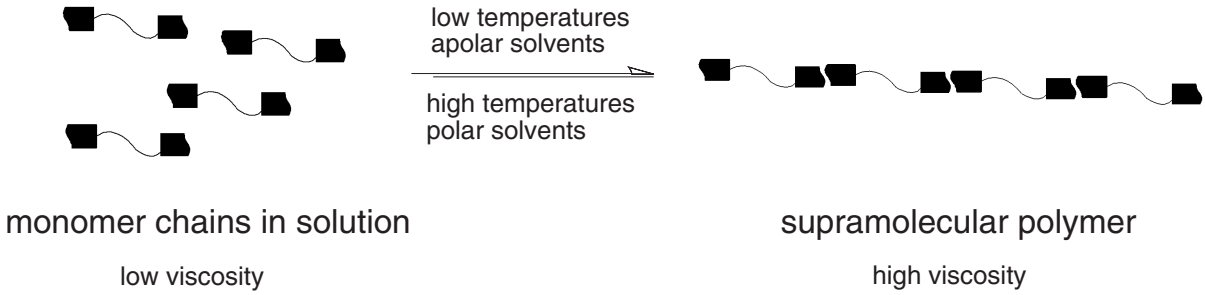

Figure 2. Supra-polymerization of bifunctional associating monomers.

Although hydrogen bonding between two neutral organic molecules is not among the strongest non-covalent interactions, it holds a prominent place in supramolecular chemistry because of its versatility and directionality. The strong dependency of the degree of (non-covalent) polymerization on the association constant makes it is necessary to either have multiple hydrogen bonds or enforce hydrogen bonding by e.g. liquid crystallinity or phase separation.

Meijer and co-workers have developed the ureidopyrimidinone unit, a synthetically very accessible quadruple hydrogen bonding moiety with a very high association constant, with which a variety of supramolecular polymer systems with high molecular weight can be synthesized[9]. In addition to modification of monomeric units with associating end-groups, also telechelic polymers can be modified. Since the aggregation of end-groups is sufficiently strong and directional, even low molecular weight telechelic building blocks (Mw ‹ 10^3 g/mol) result in materials in which chain entanglements give rise to polymer-like properties[10, 11] (figure 3).

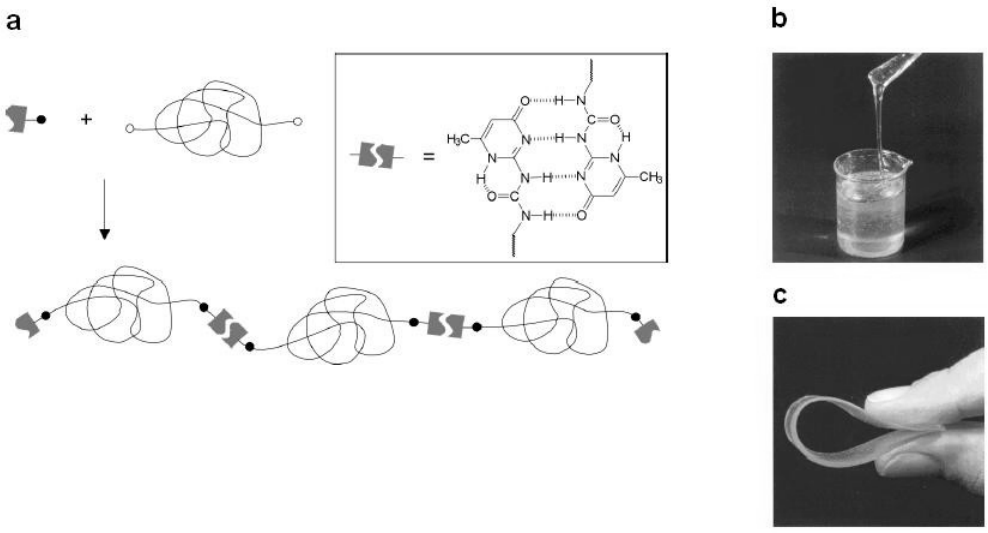

Figure 3. a) Schematic drawing of functionalization of telechelic polymers with quadruple hydrogen bonding ureidopyrimidinone units; b) poly(ethylene/butylene) with OH end groups; c) poly(ethylene/butylene)functionalized with hydrogen-bonded units[12].

Drawback of some supramolecular systems is that the hydrogen bonding motifs are self-complementary. Therefore, researchers have looked for several ways to create complementary hydrogen bonding units that would expand the scope of supramolecular polymers[13]. Since nature has already developed a complementary hydrogen bonding system, the use of Watson Crick base pairing in supramolecular polymer chemistry can be regarded as a logical choice. This approach has been studied by a number of researchers. Protected single nucleobase monomers attached to telechelic polymers were prepared and appeared to induce supramolecular properties[14, 15], which is remarkable, since these hydrogen bonding interactions are relatively weak.

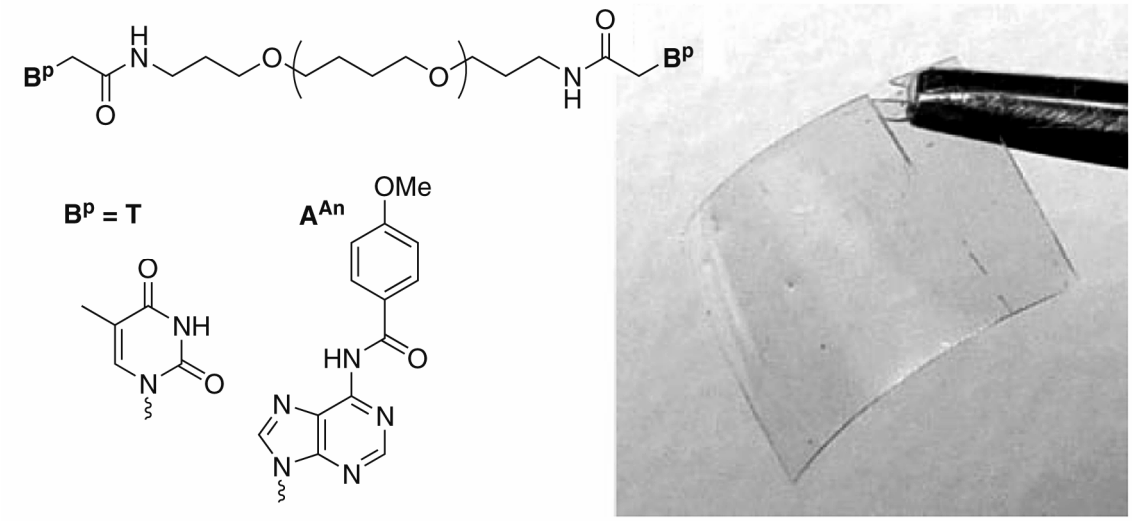

Figure 4. (left) Supramolecular nucleobase functional telechelic macromonomer based on poly THF. (right) A film prepared from only adenine modified macromonomer.

In order to tune material properties and thus gain more control over the supramolecular polymer materials, it would be advantageous to be able to control the strength of the hydrogen bonding moieties as was shown by Craig et al[16-18]. However, the use of natural DNA limits the scale at which supramolecular materials can be prepared since often DNA sequences are prepared in μg quantities, using solid phase synthesis techniques. Since previous chapters have already described the successful synthesis and polymerization of nucleobase functional monomers using Atom Transfer Radical Polymerization (ATRP), we envisioned that a facile, controlled synthesis of small oligomers with nucleobase functionality using ATRP would allow convenient access to multiple and hence stronger complementary nucleobase interactions resulting in improved supramolecular materials.

In order to construct supramolecular polymers it is necessary to prepare ABA-type triblock copolymers in which the A block contains nucleobase functionality. By mixing two different ABA-type block copolymers with complementary nucleobase functionality assembly into supramolecular materials could be accomplished.

There are several methods envisaged to build up ABA triblock copolymers, which all rely on the application of a controlled polymerization technique, such as ATRP. The first method employs a straightforward approach by polymerizing the monomers in sequential order. In this way, ABA triblock copolymers can be built up, as illustrated in figure 5.

Figure 5. Sequential build up of ABA triblock copolymer by polymerization of monomer A, followed by macro initiation from polymer A with monomer B, and finally initiation from polymer AB to polymerize monomer A.

A possible drawback of this straightforward method is the number of initiation steps involved. Although the termination reaction can be strongly suppressed in the ATRP process, it cannot be excluded that there will be polymer chains present that will not re-initiate the polymerization of a second or third block. Consequently, the final product will be a mixture of A, AB and ABA block copolymers, which is laborious, or even impossible, to separate.

An improvement for this method would be to limit the amount of initiation steps. Because the two flanking blocks have the same composition, a more simple approach can in this case be followed using a bifunctional polymeric initiator B. Initiation from this polymer with the second monomer results in the desired ABA triblock copolymer (figure 6). This approach will be described in section 5.2.

Figure 6. Synthesis of an ABA triblock copolymer by polymerization of monomer A from telechelic polymer B.

Although the number of initiation steps in the macroinitation method is reduced by using a bifunctional initiator, defects in the final tri block copolymer cannot be excluded. An alternative, modular approach is to synthesize the polymeric blocks separately and subsequently couple them together. In order for this to be a viable approach, the blocks have to be quantitatively functionalized with moieties that can react with each other with high efficiency. ATRP opens up the possibility to use functional initiators, and hence create polymers with 100% functional end groups. In addition, it was shown in literature[19-21] that modification of the halogen end group by substitution can be performed.

Equipped with these methods for introducing end group functionality, it should be possible to polymerize monomers A and B separately and couple the polymeric blocks afterwards as shown schematically in figure 7. This modular approach will be explored as described in section 5.3.

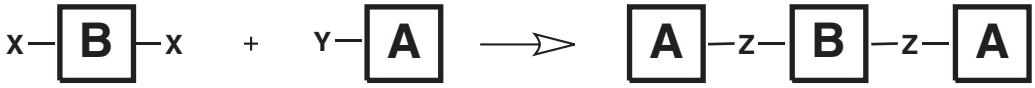

Figure 7. Modular method to synthesize ABA triblock copolymers, by coupling of telechelic polymer B containing reactive end group X with polymer A containing end group Y.

Inherent disadvantages for all of these methods is that 100% endgroup functionality is required for successful implementation of these methods. It must be noted that the coupling method will also result in a polymer mixture upon incomplete coupling. However, the resulting polymer mixture would in that case contain only the polymers that were used as building blocks, which facilitates identification of incomplete coupling and could lead to a more effcieint purification strategy.

5.2 Macroinitiation build-up method

5.2.1 Triblock copolymer synthesis by macro initiation from telechelic PMMA

For the ATRP-mediated synthesis of triblock copolymers via the macroinitiation method, an α-bromo ester functional telechelic polymer had to be employed. Since the nucleobase-functional monomers that have been prepared in chapter 2 are methacrylate type monomers, an isobutyric bromide initiating moiety was furthermore desired. In order to fulfill these macroinitiation requirements, it was chosen to prepare telechelic poly methyl methacrylate (pMMA) by ATRP of methyl methacrylate (MMA) using a low molecular weight bifunctional initiator. This initiator **1** was prepared by esterification of 1,4-benzenedimethanol with 2-bromoisobutyric bromide under basic conditions as depicted in scheme 1. Haddleton and co-workers have shown that the synthetically very accessible alkylpyridylmethanimine type ligands can be successfully used for the controlled polymerization of MMA[22].

For that reason the Schiff base *N*-(n-propyl)-2-pyridylmethanimine **2** was prepared via condensation of propyl amine with pyridine-2-carboxaldehyde (scheme 1), and used as ATRP ligand in the polymerization of MMA.

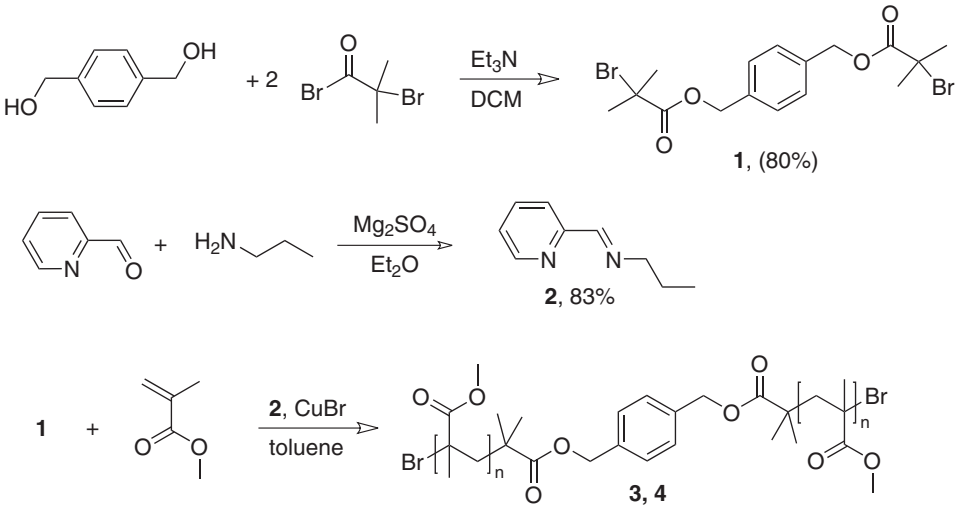

scheme 1. Synthesis of bifunctional initiator **1**, ligand **2** and polymerization of MMA.

Polymerization of MMA could be monitored using GC with toluene as the internal standard. Depicted in figure 8 is the kinetic plot obtained from the polymerization using bifunctional initiator **1**. Good first order kinetics (figure 8) and a low PDI (table 1) indicated control over the polymerization and the presence of a high percentage of active chain ends.

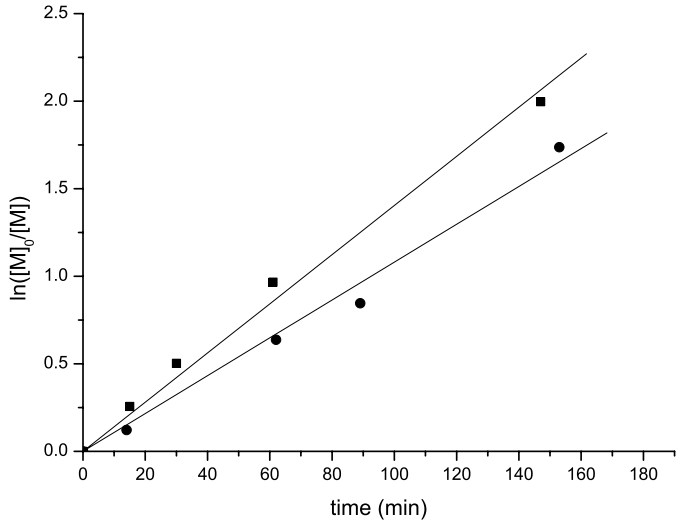

Figure 8. kinetic plot of MMA polymerization using bifunctional initiator **1** and CuBr/**2** complex as catalyst (■ polymer **3**, ♦ polymer **4**).

Table 1. ATRP of MMA using bifunctional initiator **1**

polymer	ratio[a] M/I/Cu/L	Solvent	Temp (°C)	$M_{n,\ NMR}$ (kg/mol)	M_n[b] (kg/mol)	M_w/M_n[b]
3	36/1/1/1	toluene	80	7.2	6.9	1.15
4	28/1/1/1	toluene	80	7.1	5.8	1.19

a) molar ratio per initiating moiety, M = MMA, I=**1**, Cu=Copper(I)bromide, L= **2**. b) determined using SEC with THF as eluent and RI detection.

Macroinitiation of PMMA with nucleobase monomers **5** (adenine) and **6** (thymine) using DMSO-d_6 as solvent, CuBr/bpy as catalyst at 35 and 30°C respectively, proceeded with relative good first order kinetics, indicating control over the polymerization, as can be seen in figure 9. It must be noted that the rate of polymerization was relatively fast.

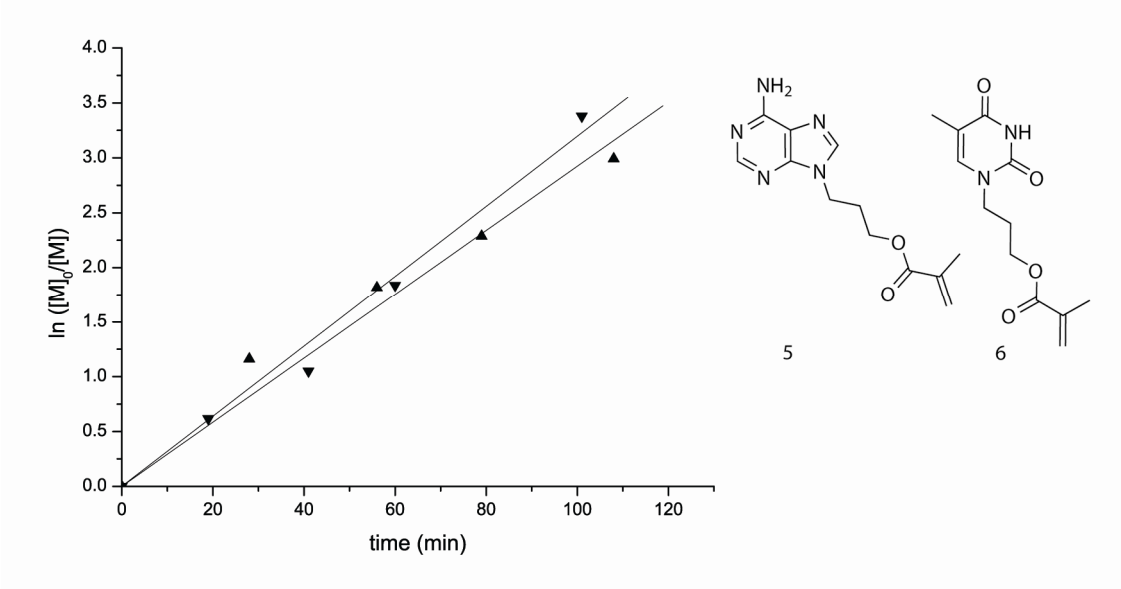

Figure 9. kinetic plot of the macroinitiation of PMMA with adenine monomer at 35°C ▲ (**5** = 0.292 M, **3** = 0.022 M, CuBr = 0.046 M, bpy = 0.089 M), and thymine monomer at 30°C ▼ (**6** = 0.341 M, **4** = 0.020 M, CuBr = 0.043 M, bpy = 0.088 M).

Unfortunately, GPC analysis of the triblock copolymer products revealed for both the adenine and thymine functionalized triblock copolymers a bimodal distribution, as depicted in figure 10.

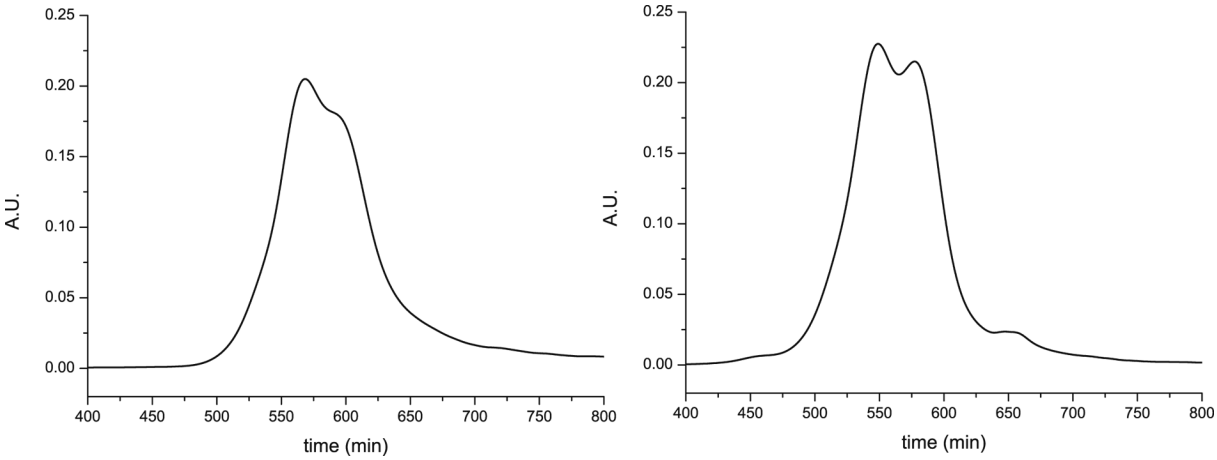

Figure 10. SEC spectra after PMMA macro initiation. Left, macroinitiation of PMMA **3** with adenine monomer **5**. Right, macroinitiation of PMMA **4** with thymine monomer **6.**

5.2.2 Block copolymer synthesis by macro initiation from telechelic PEG

To circumvent possible termination occurring during the polymerization of the center block and to extend the exploration of ABA type block copolymer synthesis via the macro initiation technique, poly ethylene glycol (PEG) was chemically modified and investigated for usage as a macroinitiator.

PEG-based initiator **7** was successfully synthesized by treatment of a commercially available PEG (2 kDa) with 2-bromoisobutyryl bromide in the presence of Et_3N (scheme 2). ATRP of both adenine and thymine monomers **5** and **6** using **7** with CuCl/bpy as catalyst was performed.

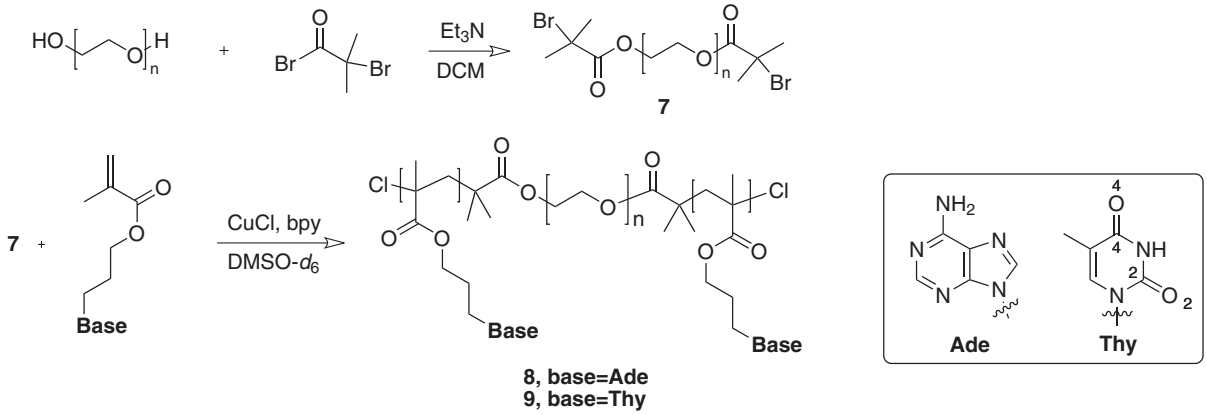

scheme 2. synthesis of telechelic PEG initiator **7** and polymerization of both adenine and thymine monomers to triblock copolymer **8** and **9**, respectively.

As can be seen in figure 11, the polymerization of both the thymine and adenine monomers proceeded with good first order kinetics, indicating control over the

polymerization. These findings were supported by the low polydispersities found by SEC analysis (table 2). From the ^{1}H NMR spectra it was observed that initiation occurred at both α-bromoesters, since the methyl protons from the initiator (δ 3.33 ppm) shifted upfield upon polymerization.

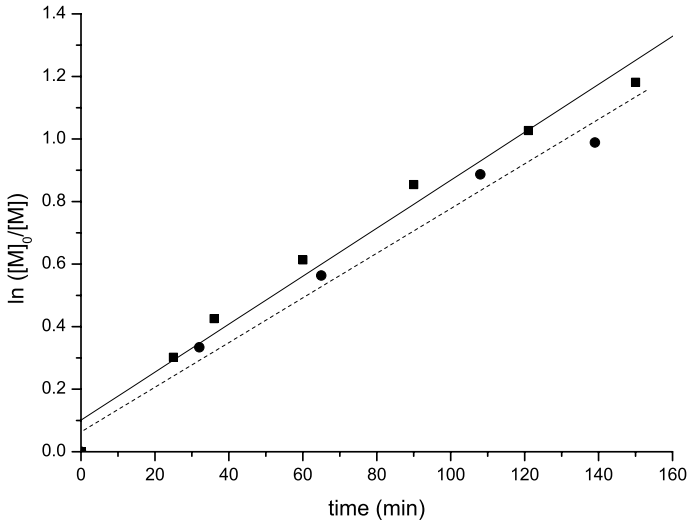

Figure 11. kinetic plot of polymerization of adenine monomer (●, 35°C) and thymine monomer (■, 30°C) using telechelic PEG initiator **7**.

Table 2. ATRP of adenine and thymine monomers using bifunctional PEG initiator

Polymer	ratio[a] M/I/Cu/L	Temp (°C)	M_n, theo (kg/mol)	DP[b]	M_n[c] (kg/mol)	M_n[d] (kg/mol)	M_w/M_n[d]
8, A10-PEG-A10	15/1/1/2	35	7.3	19.2	8.3	7.2	1.21
9, T10-PEG-T10	15/1/1/2	30	7.4	22.8	7.1	7.5	1.19

a) M = monomer (**5** in case of **8**, **6** in case of **9**), I=Initiator, Cu=Copper(I)chloride, L= bpy. b) DP is the sum of the DP of both nucleobase blocks. c) M_n is calculated using the integral ratio in the ^{1}H NMR spectra between the PEG block and the nucleobase block. d) Determined using SEC with DMSO as eluent and RI detection.

5.2.3 Discussion

To obtain ABA type triblock copolymers two macroinitiation systems were investigated. The first started with a bifunctional initiator from which the center polymer block was prepared. The bifunctional polymer thus obtained was used as a macroinitiator for a second polymerization of the outer polymer block with a different second monomer.

From the kinetic plots of the polymerization of MMA and the successive polymerization of the nucleobase monomers, good first order kinetics were observed.

However, SEC analysis of the final ABA-type triblock copolymer revealed a bimodal weight distribution. A first explanation could be that a significant amount of termination occurred during polymerization of MMA. This explanation is unlikely, since SEC analysis revealed a narrow molecular weight distribution of the telechelic PMMA, indicating a controlled living polymerization had occurred. A more likely explanation could be that the macroinitiation step has a very low initiator-efficiency under the applied conditions. Combined with the observed relative fast polymerization rate of the nucleobase monomers in DMSO-d_6 the result would be that only a few PMMA chain ends re-initiate resulting in a mixture of products.

The second method used a commercially available telechelic polymer of which both endgroups were chemically modified into initator groups, from which the outer block was polymerized in a single polymerization step. The triblock copolymers obtained after polymerization from bifunctional PEG initiator **7** revealed no bimodal size distribution by SEC analysis, additionally ^{1}H NMR spectra of both the adenine and thymine block copolymers indicated both PEG chain ends initiated upon polymerization. These combined results strongly indicate that the main product is the desired triblock copolymer.

A possible explanation for the difference in initiator efficiency of both the macroinitiator polymers could be that the solubility in DMSO-d_6 is much higher for PEG than for PMMA. As a result, the α-bromo esters are more available in case of PEG and consequently will be more efficient in initiating the polymerization.

Although chemically modifying a telechelic PEG to prepare nucleobase functionalized ABA type triblock copolymers was the most successful, it limits the scope of available center polymer blocks. On the other hand a further fine-tuning of the macroinitiation step by changing for example the solvent or lowering the polymerization rate could enhance the overall initiator efficiency toward triblock copolymers.

5.3 Block copolymer synthesis using modular approach

In order for the modular approach to be successful, a very efficient coupling chemistry has to be employed for the connection of the individual polymer building blocks. From literature, it is known that during condensation polymerization yielding polyurethanes[23] high molecular weight alcohols and isocyanates can be coupled. The

excellent reactivity of the isocyanate group towards nucleophiles makes this functionality therefore a good candidate for our modular block copolymer synthesis approach.

Matyjaszewski et al. have demonstrated it to be possible to convert bromide end-groups of mono-functional poly methyl acrylate (pMA) into amine end-groups, via a substitution with sodium azide and subsequent reduction of the azide via a Staudinger reaction[19, 20]. Furthermore, from literature it is known that isocyanates can easily be prepared out of amines[24]. Based on these facts it was decided to investigate the modular approach with a B-block consisting of isocyanate functional telechelic pMA and A-blocks that consisted of amine end functionalized oligonucleobases. The envisaged synthesis of telechelic PMA containing isocyanate end-groups is retrosynthetically depicted in scheme 3.

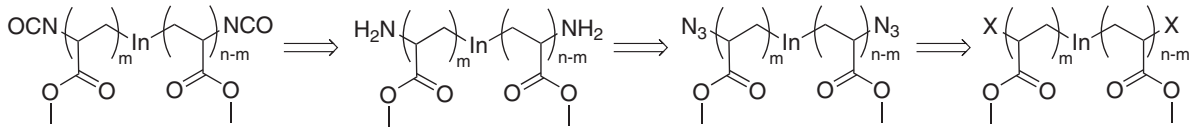

scheme 3. Retrosynthetic scheme outlining the preparation of isocyanate functionalized telechelic pMA starting from halide end-functionalized pMA.

5.3.1 Synthesis of telechelic polymethyl acrylate by ATRP

For the synthesis of telechelic poly methyl acrylate (pMA), a suitable bifunctional initiator had to be synthesized. Initiator **10** was prepared by esterification of hydroquinone with 2-bromopropanoyl chloride under basic conditions. Since the aromatic protons in **10** appear in ^{1}H-NMR spectra completely separated from the resonances of protons present in pMA, they can conveniently be used as an internal standard for monitoring end-group modifications.

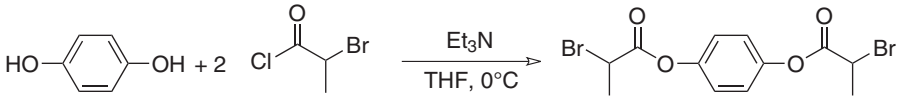

10, 79%

scheme 4. Preparation of bifunctional initiator **10**

Initially MA was polymerized from **10** using CuCl/bpy complex as catalyst at 80°C in toluene. Conversion was monitored using GC with the solvent as internal standard. Depicted in figure 12 is part of the ^{1}H NMR spectrum of the final polymer. A complete shift of the initiator methyl protons (ii, 6H) from δ 1.94 ppm to δ 1.22 ppm was observed, indicating

initiation occurred from both bromides. In addition the integral value of the OCH_3 end-groups (iii, 6H), compared to the aromatic protons of the initiator (i, 4H) was determined to be 6:4.

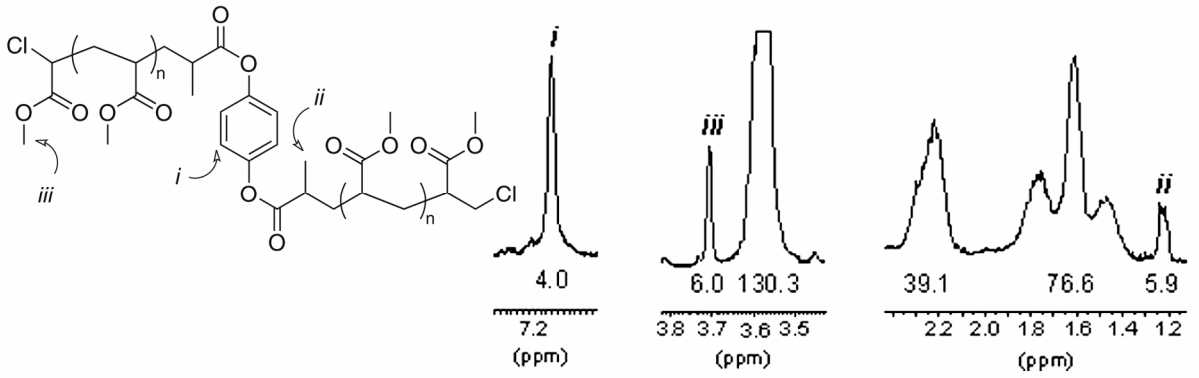

Figure 12. Parts of the ^1H NMR spectrum of telechelic pMA (entry 1, table 1) in $CDCl_3$.

Although the polymerization seemed to be controlled, polymerization conditions were not optimal since the kinetic plot deviated from first order (figure 13) and the observed polydispersity (M_w/M_n=1.34) was relatively high. Attempts to optimize the polymerization conditions using the CuCl/2 bpy catalyst did not result in better kinetics and a lower PDI, therefore different catalytic systems were investigated. From literature and our previous results with respect to the polymerization of MMA it was known that good control over polymerization could be achieved using N-(n-propyl)-2-pyridylmethanimine **2** or N,N′,N′,N″,N″-pentamethyldiethyltriamine (PMDETA) as ligand.

As can be seen in figure 13, the polymerization rate of MA using ligand **2** was very low, compared to bpy or PMDETA as a ligand. Nevertheless, good first order kinetics and an improved polydispersity index (PDI = 1.26) were observed when compared to the usage of bpy as ligand. Polymerization of MA using PMDETA resulted in good first order kinetics and an even better molecular weight distribution (PDI = 1.15).

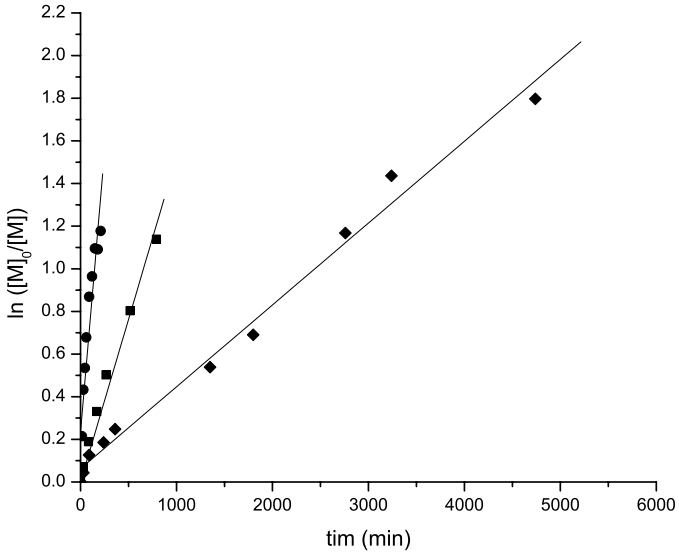

Figure 13. Kinetic plot for the ATRP of MA using different catalysts and monomer concentrations (see table 3), ● (polymer **11**), ♦ (polymer **12**), ■ (polymer **13**).

Table 3. ATRP of MA using a bifunctional initiator and different ligands

Polymer	Ligand	ratio[a] M/I/Cu/L	Solvent	Temp (°C)	Mn, theo (kg/mol)	Mn[b] (kg/mol)	Mw/Mn[b]
11	Bpy	56/1/2/4	toluene	80	3.6	3.6	1.34
12	**2**	116/1/2/4	xylene	90	8.9	6.7	1.26
13	PMDETA	115/1/2/2	toluene	70	6.1	6.9	1.15

a) M = monomer, I=Initiator, Cu=Copper (I) chloride, L= ligand. b) determined using SEC with THF as eluent and RI detection.

5.3.2 End-group modification towards isocyanate

The chloride endgroups in polymer **12** were substituted by reaction with sodium azide resulting in polymer **14**. Substitution of the end groups was determined by the complete upfield shift in the 1H NMR spectrum of the methine proton resonances adjacent to the end-groups from δ = 4.29 ppm to 3.91 ppm, and the appearance of the azide stretch vibration in the IR spectrum at υ = 2114 cm^{-1}. Subsequent reduction of the azide functionality into an amine using the Staudinger reaction was not successful. Although treatment of azide terminated polymer 1**4** with triphenylphosphine resulted in the disappearance of the azide signal in the IR spectrum, hydrolysis resulted in a negative bromophenol blue test, indicating no amines were present in the final product.

An alternative route is the reduction of azides via hydrogenation[25] (scheme 5). Treatment of 1**4** with hydrogen gas and a catalytic amount of Pd/C yielded amino terminated polymer **15**. Complete disappearance of the azide signal in the IR spectrum, a positive bromophenol blue test and complete downfield shift of the end-group protons in the ^{1}H-NMR spectrum from δ 3.91 ppm to 4.18 ppm, indicated hydrogenation was complete.

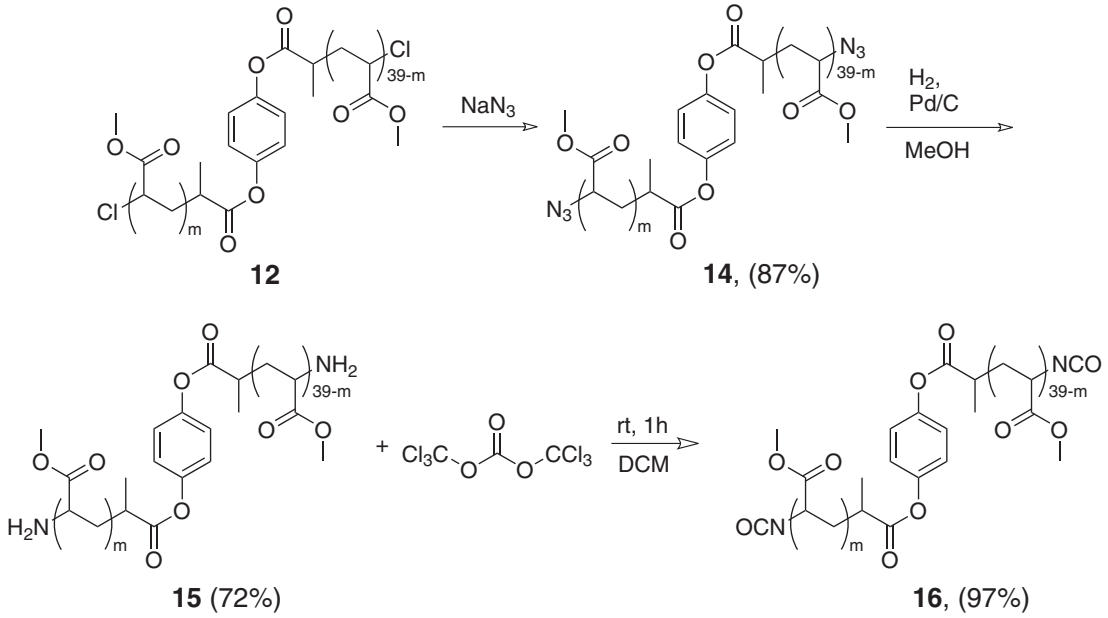

scheme 5. End-group modification of telechelic chloride functional pMA into isocyanate functional PMA.

The last step in the synthesis of isocyanate end-functionalized PMA is the transformation of the amine groups of **15** into isocyanates. The most common method comprises the reaction of phosgene with aliphatic and aromatic amines[24]. This method was modified over the years using various substitutes for the highly toxic phosgene[26]. An elegant route towards isocyanates starting from amines, developed by Meijer et al., involved treatment of the amine with di-tert-butyltricarbonate[27]. Although the appearance of the isocyanate stretch vibration in the IR spectrum (2337 cm^{-1}) demonstrated the formation of isocyanates, the bromophenol blue test indicated incomplete conversion upon treatment of polymer **15** with di-tert-butyltricarbonate. Therefore, polymer **15** was treated with the more reactive triphosgene, which led to complete transformation of **15** to **16** in one hour, as was indicated by the appearance of the isocyanate peak in the IR spectrum, a negative bromophenol blue test and a downfield shift of the protons adjacent to the end-groups (from

δ 4.18 ppm to 4.41 ppm). Furthermore, in the SEC chromatogram no high molecular weight material was observed, which could be formed if coupling of **15** with **16** had occurred.

Besides pMA, polyethylene glycol was also subjected to endgroup modification in order to introduce isocyanate functionality. In case of pMA, a secondary isocyanate group was obtained, which might hamper reactivity with the amine end group upon coupling of the nucleobase functionalized polymers. Using PEG a primary isocyanate group will be obtained which is expected to be more reactive towards nucleophiles. The synthesis of telechelic PEG with isocyanate end groups (**9**) was performed according to the route depicted in scheme 6.

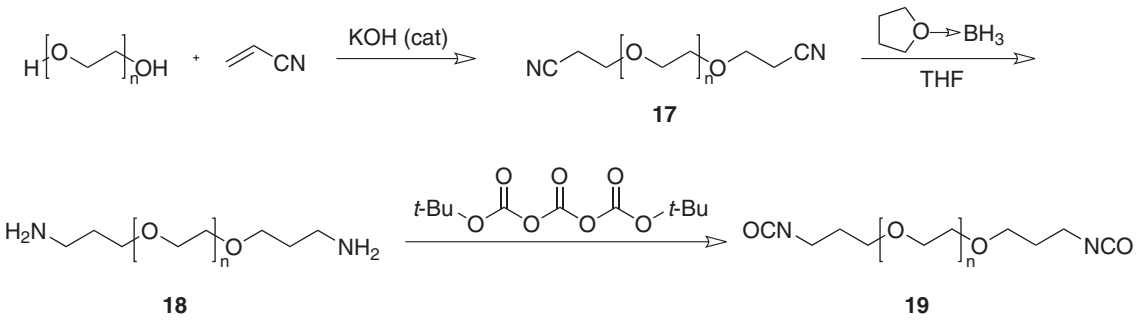

scheme 6. Endgroup modification of telechelic PEG_{6000} to isocyanates

Michael addition of PEG on acrylonitrile using a catalytic amount of potassium hydroxide followed by hydroboration of the nitrile with borane-tetrahydrofuran complex (BH_3●THF), resulted in telechelic PEG with amine endgroups **18**. Upon treatment of polymer **18** with a large excess of di-*tert*-butyl tricarbonate, the desired isocyanate endgroups were obtained. To obtain evidence for quantitative end group modification and to analyze the reactivity of the isocyanate group, a model reaction of the telechelic polymers with benzyl amine was performed (scheme 7).

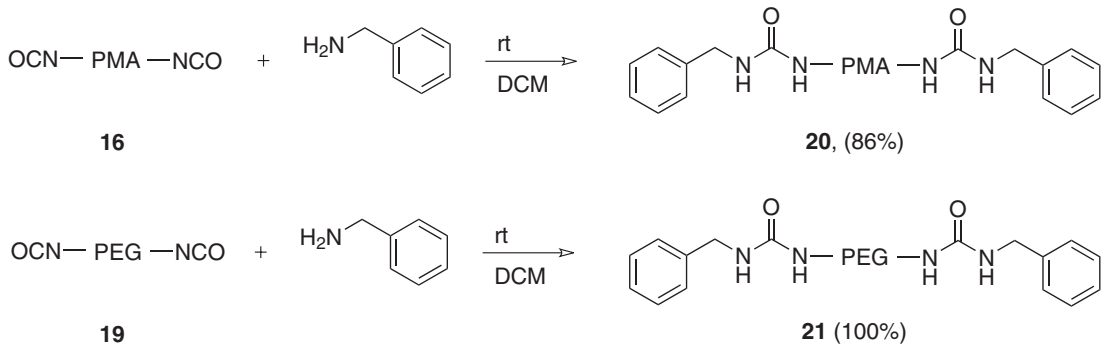

scheme 7. Coupling of benzyl amine with isocyanate functionalized polymers **16** and **19**

In case of the telechelic isocyanate functional PEG **19,** SEC analysis of the isocyanate polymer after work up revealed a bimodal distribution. Increasing the amount of tricarbonate did not circumvent this problem. It was found that the best results were obtained when a slight excess of tricarbonate was used, followed by *in situ* addition of benzylamine directly after a negative bromophenol blue test indicated complete conversion of all PEG amine groups.

Coupling between pMA polymer **16** and benzyl amine proceeded effectively, as was determined by the disappearance of the characteristic IR absorption of the isocyanate groups at 2253 cm^{-1} and the presence of urea stretch vibrations at 3405 and 1685 cm^{-1}. In addition, from the ^{1}H-NMR spectrum of polymer **20** the ratio between the integrals of the aromatic end groups (*ii*, 10H) and the aromatic initiator protons (*i*, 4H) was in excellent agreement with the expected ratio of 10:4 as can be seen in figure 14. These combined results are indicative that all end group transformations starting from telechelic pMA **12** to telechelic isocyanate pMA **16** and successive coupling with an amine model compound could be performed quantitatively.

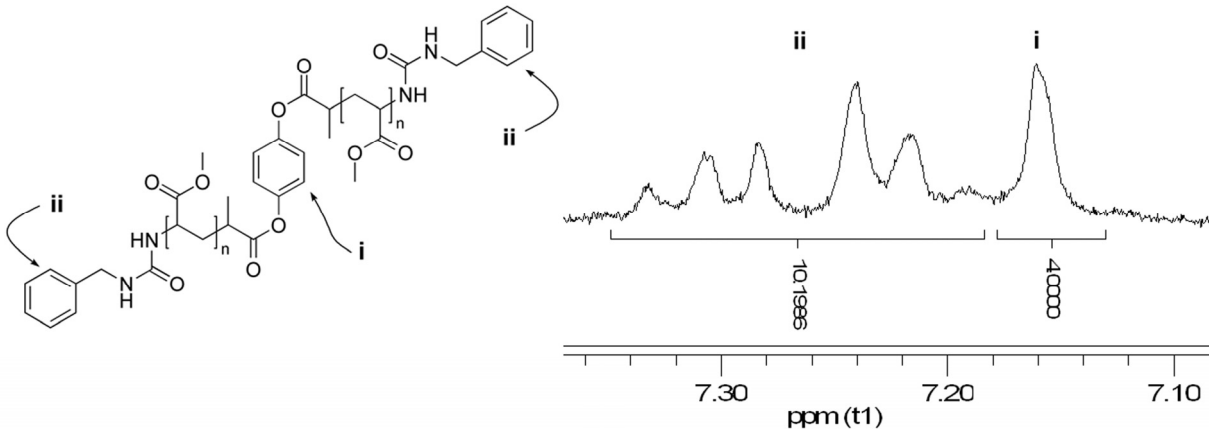

Figure 14. Part of the ^{1}H-NMR spectrum of benzylurea functionalized pMA **20** in $CDCl_3$

5.4 Amine functionalized oligo nucleobase polymer synthesis

The most convenient method for introducing end group functionality into polymers prepared by ATRP is to use a functional initiator[28]. Therefore, a protected amine functional initiator was prepared as described in scheme 8.

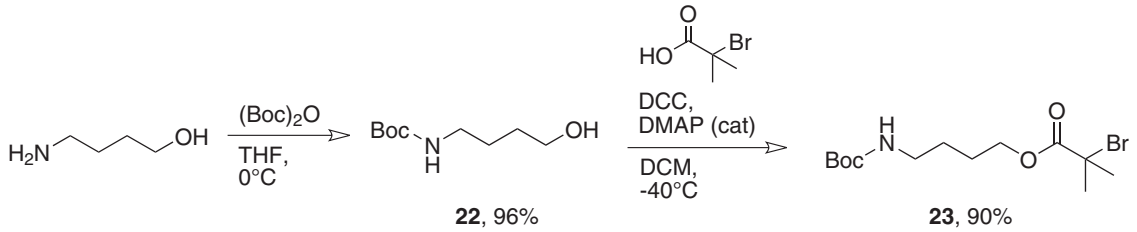

scheme 8. Synthesis of amine functionalized initiator **23**

4-amino-butanol was treated with di-*tert*-butyl dicarbonate to yield *tert*-butyl 4-hydroxybutylcarbamate **22**. Successively, the alcohol was coupled with 2-bromo isobutyric acid using DCC as a coupling agent and a catalytic amount of DMAP, resulting in the Boc protected amino initiator **23**. Both the adenine (**5**) and thymine (**6**) monomers showed good first order kinetics (figure 15) upon polymerization from this Boc protected initiator. Additionally with GPC analysis reasonably narrow molecular weight distributions were observed, indicating control over the polymerization.

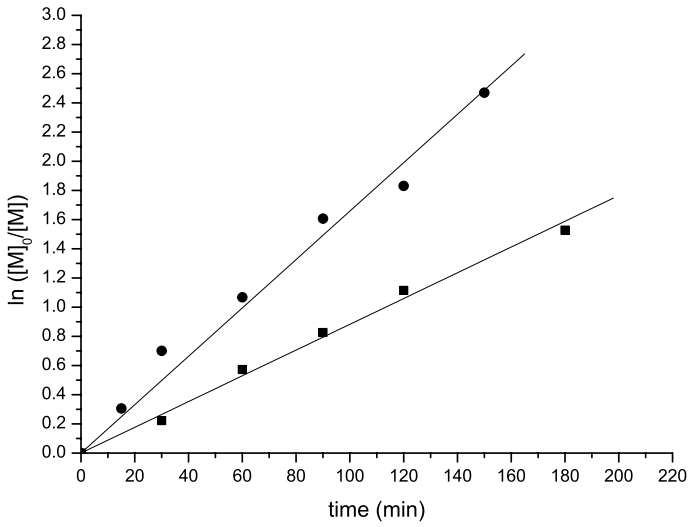

Figure 15. Kinetic plot of ATRP of nucleobase monomers ■ (**5**), ● (**6**) using initiator **23** (see table 4 for conditions)

Table 4. Synthesis of nucleobase oligomers by ATRP of adenine and thymine monomers using Boc initiator **23**

Polymer	Monomer	ratio[a] M/I/Cu/L	Solvent	Temp (°C)	$M_{n,\ theo}$ (kg/mol)	M_n[b] (kg/mol)	M_w/M_n[b]
24	**5**	10/1/1/2	DMSO-d_6	35	2.3	2.6	1.26
25	**6**	10/1/1/2	DMSO-d_6	45	2.6	3.2	1.32

a) M = monomer, I=Initiator **23**, Cu=cuprous chloride, L= bpy. b) determined using SEC with DMSO as eluent and UV detection (λ = 275 nm)

5.5 Coupling between nucleobase polymers and telechelic pMA

Complete removal of the Boc group was achieved for both polymer **24** and **25** by treatment with trifluoro acetic acid, resulting in the TFA salt of the oligonucleobase polymers. To obtain the free amine, the oligonucleobase polymers were dissolved in DMF and DIPEA was added.

The high reactivity of the isocyanate group towards free amines should result in quantitative coupling reactions and allow for the use of stoichiometric amounts of reagents. Consequently, purification of the final triblock copolymer should become straightforward. Coupling of the polymers was achieved by addition of a solution containing the isocyanate-functional PMA polymer, to a solution containing the amine functionalized nucleobase oligomer. Completion of the coupling between thymine polymer **25** and telechelic pMA **16** was indicated by the disappearance of the characteristic isocyanate IR absorption of **16** at 2253 cm^{-1} and a negative bromophenol blue test. SEC analysis of the product (figure 16) revealed a complete shift towards higher molecular weight. Additionally, the product obtained (figure 16, ii) also showed a UV-absorption at 254 nm, indicating the new polymer must contain nucleobase functionality. Furthermore, a change in morphology of the isolated product from a sticky waxy polymer to a white solid was observed. These observations demonstrate that the thymine–functional triblock copolymer was successfully synthesized.

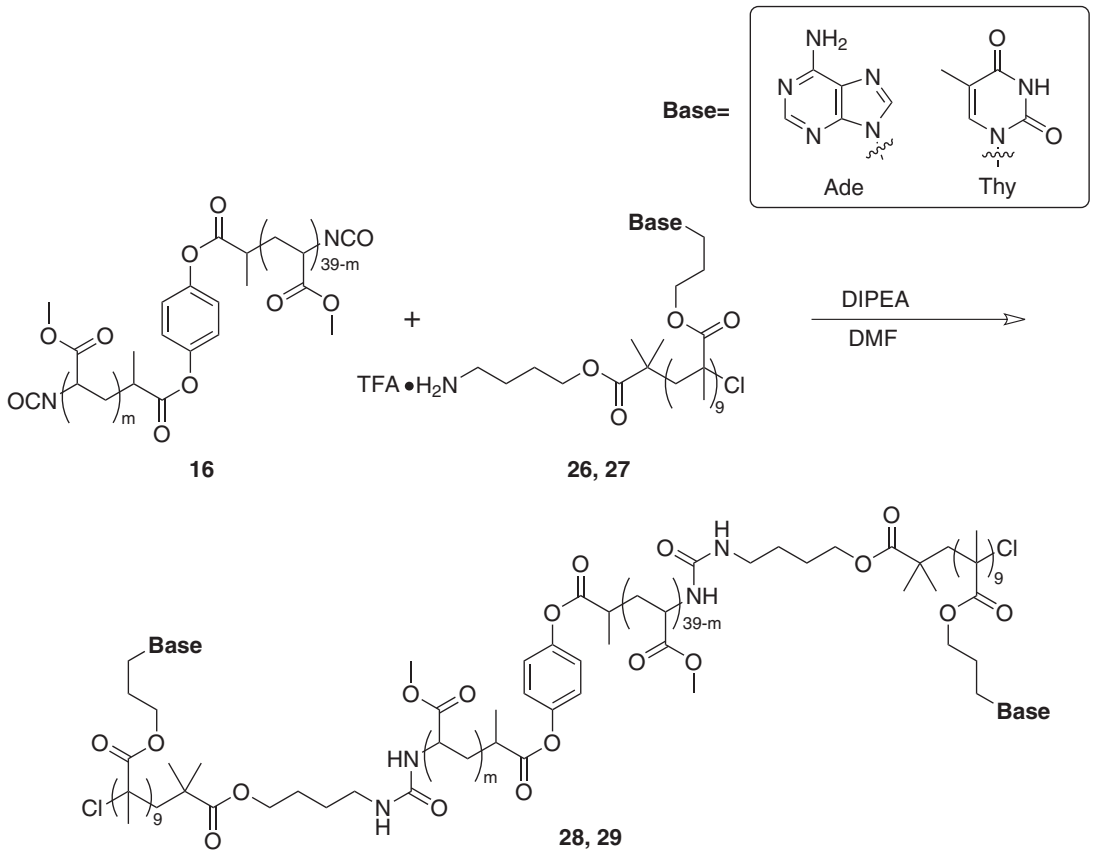

scheme 9. A modular approach for the synthesis of nucleobase functionalized ABA type triblock copolymers.

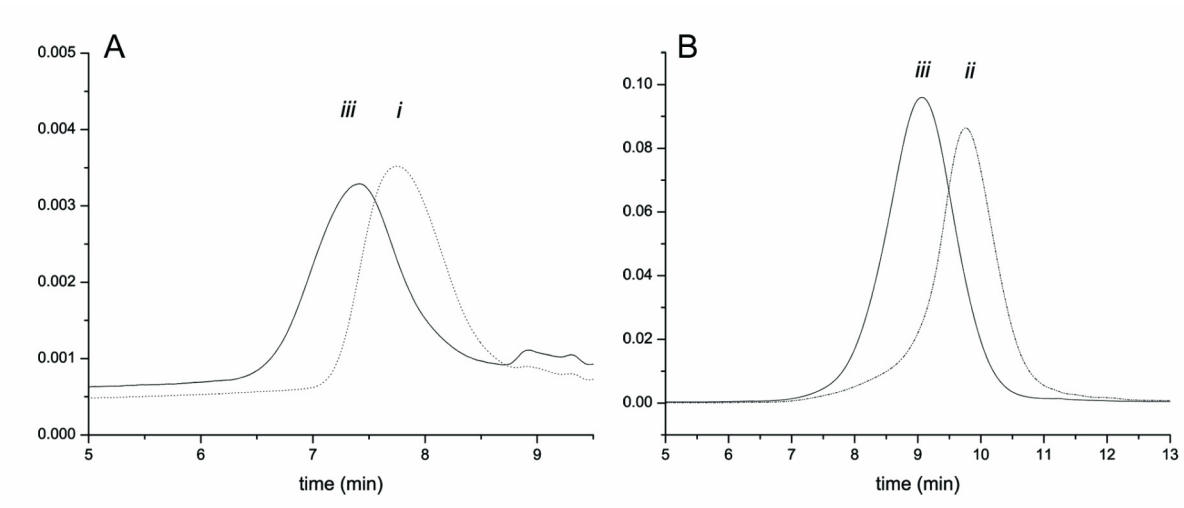

Figure 16. SEC chromatograms indicating the formation of oligothymine-PMA triblock copolymers; **A**) measured in THF using RI detection (i) isocyanate PMA **16**, (iii) thymine PMA triblock copolymer **29**; **B**) measured in DMSO with UV detection (ii) thymine PMA triblock copolymer **29**, (ii) thymine polymer **27.**

Table 5. Molecular weight data of triblock copolymer synthesis via coupling between isocyanate functionalized PMA **16** and amine-functionalized oligo thymine.

Polymer	$M_{n,\ theo}$ (kg/mol)	M_n (kg/mol)	M_w/M_n
16	3.6[a]	3.6[a]	1.34[a]
27	2.6[b]	3.2[b]	1.42[b]
29	8.9[a]	7.6[a]	1.63[a]
29	8.9[b]	8.4[b]	1.28[b]

a) Samples measured with THF as an eluent, using RI detection. b) Samples measured with DMSO as an eluent, using UV detection (λ = 254 nm).

Unfortunately, coupling of adenine-functionalized polymer **26** to pMA **16** was unsuccessful. It was found that adenine oligomer **26** contained after BOC removal large amounts of TFA salts, therefore a larger excess of base was needed to liberate the amine for nucleophilic attack. However, upon addition of a large excess of base, precipitation was observed and analysis of the reaction mixture revealed that no coupling had occurred. Unfortunately, changing solvent from DMF to DMSO to improve solubility did not have the desired effect.

5.5.1 Coupling between nucleobase polymers and telechelic PEG

As was determined in paragraph 5.3.2, optimal conditions for coupling amine nucleophiles to PEG isocyanate, is to prepare the PEG_{6000}-isocyanate polymer under dry conditions using a large excess of the tricarbonate, followed by in situ coupling. However, applying these conditions would require a large excess of nucleobase functionalized oligomer, since addition of the amine to the isocyanate endgroup has to compete with reaction of the free amine with residual tricarbonate. As a result the reaction mixture would contain besides the desired product a substantial amount of nucleobase oligomer, which is difficult if not impossible to separate. Therefore, coupling between isocyanate PEG with amine functionalized oligonucleobase was first attempted using stoichiometric amounts of reagents and a slight excess of tricarbonate.

Upon addition of a basic solution of oligothymine **27** in DMF to a solution of PEG-isocyanate in DMF immediate precipitation occurred. It was found necessary to aid solubility by adding DMF to the PEG6000-isocyanate solution as well. SEC analysis of the reaction

mixture revealed that the reaction was not complete, since peaks corresponding to the starting materials could be observed. Nevertheless, a new product with a mass of about 11 kDa (Mn/Mw = 1.10) was also obtained. By semi-preparative SEC, this product could be isolated. ^{1}H NMR analysis revealed that it was indeed the expected triblock copolymer, with the correct integral values (figure 17).

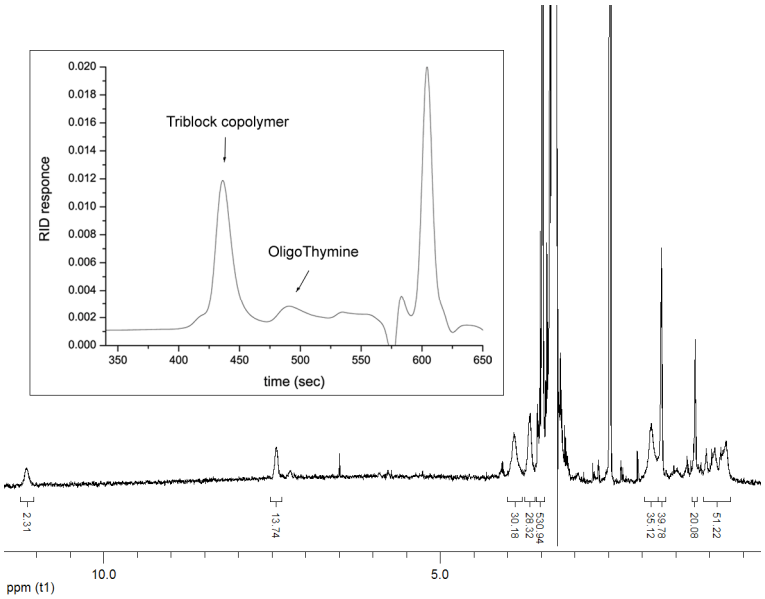

Figure 17. SEC spectrum of the coupling product between PEG_{6000}-isocyanate **9** and **27**, and the resulting ^{1}H NMR spectrum of the isolated GPC peak.

Unfortunately, solubility problems again hampered coupling between the PEG isocyanate **9** and amine functionalized oligo adenine **16**. Similar to the pMA coupling reactions involving adenine functionalized oligomers, precipitation of the adenine oligomer upon addition of an excess of base occurred and no product could be obtained.

5.5.2 Discussion

To use the modular approach for preparation of the triblock copolymers, three steps need to be performed. First, the center polymer block needs to be prepared. Second, a nucleobase functionalized polymer block containing a free amine must be prepared and finally the coupling reaction between the two polymer blocks has to be performed.

Two telechelic polymers, PMA and PEG, were chosen as center blocks. Both polymers needed some chemical endgroup modification to obtain an endgroup that is reactive enough for efficient coupling with the outer nucleobase functionalized block. In case of PMA a

bifunctional initiator was prepared from which MA could be polymerized in a controlled fashion using ATRP. Substitution of the halogen endgroup proceeded smoothly, but subsequent reduction to the amine using the Staudinger reaction appeared to be problematic. Although no evidence for the presence of the iminophosphorane end-groups was obtained, it is likely that hydrolysis by water was the problematic step, since in the IR spectrum of the product the azide stretch vibration could not be detected and the bromophenol blue test remained negative. Reason for this could be that pMA is a hydrophobic polymer and the endgroups are therefore shielded from water. Reduction of the azide by hydrogenation and successive conversion of the amine to an isocyanate group using triphosgene was successful, as was demonstrated with various analysis techniques. Additionally, coupling with benzyl amine clearly indicated that telechelic isocyanate functional PMA was efficiently produced.

Synthesis of amine-functional PEG starting from hydroxyl terminated PEG by Michael addition to acrylonitrile, followed by hydrogenation of the nitrile group was performed successfully. Conversion of the amine into an isocyanate group seemed to proceed smoothly, as was determined by IR and a negative bromophenol blue test. However, after the coupling experiments between PEG-isocyanate and benzylamine a bimodal mass distribution was obtained. This result was unexpected since it has been shown that this method for the preparation of isocyanates out of amines can normally be performed very efficiently on molecules containing multiple amines, such as dendrimers[29].

Reason for this could be that the isocyanate endgroup is hydrolyzed back to a free amine, which can then attack an isocyanate group. Although great care was taken to perform the reaction under dry conditions, it is known that due to the hygroscopic nature of PEG trace amounts of water strongly bind to the polymer chains and could therefore be present. Under the applied conditions in our hands it was impossible to circumvent this side reaction. Effective suppression of this side reaction could only be achieved by usage of a large excess of di tertbutyl tricarbonate, followed by in situ coupling with the desired amine nucleophile.

The large difference in stability of the isocyanate endgroup between PMA en PEG can therefore be explained by the difference in hydrophobicity between the polymers. The hydrophobic nature of PMA is supported by the unsuccessful hydrolysis of the iminophosphorane, during the Staudinger reduction of the azide.

The last step towards triblock copolymers is the coupling between the nucleobase polymers and the telechelic PEG and PMA center blocks. Therefore, nucleobase polymers containing a Boc protected amine endgroup were prepared using ATRP. The Boc group could be removed using TFA. Unfortunately, upon addition of base to the nucleobase polymer solutions in order to quench the excess TFA and obtain a free amine, the solubility of the adenine nucleobase polymer decreased drastically. As a result, no coupling between PEG-isocyanate or PMA-isocyanate and adenine nucleobase polymer was achieved. Changing solvent to DMSO had no effect.

In case of coupling between thymine nucleobase polymer and PEG-isocyanate no solubility problems were encountered, and thus triblock copolymer could be obtained in both cases. However, the coupling with PEG resulted in a mixture of products. This can be explained by the known hydrolysis reaction of the isocyanate endgroup of PEG. Additionally the excess of tricarbonate, in order to suppress the hydrolysis of the PEG isocyanate, has as a major drawback that leads to a possible reaction of the nucleobase polymer amine endgroup with the tricarbonate. As a result another isocyanate group can be formed, leading to a mixture of polymer products. Nevertheless, the main product peak appeared to be the desired triblock copolymer as was shown by ^{1}H NMR.

Upon coupling thymine nucleobase polymer and PMA-isocyanate a clear shift towards higher molecular weight was observed. Remarkably, there were large difference between the polydispersities of triblock copolymer **29** observed when measured in THF or DMSO. Most likely, this is the result of aggregation of the triblock copolymer since the diblock copolymers prepared in chapter 4 also show aggregation behavior due to nucleobase functionality. As a result, the GPC spectrum in THF will give a rather broad molecular weight distribution peak. When DMSO is used as a solvent, polymer aggregation is less likely to occur, therefore the observed polydispersity and molecular weight will be more close to the actual figure.

5.6 Towards nucleobase directed supramolecular polymers.

Because the macroinitiation method for preparation of nucleobase functionalized triblock copolymers was the most successful (paragraph 5.2), well-defined polymers **10** and **11** were used for the construction of supramolecular materials. To investigate whether interactions between the two triblock copolymers occurred as a result of hydrogen bonding between the complementary thymine and adenine moieties, equimolar amounts of the block copolymers were dissolved in different deuterated solvents. Upon mixing of the adenine and thymine triblock copolymers in DMSO-d_6, no chemical shift of the nucleobase protons in the ^{1}H NMR spectrum could be observed. This could be expected from the known hydrogen bond breaking effect of this solvent. Upon using $CDCl_3$, a cloudy mixture was obtained for both the separate polymers and the mixture, indicating incomplete solubilization or aggregation of the polymers. The resulting ^{1}H NMR spectrum showed in all cases only the PEG part of the block copolymers. Addition of CD_3OD (10%) to the dispersion produced an optically clear solution. However, in this solvent mixture the ^{1}H NMR spectra of the separate block copolymers showed the resonances of the imide protons of thymine and the amine protons of adenine were found at already a relatively high chemical shift (δ 7.2 and 8.0 ppm resp.), indicating the presence of hydrogen bonded protons. Upon mixing no additional change in chemical shift of the nucleobase protons could be observed.

FTIR studies were also performed on the polymer solutions. For this purpose, the triblock copolymers were dissolved in $CDCl_3$ after which 3% CD_3OD was added, resulting in an optical clear solution, with a total polymer concentration of 2 mg/mL. The spectral range shown in figure 18 contains absorption bands of the in-plane double bond stretching vibrations of the thymine and adenine bases. The calculated spectrum was obtained by averaging the IR spectra of the separate block copolymers, as to simulate a mixture of non-interacting oligonucleobase polymers. Selected vibrations are depicted in table 6 and figure 18.

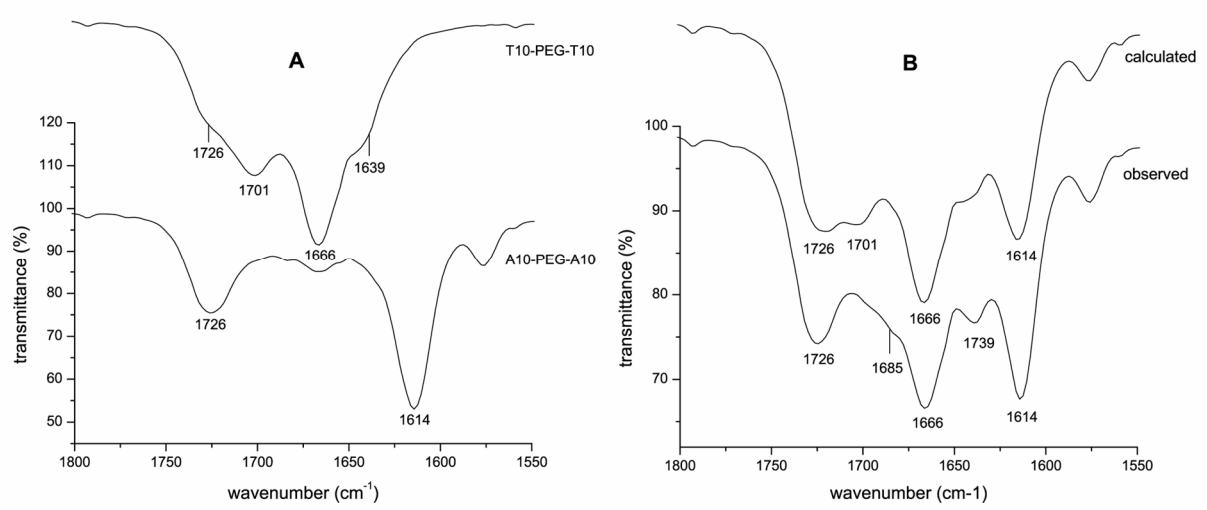

Figure 18. FTIR spectra recorded in 3% CD_3OD / $CDCl_3$ of **A**) A10-PEG-A10 and T10-PEG-T10. **B**) equivalent mixture of A10-PEG-A10 and T10-PEG-T10 (total 2 mg polymer/mL); calculated curve obtained by averaging the curves in A.

Table 6. The wavenumbers and spectral assignments of selected IR bands in polymer **8, 9**

Polymer	wavenumber cm^{-1}	assignment
8	1726	C=O PMMA backbone
8	1614	C=N, C=C in plane ring
9	1726	C=O PMMA backbone
9	1701	C2=O2 thymine stretching
9	1666	C4=O4 thymine stretching
9	1639	thymine ring

From FTIR studies with DNA and RNA[30-33] it is known that duplex formation causes changes in the infrared spectrum in this region. By comparing the calculated spectrum with the observed spectrum of the mixture, the following changes were observed upon mixing (figure 8B). The C2=O2 stretch vibration at 1701 cm^{-1} decreased significantly, while the C4=O4 stretch vibration at 1666 cm^{-1} remained relatively unaffected. More pronounced were the changes in ring vibrations at 1614 $cm^{-1,}$ which decreased significantly, while the vibration at 1639 cm^{-1} increased.

The combined changes in the IR spectrum of the triblock copolymer mixture indicate thymine and adenine are involved in hydrogen bonding interactions at the measured concentration of 2 mg polymer/mL solvent. This is especially demonstrated by the shift of

the thymine C2=O2 vibration from 1701 cm^{-1} to 1685 cm^{-1}.The unaffected vibration of C4=O4 (1666 cm^{-1}) indicates this carbonyl is not involved in hydrogen bonding interactions. These findings suggest that the mode of binding between thymine and adenine occurs predominantly via a *trans* or reversed Watson Crick and/or Hoogsteen interaction (figure 19).

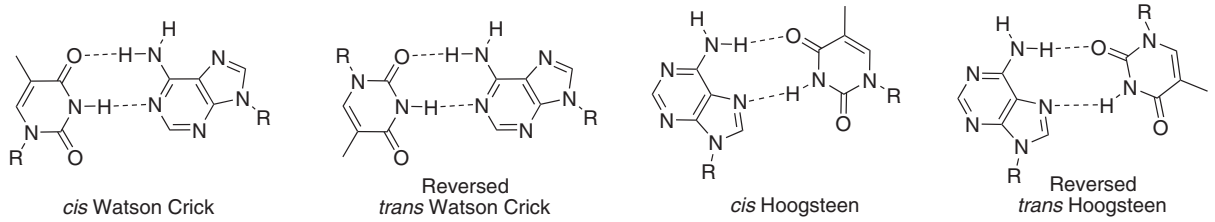

Figure 19. thymine - adenine base pair possibilities

Further studies to determine binding between the triblock copolymers were performed using DSC measurements in the solid phase. As summarized in table 2 only typical transitions involved with the Tg of the PMMA backbone could be observed. As can be expected no change in Tg was observed upon mixing of the triblock copolymers since the PMMA backbone is not directly involved in supramolecular hydrogen bonding interactions.

Table 7. Thermal transitions observed of trblock copolymers and their mixture

Polymer	Transition heating[a]	Transition cooling[a]
A10-PEG-A10	67.1	61.0
T10-PEG-T10	68.8	60.7
Mixture[b]	66.4	59.6

a) second curve 5°C/min, b) ratio approximately 1 : 1 weight

5.7 Discussion

As could be expected the triblock copolymers prepared using the macroinitiation method appeared to be amphiphilic in nature. This hampered the detection of hydrogen bonding interactions by ^1H NMR spectroscopy, since the block copolymers were only completely soluble in solvents that disrupt hydrogen bonding, such as DMSO-d_6 and CD_3OD. Only with IR spectroscopy could information be obtained about possible interactions between the thymine and adenine nucleobases. The observed IR spectrum of the mixed triblock copolymers showed distinct differences compared to the calculated mixture of non-interacting block copolymers. Detailed comparison of the observed characteristic

vibrations with known literature studies of DNA interactions suggests that hydrogen bonding interactions occur.

Since interactions between the nucleobases occurred in solution, we envisioned that these interactions might also occur in the solid state creating materials with supramolecular properties. It was anticipated that a new melting transition due to the hydrogen bonding interactions would occur or that a transition of the separate block copolymers would change upon mixing the complementary block copolymers. Unfortunately, no additional transition could be observed probably due to the weakness of the interaction or phase separation that might occur upon melting.

5.8 conclusions

Two methods for building up triblock copolymers, the macroinitiation and the modular buildup method were investigated. The macroinitiation method proved to be a straight forward method, which worked very well when commercially available bifunctional PEG was modified into an ATRP initiator from which the triblock copolymers were prepared. The second macroinitiation approach however has its limitations. ATRP from a PMMA bifunctional macroinitiator resulted in an inseparable mixture of block copolymers, probably due to a low reinitiation efficiency.

The modular build up method has the advantage that both polymer blocks can be prepared separately in a controlled fashion. Modification of the endgroups of the telechelic pMA and PEG center blocks into isocyanate groups could be achieved effectively. Amine functional oligonucleobase blocks were also constructed in a controlled manner However, the amine-isocyanate coupling chemistry was not as straightforward as anticipated. In case of PEG side reactions occurred, leading to multimodal molecular weight distributions. The amine functional oligoadenine block suffered form severe solubility problems. This therefore made the macroinitiation method the method of choice for the preparation of oligonucleobase triblock copolymers. Preliminary studies after the supramolecular assembly of these polymers in solution and in the solid state only showed some evidence for adenine-thymine interaction in solution. However, no effect of this (weak) interaction on the polymer properties could be detected.

5.9 Experimental

Materials

Glassware used was oven-dried. All reactions were performed under an argon atmosphere, unless otherwise stated. DMF was dried over anhydrous $MgSO_4$, followed by distillation under reduced pressure and storage under an argon atmosphere. Dichloromethane (DCM), heptane and ethyl acetate (EtOAc) were distilled over calcium hydride (CaH_2) and 1,4-dioxane was freshly distilled over $LiAlH_4$. Copper chloride (CuCl) was purified according to a literature procedure[34]. Silica gel column chromatography (SGCC) was performed using Acros silica gel (0.035-0.070 mm). TLC was carried out on Merck precoated silica gel 60 F-254 plates. Compounds were visualized using UV and permanganate staining agent. Other chemicals were used as received unless otherwise stated. The synthesis of compounds **5** (adenine monomer) and **6** (thymine monomer) are described in chapter 2.

Instrumentation

^{1}H NMR spectra were recorded on a Bruker AC200 or a DPX300 instrument at 200 or 300 MHz respectively. ^{13}C NMR spectra were recorded on a Bruker DPX300 instrument at 75 MHz. Chemical shifts (δ) are given in ppm relative to the internal standard (Me_4Si or DMSO-d_6). IR spectra were recorded on an ATI Matson Genesis Series FTIR spectrometer with fitted ATR cell. GPC measurements were performed using a Shimadzu LC-10ADvp system equipped with PL gel 5 μm guard column, a PL gel 5 μm mixed D column, differential refractive index detector (Shimadzu RID-10A) at 38°C and a UV detector (Shimadzu SPD-10AVvp). The system was operated with a flow of 0.8 mL·min^{-1} at 70°C using dimethylsulfoxide (DMSO, 0.02 M LiCl) as an eluent and polyethylene glycol standards in the range 1900 to 124700 Da to calibrate the SEC. In case THF was used as an eluent a flow of 1 mL·min^{-1} at 35°C was applied and polystyrene standards in the range of 580 to 377400 Da to calibrate the GPC were used. Gas chromatograms were conducted on a Hewlett-Packard 5890 Series II gas chromatograph, equipped with capillary columns (HP1, 25m x 0.32 mm x 0.17 μm; HP1701, 25m x 0.32 mm x 0.25 μm), using flame ionization detection. DSC measurements were performed on a Perkin Elmer Pyris Diamond DSC, equipped with a Perkin Elmer Intracooler 2P.

1,4-phenylenebis(methylene) bis(2-bromo-2-methylpropanoate) (1)

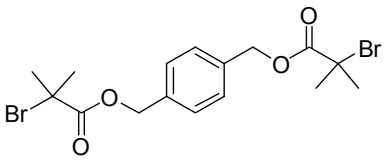

A solution of 2-bromoisobutyryl bromide (2.30 mL, 18.6 mmol) in THF (15 mL) was added dropwise to a solution of 1,4-benzenedimethanol (1.11 g, 8.00 mmol) and Et_3N (1.98 g, 19.6 mmol) in THF (25 mL) at 0°C. After complete addition, the reaction mixture was allowed to stir for 2 hours at ambient temperature. The formed precipitate was removed by filtration and the solvent was removed *in vacuo*. The crude product was further purified by SGCC (heptane/EtOAc 9:1) and isolated as a white solid which was dried under vacuum to yield 3.25 g (93%) of pure **1**. R_f (heptane/EtOAc 9:1) = 0.16. ^{1}H NMR (300 MHz, $CDCl_3$): δ 7.36 (s, 4H Ar<u>H</u>), 5.19 (s, 4H, Ar-C<u>H</u>$_2$), 1.95 (s, 12H CBr-(C<u>H</u>$_3$)$_2$). ^{13}C NMR ($CDCl_3$): δ 171.24, 135.49, 128.03, 67.34, 55.83, 31.09.

N-(n-propyl)-2-pyridylmethanimine (2)

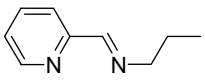

An excess of n-propylamine (1.280 g, 21.65 mmol) was added dropwise to a stirred solution of pyridine-2-carboxaldehyde (2.108 g, 19.68 mmol) in diethyl ether (2 mL), cooled in an ice bath. After complete addition of the amine, anhydrous $MgSO_4$ (500 mg) was added and the slurry was stirred for 2 hours at room temperature. The solution was filtered and concentrated in vacuo to yield 2.430 g (16.4 mmol, 83%) **2** as yellow oil. ^{1}H NMR (300 MHz, $CDCl_3$): δ 8.66-8.63 (m, 1H, pyridyl H6), 8.38 (m, 1H, pyridyl-C(=N-Pr)H), 8.01-7.97 (m, 1H, pyridyl H4), 7.76-7.71 (m, 1H, pyridyl H3), 7.33-728 (m, 1H, pyridyl H5), 3.65 (dt, 2H, ^3J = 6.9 Hz, ^4J = 1.4 Hz, CH=N-C<u>H</u>$_2$-CH$_2$), 1.82-170 (m, 2H, CH$_2$-C<u>H</u>$_2$-CH$_3$), 0.97 (t, 3H, ^3J = 7.21 Hz, CH$_2$-C<u>H</u>$_3$). ^{13}C NMR ($CDCl_3$): δ 161.83, 154.78, 149.50, 136.59, 124.66, 121.27, 63.40, 23.96, 11.93. FTIR (oil): ν 2959, 2928, 2873, 2833, 1649, 1586, 1566.

Telechelic PMMA (3)

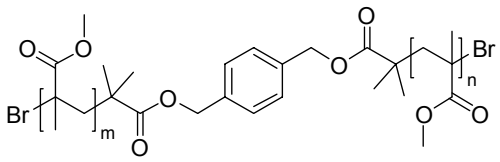

CuBr (94.8 mg, 0.66 mmol) and **1** (147.9 mg, 0.34 mmol) were placed in a Schlenk tube. Deoxygenation was performed by three cycles of evacuation, followed by refilling with nitrogen. Toluene (2 mL) and MMA (2.43 g, 24.2 mmol) were added. The reaction mixture was placed in an oil bath at 80°C after which the polymerization was started by addition of **2** (100 mg, 0.67 mmol). Samples were taken periodically for conversion analysis. Conversions were determined by GC, using the solvent as an internal standard. The reaction was stopped by rapid cooling to RT and dilution with 2 mL of toluene. The crude product was purified by filtration over a bed of basic alumina, which was thoroughly washed with toluene. After concentration to about 10 mL, the polymer was further purified by precipitation in heptane to yield 1.11 g (53%) of pure **3**. ^{1}H NMR (300 MHz, $CDCl_3$): δ 7.33 (s, arom. H), 5.10 (s, 2x Ar-C$\underline{H}_2$-), 3.77 (s, 2x OC$\underline{H}_3$ endgroup), 3.60 (br s, OC$\underline{H}_3$ backbone), 2.0-1.78 (br m, C$\underline{H}_2$ backbone), 1.21-1.15 (br m, 2x CH_2O_2C-C-C$\underline{H}_3$-), 1.1-0.8 (br m, C$\underline{H}_3$ backbone). SEC (THF): M_n = 6.9 kDa, M_w/M_n = 1.15, DP_{NMR}=68, $M_{n\ NMR}$ = 7.2 kDa.

Telechelic PMMA 4

MMA was polymerized according to the procedure described for polymer **3** using MMA (3.78 g, 37.8 mmol), **1** (295 mg, 0.68 mmol), CuBr (188 mg, 1.31 mmol) and **2** (200 mg, 1.34 mmol) in 4.0mL toluene at 80°C. ^{1}H NMR (400 MHz, $CDCl_3$): δ 7.33 (s, arom. H), 5.10 (s, 2x Ar-C$\underline{H}_2$-), 3.77 (s, 2x OC$\underline{H}_3$ endgroup), 3.60 (br s, OC$\underline{H}_3$ backbone), 2.0-1.78 (br m, C$\underline{H}_2$ backbone), 1.21-1.15 (br m, 2x CH_2O_2C-C-C$\underline{H}_3$-), 1.1-0.8 (br m, C$\underline{H}_3$ backbone). SEC (THF): M_n = 5.8 kDa, M_w/M_n = 1.19. DP_{NMR}=67, $M_{n\ NMR}$ = 7.1

α, ω-(2-bromo-2-methyl propionate)-poly(ethylene glycol) (7)

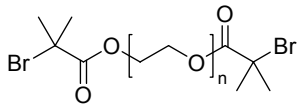

Poly(ethylene glycol) 2000 g/mol (5.00 g, 2.5 mmol) and Et_3N (1.143 g, 11.3 mmol) were dissolved in DCM (100 mL) and cooled to 0 °C. 2-bromo-isobutyrylbromide (1.379 g, 7.99 mmol) was added in a dropwise fashion and the mixture was slowly allowed to heat to ambient temperature. The remaining 2-bromo-isobutyrylbromide was quenched with MeOH (10 mL). The mixture was washed with a saturated $NaHCO_3$ solution (50 mL) and water (50 mL). The organic phase was dried over anhydrous $MgSO_4$ and concentrated under reduced pressure, yielding a waxy yellowish solid which could be further purified using column chromatography (MeOH/DCM; 1:9) to yield 5.22 g (95%) of product **7** as a white, waxy solid. ^{1}H NMR (400 MHz, $CDCl_3$): δ 4.34-4.30 (m, 4H, CH_2-C$\underline{H}_2$-O-C(=O)), 3.75-3.72 (m, 4H, C$\underline{H}_2$-CH_2-O-C(=O)), 3.64 (br s, 182H {C$\underline{H}_2$-C$\underline{H}_2$-O}), 1.94 (s, 12H, 2x C(=O)-C(C$\underline{H}_3$)$_2$-Br). ^{13}C NMR ($CDCl_3$): δ 171.59, 70.73, 70.58, 68.76, 65.14, 55.74, 30.79. FTIR (Solid): ν 1731, 1102. SEC (THF) M_n = 2.1 kg/mol, M_w/M_n = 1.06. MALDI-TOF $[M+Na]^+$ calc. for n = 41, m/z = 2143.98 g/mol, found m/z = 2142.62 g/mol.

Polymerization of adenine monomer using telechelic PEG initiator 7, A10-PEG-A10 (8)

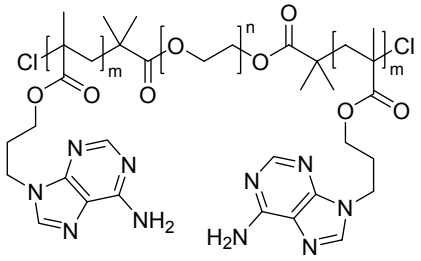

3-(adenin-9-yl)propyl methacrylate (**5**) (500.6 mg, 1.917 mmol), CuCl (13.0 mg, 0.131 mmol) and 2,2'-bipyridyl (bpy) (42.0 mg, 0.269 mmol) were placed in a Schlenk tube, followed by three vacuum – argon refill cycles. DMSO-d_6 (5.00 mL) was added and the mixture was argon purged for 10 minutes, followed by heating to 35°C. The polymerization was started by addition of 0.98 mL of an argon purged stock solution of PEG-based macro-initiator **7** (331.6 mg, 0.144 mmol) in DMSO-d_6 (2.24 mL). Samples were taken periodically in order to analyze the monomer conversion with ^{1}H NMR spectroscopy. At the desired conversion, the reaction mixture was poured into an aqueous EDTA solution (0.055 M), followed by extraction of the crude product with dichloromethane (DCM) (3 times 50 mL). After addition of brine to the aqueous phase another three extractions with DCM were performed. The combined organic phases were dried over anhydrous $MgSO_4$, filtered and concentrated under reduced pressure. The crude product was further purified using sephadex column chromatography (LH-20, MeOH/DCM; 1:1) resulting in 287 mg (92%) of product as a pure white solid after freeze drying. ^{1}H NMR (DMSO-d_6): δ 8.15 (br s, purine-C$\underline{H}$), 8.10 (br s, purine-C$\underline{H}$), 7.24 (br purine-N$\underline{H}_2$), 4.21 (br s, O-C$\underline{H}_2$-CH_2), 3.90 (br s, C$\underline{H}_2$-CH_2-N_{purine}), 3.50 (br s, {O-C$\underline{H}_2$-C$\underline{H}_2$}), 2.12 (br s, O-CH_2-C$\underline{H}_2$-CH_2-N_{purine}), 1.89-1.40 (br s, {C$\underline{H}_2$-C(CH_3)}), 1.10-0.70 (br m, {CH_2-C(C$\underline{H}_3$)}). SEC (DMSO, RID): M_n = 7.2 kg/mol, M_w/M_n = 1.21, M_n (^{1}H NMR) = 7.1 kg/mol.

Polymerization of thymine monomer using telechelic PEG initiator T10-PEG-T10 (9)

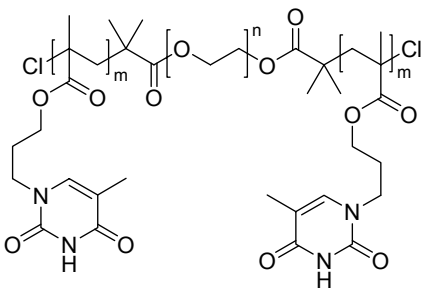

3-(thymin-1-yl)propyl methacrylate (**6**) was polymerized at 30°C using the procedure described for polymer **8** with **6** (504.3 mg, 1.999 mmol), CuCl (13.2 mg, 0.133 mmol) and bpy (41.7 mg, 0.267 mmol) in 4.73 ml DMSO-d_6 The polymerization was started by addition of 1.0 mL of a stock solution containing **7** (324.9 mg, 0.141 mmol) in 2.07 mL DMSO-d_6. Yield: 360 mg ^{1}H NMR (DMSO-d_6): δ 11.17 (br s, pyrimidine-NH), 7.46 (br s, pyrimidine-H6), 3.92 (br s, O-C$\underline{H}_2$-CH_2), 3.69 (br s, CH_2-C$\underline{H}_2$-N), 3.50 (br s, {C$\underline{H}_2$-C$\underline{H}_2$-O}), 1.88 (br s, CH_2-C$\underline{H}_2$-CH_2-N), 1.74 (br s, pyrimidine-CH_3), 1.70-1.30 (br m, {C$\underline{H}_2$-C(CH_3)}, 1.10-0.65 (br m, {CH_2-C(C$\underline{H}_3$)}). SEC (DMSO): M_n = 7.5 kg/mol, M_w/M_n = 1.19, M_n (^{1}H NMR) = 8.3 kg/mol.

1,4-phenylene bis(2-bromopropanoate) (10)

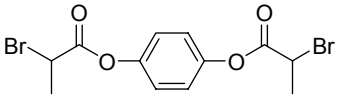

An excess of 2-bromopropionyl chloride (9.338 g, 43.5 mmol) was added dropwise to a stirred solution of hydroquinone (2.2037 g, 20.01 mmol) and Et_3N (4.498 g, 44.5 mmol) in THF (80 mL), cooled in an ice bath. After complete addition of the acid chloride, the reaction mixture was stirred for 6 hours at room temperature. After TLC (acetone / DCM 1:1) indicated the reaction was finished, the excess of acid chloride was quenched with MeOH. Precipitated triethylammonium chloride was removed by filtration, after which the filtrate was concentrated under reduced pressure to give the crude product as a yellowish solid. The crude product was further purified by two recrystallizations from isopropanol to yield 6.043 g (15.9 mmol, 79%) of pure **10** as a white solid. mp = 89.9 °C. R_f (acetone / DCM 1:1) = 0.82. ^{1}H NMR (300 MHz, $CDCl_3$): δ 7.17 (s, 4H, Ar-H), 4.58 (q, 2H, ^3J = 6.91 Hz, 2x O_2C-C$\underline{H}$Br-CH_3), 1.94 (d, 6H, ^3J = 6.91 Hz, 2x O_2C-CHBr-C$\underline{H}_3$). ^{13}C NMR ($CDCl_3$): δ 168.71, 148.29, 122.23, 39.57, 21.55. FTIR (solid): ν 2997, 1753.

Polymerization of methyl acrylate using bpy as ligand (11)

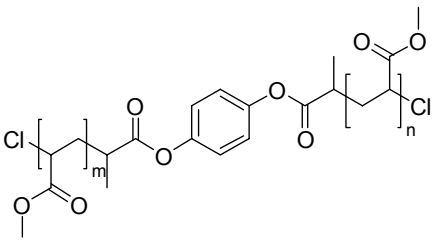

CuCl (397 mg, 4.01 mmol), bpy (1.25 g, 8.01 mmol) and **10** (759 mg, 2.00 mmol) were placed in a Schlenk tube. Deoxygenation was performed by three cycles of evacuation, followed by refilling with nitrogen. Toluene (18 mL) and methyl acrylate (MA) (9.644 g, 112.0 mmol) were added and the reaction mixture was cooled in an ice bath, followed by purging with dry nitrogen for 10 minutes. The reaction mixture was placed in a statically controlled oil bath at 80°C. Samples were taken periodically for conversion analysis. Conversions were determined by GC, using the solvent as an internal standard. Polymers were purified by precipitation in a 0.060 M aqueous EDTA solution, followed by addition of 1 mL 1M aqueous HCl solution and subsequent extraction with DCM. The organic layer was washed with 3 x 200 mL water, dried over anhydrous $MgSO_4$, filtered and concentrated in vacuo to yield 6.92 g (95.4%) of **11**. ^{1}H NMR (300 MHz, $CDCl_3$): δ 7.09 (s, arom. H), 4.29 (br m, 2x CH_2-C$\underline{H}$(Cl) endgroup}, 3.78 (s, 2x OC$\underline{H}_3$ endgroup), 3.66 (s, {CH_2-CH(CO_2C$\underline{H}_3$)}), 2.45-2.22 (br m, {CH_2-C$\underline{H}$(CO_2CH_3)}), 2.05-1.37 (br m, {C$\underline{H}_2$-CH(CO_2CH_3)}), 1.35-1.24 (br m, 2x ArO_2C-C$\underline{H}_3$-). FTIR (solid): ν 2996, 2953, 2849, 1730.SEC (THF): M_n = 3.8 kDa, M_w/M_n = 1.32, $M_{n\ NMR}$ = 3.9 kDa.

Polymerization of MA using 2 as ligand (12)

MA was polymerized according to the procedure described for polymer **11** using MA (5.183 g, 60.2 mmol), **10** (190 mg, 0.50 mmol), CuCl (101 mg, 1.02 mmol) and **2** (299 mg, 2.02 mmol) in 4.0mL xylene at 90°C. Yield: 4.06 g (94.5%). SEC (THF): M_n = 6.7 kDa, M_w/M_n = 1.26.

Polymerization of MA using PMDETA as ligand (13)

MA was polymerized according to the procedure described for polymer **11** using MA (4.843 g, 56.3 mmol), **10** (186 mg, 0.50 mmol), CuCl (97 mg, 0.98 mmol) and PMDETA (197 mg, 1.14 mmol) in 5.1 mL toluene at 70°C. Yield: 2.74 g (90.1%). $M_{n\ NMR}$ = 6.1 kDa. SEC (THF): M_n = 6.8 kDa, M_w/M_n = 1.15.

Azide functionalized telechelic PMA (14)

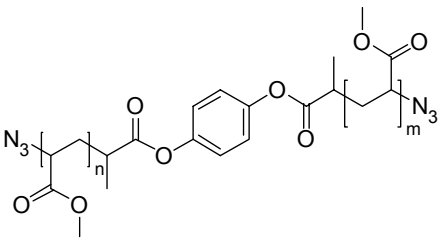

Telechelic PMA **12** (3.152 g, 0.80 mmol) was dissolved in DMF (16 mL). NaN_3 (211 mg, 3.24 mmol) was added to the stirred solution. After stirring for 65 h at room temperature, the reaction mixture was diluted with water followed by three extractions with $CHCl_3$. The organic layer was dried over anhydrous $MgSO_4$, filtered and concentrated in vacuo yielding 2.684 g (85%) product as a dark yellowish viscous polymer. ^{1}H NMR (300 MHz, $CDCl_3$): δ 7.09 (s, arom. H), 3.91 (br m, 2x -CH_2-C<u>H</u>(N_3)- endgroup), 3.80 (s, 2x O<u>C</u>H_3 endgroup), 3.66 (s, {CH_2-CH(CO_2C<u>H</u>$_3$)}), 2.45-2.22 (br m, {CH_2-C<u>H</u>(CO_2CH_3)}), 2.05-1.37 (br m {C<u>H</u>$_2$-CH(CO_2CH_3)}), 1.35-1.24 (br m, 2x ArO_2C-C<u>H</u>$_3$-). FTIR (solid): ν 2998, 2953, 2849, 2114, 1738. SEC (THF, RID) M_n = 3.8, M_w/M_n = 1.36.

Typical procedure for bromophenol blue test

A few drops of the reaction mixture were mixed with a few drops of the bromophenol blue stock solution containing 1 g bromophenol blue sodium salt in 100 g N,N-dimethylacetamide (DMA). This solution selectively stains both primary and secondary amines. A positive test produces a blue color indicating the presence of primary or secondary amines, otherwise it remains yellow.

Amine functionalized telechelic PMA (15)

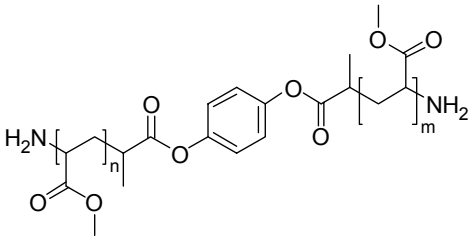

Azide functionalized telechelic PMA **14** (2.514 g, 0.692 mmol) was dissolved in MeOH (50 mL). A catalytic amount of Pd/C was dispersed into the stirred reaction mixture. The flask was evacuated and flushed with hydrogen three times. After the evacuating cycles, the reaction mixture was purged with hydrogen and stirred for two hours at room temperature. Completion of the reaction was determined by a positive bromophenol blue test and complete disappearance of the azide signal in the IR spectrum. The reaction mixture was filtered over hyflo and concentrated in vacuo to yield 1.782 g (72%), slightly orange colored pure viscous polymer. ^{1}H NMR (300 MHz, $CDCl_3$): δ 7.09 (s, Ar<u>H</u>), 4.18 (br m, -C<u>H</u>(NH_2)- endgroup), 3.77 (s, O<u>C</u>H_3 endgroup), 3.66 (br s, {CH_2-CH(CO_2C<u>H</u>$_3$)}), 2.45-2.22 (br m, {CH_2-C<u>H</u>(CO_2CH_3)}), 2.05-1.37 (br m, {C<u>H</u>$_2$-CH(CO_2CH_3)}), 1.35-1.24 (br m, ArO_2C-C<u>H</u>$_3$-). FTIR (solid): ν 2996, 2953, 2849, 1735. SEC (THF): M_n = 3.4 kDa, M_w/M_n = 1.32.

Isocyanate functionalized telechelic PMA (16)

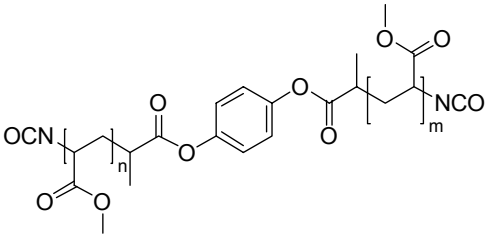

A solution of amine functionalized telechelic PMA **15** (1.754 g, 0.49 mmol) in DCM (20 mL) was added drop wise to a stirred solution of triphosgene (119.8 mg, 0.40 mmol) in DCM (30 mL). After complete addition of the polymer, the reaction mixture was stirred for at least one hour at ambient temperature until complete conversion was ascertained by the negative bromophenol blue test and the appearance of an isocyanate peak in the IR spectrum. The crude product was purified by precipitation in heptane, filtered and dried in vacuo to yield 1.724 g (97%) of a slightly green colored viscous polymer, which was dried under vacuum. ^{1}H NMR (300 MHz, $CDCl_3$): δ 7.09 (s, Ar<u>H</u>), 4.41 (br m, -C<u>H</u>(NCO)- endgroup), 3.77 (s, OCH_3 endgroup), 3.66 (s, {CH_2-CH(CO_2C<u>H</u>$_3$)}), 2.45-2.22 (br m, {CH_2-C<u>H</u>(CO_2CH_3)}), 2.05-1.37 (br m, {C<u>H</u>$_2$-CH(CO_2CH_3)}), 1.35-1.24 (br m, ArO_2C-C<u>H</u>$_3$-). FTIR (solid): ν 2952, 2862, 2253, 1735. SEC (THF) M_n = 3.87 kDa, M_w/M_n = 1.35

Bis(2-cyanoethyl)-polyethylene glycol (17)

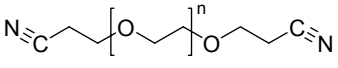

Poly ethylene glycol 1000 (10.0 g, 10 mmol) was dried by two co-evaporations with benzene, after which the dried PEG was dissolved in acrylonitrile and cooled to 0°C. Powdered potassium hydroxide (16.0 mg, 0.285 mmol) was added and the reaction mixture was stirred at 0°C for 110 min. The reaction mixture changed from a colorless clear solution to a clear slightly yellow solution. At this point, the reaction was quenched by addition of 1 drop of concentrated hydrochloric acid (37%). The reaction mixture was concentrated in vacuo, the residue was taken

up into dry DCM. The resulting cloudy solution was filtered and concentrated in vacuo resulting in 10 g (100%) of product as a slightly yellow powder.
^{1}H NMR ($CDCl_3$): δ 3.73 (t, -O-C$\underline{H}_2$-CH_2-CN endgroup), 3.65 (br s, -C$\underline{H}_2$-C$\underline{H}_2$-O- backbone), 2.62 (t, -O-CH_2-C$\underline{H}_2$-CN endgroup). SEC (THF): M_n = 1.8 kDa, PDI = 1.04. MALDI-TOF $[M+Na]^+$ calc. for n = 22, m/z = 1115.6 g/mol, found m/z = 1115.0 g/mol.

Bis(3-aminopropyl)-poly(ethyleneglycol) (18)

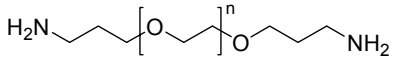

To a cooled (0°C) solution of borane tetrahydrofuran complex (80 mL, 1M in THF, 80 mmol) in dry THF (50 mL) was slowly added a solution of **17** (10 g, 10 mmol) in 100 mL THF. The solution was stirred at 0°C for 60 min, heated to reflux for 4 h. After cooling to room temperature the reaction was quenched by slow addition of 80 mL MeOH (note: gas evolves) followed by addition of 4 mL concentrated HCl (37%). The mixture was stirred at ambient temperature for 45 min after which solvent was removed in vacuo. Residual borate salts were removed by three coevaporations with MeOH (50 mL). The resulting crude product was further purified by dissolving in 1M NaOH solution (150 mL) followed by extraction with DCM. The combined organic layers were dried with $MgSO_4$, filtered and concentrated in vacuo to yield 10.6 g (95%) of white powder.
^{1}H NMR ($CDCl_3$): δ 3.65 (br s, -C$\underline{H}_2$-C$\underline{H}_2$-O- backbone), 3.56 (t, -O-C$\underline{H}_2$-CH_2- endgroup), 2.83 (t, -CH_2-C$\underline{H}_2$-NH_2 endgroup), 1.78-1.72 (m, CH_2-C$\underline{H}_2$-CH_2 and -CH_2-CH_2-N$\underline{H}_2$, endgroup). ^{13}C NMR ($CDCl_3$): δ 70.69, 70.20,69.59, 39.84, 33.02. MALDI-TOF $[M+Na]^+$ calc. for n = 22, m/z = 1123.7 g/mol, found m/z = 1123.1 g/mol.

Coupling of isocyanate functionalized PMA with benzylamine (20)

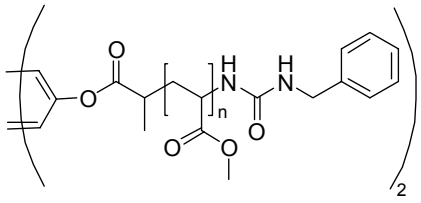

A solution of benzylamine (4.9 mg, 0.046 mmol) in DCM (2 mL) was slowly added to a solution of **16** (81.8 mg, 0.023 mmol) in DCM (5 mL). After complete addition of benzylamine the reaction mixture was stirred at ambient temperature until completion of the reaction was determined by the disappearance of the isocyanate peak in the IR spectrum. The polymer was purified by precipitation in heptane yielding 74.5 mg (86%) of a brownish colored viscous polymer, after drying in high vacuum. ^{1}H NMR (300 MHz, $CDCl_3$): δ 7.34-7.18 (br m, Ar$\underline{H}$ benzyl amine), 7.09 (s, Ar$\underline{H}$ initiator), 4.20 (br m, -C$\underline{H}$(NH-C(=O)-NH)- endgroup), 3.61 (s, OCH_3 endgroup), 3.66 (s, {CH_2-CH($CO_2C\underline{H}_3$)}), 2.45-2.22 (br m, {CH_2-C$\underline{H}$(CO_2CH_3)}), 2.05-1.37 (br m, {C$\underline{H}_2$-CH(CO_2CH_3)}), 1.35-1.24 (br m, ArO_2C-C$\underline{H}_3$-). FTIR (solid): ν 3405, 3064, 1734, 1685.

Coupling of isocyanate functionalized PEG with benzylamine (21)

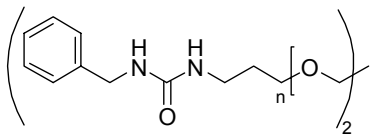

62 mg **18** was dried by coevaporation with dry toluene followed by dissolving in 2.5 mL DCM. This mixture was added dropwise to a solution of 253 mg (0.96 mmol, 48 eq) di tert butyl tricarbonate in 2.5 mL DCM and stirred at ambient temperature for 10 min. 75 µL (0.54 mmol) Et_3N was added and the mixture was stirred for another 10 min., after which 100 µL (0.92 mmol) benzylamine was added. The reaction mixture was concentrated in vacuo and dried under high vacuum. ^{1}H NMR ($CDCl_3$): δ 7.35-7.26 (m, ArH), 4.37 (d, C$\underline{H}_2$-Ar), 3.65 (br s, -C$\underline{H}_2$-C$\underline{H}_2$-O- backbone), 3.56 (t, -O-C$\underline{H}_2$-CH_2- endgroup), 3.41 (t, -CH_2-C$\underline{H}_2$-N endgroup), 1.78-1.72 (m, CH_2-C$\underline{H}_2$-CH_2, -CH_2-CH_2-N$\underline{H}_2$, endgroup). SEC (THF): M_n = 1.8 kDa, PDI = 1.04.

4-*tert*-butyloxycarbonyl-amino butan-1-ol (22)

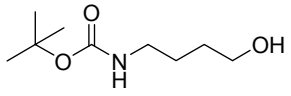

4-amino-1-butanol (1.726 g, 19.36 mmol) was slowly added to a stirred solution of di(tert-butyl) dicarbonate (4.429 g, 19.47 mmol) in THF (30 mL), cooled in an ice bath (0°C). After complete addition of the amino alcohol, the reaction mixture was stirred for another 18 hours at ambient temperature. DCM (50 mL) was added and the organic layer was washed two times with saturated aqueous $NaHCO_3$ (50 mL), two times with brine (50 mL) and distilled water (50mL). The organic layer was dried over anhydrous $MgSO_4$, filtered and concentrated in vacuo, to yield 3.56 g (97%) as a white solid. ^{1}H NMR (200 MHz, $CDCl_3$): δ 4.66 (br s, 1H, O_2C-N$\underline{H}$-CH_2), 3.67 (m, 2H, CH_2-C$\underline{H}_2$-OH), 3.16 (m, 2H, -NH-C$\underline{H}_2$-CH_2), 1.82 (br s, 1H, O$\underline{H}$), 1.59 (m, 4H, CH_2-(C$\underline{H}_2$)$_2$-CH_2), 1.44 (s, 9H, (C$\underline{H}_3$)$_3$-C-O-).

4-*tert*-butyloxycarbonyl-aminobutyl-2-bromoisobutyrate (23)

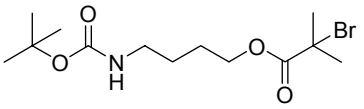

22 (3.498 g, 18.49 mmol), 4-dimethylaminopyridine (227.6 mg, 1.85 mmol) and 2-bromoisobutyric acid (3.0842 g, 18.46 mmol) were dissolved in DCM (150 mL). A solution of N,N'-dicyclohexylcarbodiimide (3.8611 g, 18.71 mmol) in DCM (50 mL) was added dropwise to the stirred reaction mixture at -40 °C. After complete addition, the reaction mixture was stirred for another 18 hours at ambient temperature. TLC indicated complete conversion of substrate. The crude reaction mixture was filtered over hyflo, followed by washing with saturated aqueous $NaHCO_3$ (300 and 100 mL) and distilled water. The organic layer was dried over anhydrous $MgSO_4$, filtered and concentrated in vacuo. The product was further purified by column chromatography (33% heptane / EtOAc) to yield 5.65 g (90%) pure product as a yellowish solid. R_f (33% heptane / EtOAc) = 0.36. ^{1}H NMR (300 MHz, $CDCl_3$): δ 4.60 (br s, 1H, O_2C-NH-CH_2), 4.19 (t, 2H, *J* = 6.6 Hz, CH_2-CH_2-O), 3.17 (q, 2H, *J* = 6.6 Hz, NH-CH_2-CH_2), 1.93 (s, 6H, O_2C-$C(CH_3)_2$Br), 1.73 (m, 2H, CH_2-CH_2-CH_2-O), 1.61 (m, 2H, NH-CH_2-CH_2-CH_2), 1.44 (s, 9H, $(CH_3)_3$-C-O). ^{13}C NMR ($CDCl_3$): δ 171.76, 156.06, 65.72, 56.00, 40.23, 30.88, 28.53, 26.71, 25.86. FTIR (solid): ν 3363, 2973, 2932, 2867, 1732, 1692, 1514, 1458.

α-(4-(tert-butoxycarbonylamino)butyl isobutyrate)-ω-chloropoly[3-(adenin-9-yl)propyl methacrylate] (24)

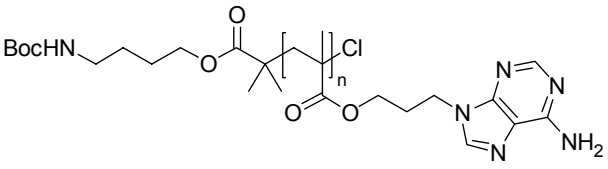

3-(adenin-9-yl)propyl methacrylate **5** (522.9 mg, 2.00 mmol), CuCl (20.2 mg, 0.20 mmol) and bpy (62.4 mg, 0.40 mmol) were placed in a Schlenk tube, followed by three vacuum – nitrogen refill cycles. DMSO-d_6 (5.00 mL) was added and the mixture was nitrogen purged for 5 minutes, followed by heating to 35°C. The polymerization was started by addition of 1.0 mL of a nitrogen purged stock solution of functional initiator **23** (105.2 mg, 0.31 mmol) in DMSO-d_6 (1.50 mL). Samples were taken periodically in order to analyze the monomer conversion with ^{1}H NMR spectroscopy. At the desired conversion, the reaction was stopped by precipitation in an aqueous EDTA solution (0.060 M). The product was filtered, washed with water and dried in vacuum to yield 363 mg (77%) of product.

^{1}H NMR (DMSO-d_6): δ 8.15 (br s, purine-H2,8), 7.21 (br s purine-NH_2), 4.21 (br s, O-CH_2-CH_2 + O-CH_2 init), 3.90 (br s, CH_2-CH_2-N_{purine}), 2.91 (br s, N-CH_2, init) 2.16 (br s, O-CH_2-CH_2-CH_2-N_{purine}), 1.81-1.31 (m, {CH_2-$C(CH_3)$} + Boc CH_3 + CH_2-CH_2 init), 1.00-0.65 (br m, {CH_2-$C(CH_3)$}). SEC (DMSO): M_n = 2.6 kg/mol, M_w/M_n = 1.26.

α-(4-(tert-butoxycarbonylamino)butyl isobutyrate)-ω-chloropoly[3-(thymin-1-yl)propyl methacrylate] (25)

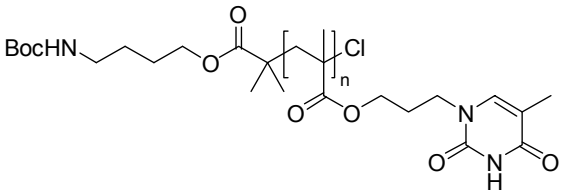

Polymer **25** was prepared according to the same procedure as described for polymer **24**, using 3-(thymin-1-yl)propyl methacrylate **6** (505.6 mg, 2.00 mmol), CuCl (20.8 mg, 0.21 mmol) and bpy (62.7 mg, 0.40 mmol) in 4.00 ml DMSO-d_6. The polymerization was performed at 45°C and started by addition of 1.0 mL of a stock solution containing **23** (68.8 mg, 0.20 mmol) in 1.0 mL DMSO-d_6.

^{1}H NMR (DMSO-d_6): δ 11.18 (br s, pyrimidine-NH), 7.45 (br s, pyrimidine-H6), 4.11 (br s, O-CH_2 init), 3.93 (br s, O-CH_2-CH_2), 3.69 (br s, CH_2-CH_2-N), 2.90 (br s, CH_2-N), 1.90-1.70 (br s, CH_2-CH_2-CH_2-N,), 1.80-1.60 (br m, {CH_2-$C(CH_3)$} + pyrimidine-CH_3 + CH_2-CH_2 init), 1.35 (s, CH_3 Boc) 1.10-0.65 (br m, {CH_2-$C(CH_3)$}). M_n (^{1}H NMR) = 2.6 kg/mol, DP (^{1}H NMR) =9.3. SEC (DMSO): M_n = 3.2 kg/mol, M_w/M_n = 1.42.

α-(4-aminobutyl isobutyrate)-ω-(chloro)poly[3-(adenin-9-yl)propyl methacrylate.*x*TFA (26)

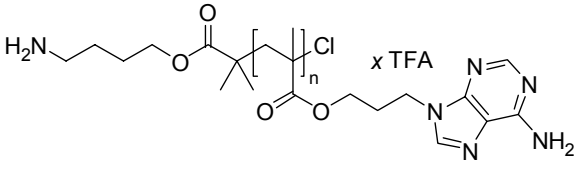

Boc protected oligo-adenine **24** (330.3 mg, 0.14 mmol) were dissolved in TFA (4 mL) and the reaction mixture was stirred for 4 hours. The reaction mixture was precipitated in Et_2O, collected and dried under vacuum. Yield: 451 mg.

^{1}H NMR (DMSO-d_6): Characteristic peak at δ = 1.35 ppm (s, Boc CH_3) was no longer present.

α-(4-aminobutyl isobutyrate)-ω-(chloro)poly[3-(thymin-1-yl)propyl methacrylate.*x*TFA (27)

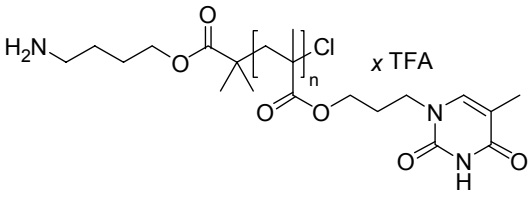

Boc protected oligo-thymine **25** (165.0 mg, 0.059 mmol) and PhSH (10 μL, 0.097 mmol) were dissolved in TFA (2 mL) and the reaction mixture was stirred for 4 hours. The reaction mixture was precipitated in Et_2O, collected and dried under vacuum. Yield: 122 mg (76%).
^{1}H NMR (DMSO-d_6): Characteristic peak at δ = 1.35 ppm (s, Boc C$\underline{H}_3$) was no longer present.

Coupling of amine functionalized oligo-thymine 27 with isocyanate functionalized telechelic PMA (29)

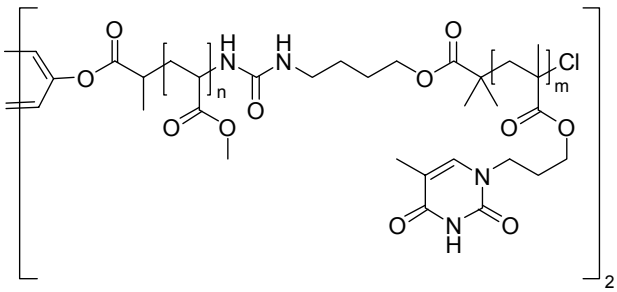

A solution of **16** (54.3 mg, 0.0092 mmol) in DMF (2.5 mL) was added dropwise to a solution of **27** (54.3 mg, 0.019 mmol) and DiPEA (6 μL, 0.034 mmol) in DMF (2.5 mL). After 6 hours stirring at room temperature, completion of the reaction was determined by a negative bromophenol blue test and the disappearance of the isocyanate peak in the IR spectrum. The polymer was purified by precipitation in 0.1 M aqueous HCl solution, triturated in water, collected and dried under vacuum to yield 67 mg (89%) of product. SEC (DMSO): M_n = 8.4 kg/mol, M_w/M_n = 1.28. FTIR (solid): ν 1730, 1687, 1664. ^{1}H NMR ($CDCl_3$): δ 11.17 (br s, pyrimidine-NH) 7.46 (br s, pyrimidine-H6), 7.16 (s, Ar$\underline{H}$), 3.93 (br s, O-C$\underline{H}_2$-CH_2), 3.65 (br s, -C$\underline{H}_2$-C$\underline{H}_2$-O- backbone), 3.56 (t, -O-C$\underline{H}_2$-CH_2- endgroup), 3.41 (t, -CH_2-C$\underline{H}_2$-N endgroup), 1.78-1.72 (m, CH_2-C$\underline{H}_2$-CH_2, -CH_2-CH_2-N$\underline{H}_2$, endgroup).

Coupling of amine functionalized oligo-thymine 27 with isocyanate functionalized telechelic PEG (30)

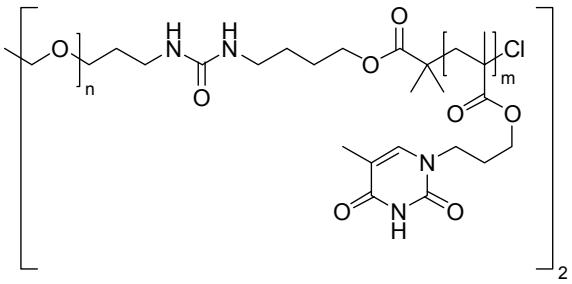

70.4 mg (0.0117 mmol) of **18** was dissolved in dry benzene and evaporated to dryness two times after which the dried PEG was dissolved in 4 mL dry DCM. This solution was added to a solution containing 9.2 mg (0.035 mmol) in 1.5 mL DCM. A solution of 194.7 mg (0.0885 mmol) **27** and 0.1 mL Et_3N in 1.5 mL DMF was added in a dropwise fashion to the PEG reaction mixture, while additional DMF was added to aid solubility, the reaction mixture was allowed to stir overnight. The crude product was concentrated in vacuo, co-evaporated with toluene to remove excess DMF, followed by suspension in THF. The product was isolated by spinning down the precipitate in a centrifuge after which decantation of the supernatant was followed by resuspending the pellet in heptane, centrifuging and decantation. The pellets were collected by dissolution in DCM and concentrated in vacuo to yield 17 mg of product. SEC (THF): M_n = 11.3 kg/mol, M_w/M_n = 1.10. ^{1}H NMR (DMSO-d_6): δ 11.17 (br s, pyrimidine-NH), 7.46 (br s, pyrimidine-H6), 3.91 (br s, O-C$\underline{H}_2$-CH_2), 3.68 (br s, CH_2-C$\underline{H}_2$-N), 3.51 (br s, O-C$\underline{H}_2$-C$\underline{H}_2$-), 1.89 (br s, CH_2-C$\underline{H}_2$-CH_2-N,), 1.73 (s, pyrimidine-C$\underline{H}_3$), 1.10-0.65 (br m, {CH_2-C(C$\underline{H}_3$)}).

5.10 References

1. C. J. Pedersen. *J. Am. Chem. Soc.* **1967**, *89*, 7017-7036.
2. J. M. Lehn. *Angew. Chem., Int. Ed.* **1988**, *27*, 89-112.
3. D. J. Cram. *Angew. Chem., Int. Ed.* **1988**, *27*, 1009-1020.
4. M. Kotera, J. M. Lehn and J. P. Vigneron. *Tetrahedron* **1995**, *51*, 1953-1972.
5. M. Muller, A. Dardin, U. Seidel, V. Balsamo, B. Ivan, H. W. Spiess and R. Stadler. *Macromolecules* **1996**, *29*, 2577-2583.
6. H. A. Klok, K. A. Jolliffe, C. L. Schauer, L. J. Prins, J. P. Spatz, M. Moller, P. Timmerman and D. N. Reinhoudt. *J. Am. Chem. Soc.* **1999**, *121*, 7154-7155.
7. T. J. Katz. *Angew. Chem., Int. Ed.* **2000**, *39*, 1921-+.
8. L. Brunsveld, B. J. B. Folmer, E. W. Meijer and R. P. Sijbesma. *Chem. Rev.* **2001**, *101*, 4071-4097.
9. F. H. Beijer, R. P. Sijbesma, H. Kooijman, A. L. Spek and E. W. Meijer. *J. Am. Chem. Soc.* **1998**, *120*, 6761-6769.
10. J. Hirschberg, F. H. Beijer, H. A. van Aert, P. Magusim, R. P. Sijbesma and E. W. Meijer. *Macromolecules* **1999**, *32*, 2696-2705.
11. B. J. B. Folmer, R. P. Sijbesma, R. M. Versteegen, J. A. J. van der Rijt and E. W. Meijer. *Adv. Mater.* **2000**, *12*, 874-878.
12. R. P. Sijbesma, F. H. Beijer, L. Brunsveld, B. J. B. Folmer, J. Hirschberg, R. F. M. Lange, J. K. L. Lowe and E. W. Meijer. *Science* **1997**, *278*, 1601-1604.
13. G. Ligthart, H. Ohkawa, R. P. Sijbesma and E. W. Meijer. *J. Am. Chem. Soc.* **2005**, *127*, 810-811.
14. S. J. Rowan, P. Suwanmala and S. Sivakova. *J. Polym. Sci., Part A: Polym. Chem.* **2003**, *41*, 3589-3596.
15. S. Sivakova and S. J. Rowan. *Chem. Soc. Rev.* **2005**, *34*, 9-21.
16. E. A. Fogleman, W. C. Yount, J. Xu and S. L. Craig. *Angew. Chem., Int. Ed.* **2002**, *41*, 4026-4028.
17. J. Xu, E. A. Fogleman and S. L. Craig. *Macromolecules* **2004**, *37*, 1863-1870.
18. J. Xu and S. L. Craig. *J. Am. Chem. Soc.* **2005**, *127*, 13227-13231.
19. V. Coessens, Y. Nakagawa and K. Matyjaszewski. *Polym. Bull.* **1998**, *40*, 135-142.
20. V. Coessens and K. Matyjaszewski. *J. Macromol. Sci., Pure Appl. Chem.* **1999**, *A36*, 667-679.
21. S. A. F. Bon, A. G. Steward and D. M. Haddleton. *J. Polym. Sci., Part A: Polym. Chem.* **2000**, *38*, 2678-2686.
22. D. M. Haddleton, M. C. Crossman, B. H. Dana, D. J. Duncalf, A. M. Heming, D. Kukulj and A. J. Shooter. *Macromolecules* **1999**, *32*, 2110-2119.
23. G. Odian. Principles of Polymerization. 3rd Ed, ed., 1991; Vol.
24. S. Ozaki. *Chem. Rev.* **1972**, *72*, 457-&.
25. E. F. V. Scriven and K. Turnbull. *Chem. Rev.* **1988**, *88*, 297-368.
26. H. J. Knolker, T. Braxmeier and G. Schlechtingen. *Angew. Chem., Int. Ed.* **1995**, *34*, 2497-2500.
27. H. W. I. Peerlings and E. W. Meijer. *Tertahedron Lett.* **1999**, *40*, 1021-1024.
28. X. Zhang and K. Matyjaszewski. *Macromolecules* **1999**, *32*, 7349-7353.
29. H. W. I. Peerlings, R. A. T. Van Benthem and E. W. Meijer. *J. Polym. Sci., Part A: Polym. Chem.* **2001**, *39*, 3112-3120.
30. W. Saenger. *Principles of Nucleic Acid Structure*, ed.; Springer-Verlag: New York, 1984; Vol.
31. S. Mohammadi, R. Klement, A. K. Shchyolkina, J. Liquier, T. M. Jovin and E. Taillandier. *Biochemistry* **1998**, *37*, 16529-16537.
32. M. Banyay, M. Sarkar and A. Graslund. *Biophys. Chem.* **2003**, *104*, 477-488.
33. F. Geinguenaud, J. A. Mondragon-Sanchez, J. Liquier, A. K. Shchyolkina, R. Klement, D. J. Arndt-Jovin, T. M. Jovin and E. Taillandier. *Spectrochim. Acta, Part A* **2005**, *61*, 579-587.
34. R. N. Keller and H. D. Wycoff. *Inorganic Syntheses* **1946**, *2*, 1-4.

Chapter 6

Probing the use of nucleobase functionalized block copolymers as a gene delivery system

6 Probing the use of nucleobase functionalized block copolymers as a gene delivery system

6.1 General introduction

In principle, gene therapy is simple: putting corrective genetic material into cells diminishes the symptoms of disease. In practice, considerable obstacles have emerged before gene therapy can be safely applied in the clinic. A key limitation to development of human gene therapy remains the lack of safe, efficient and controllable methods for gene delivery[1]

In general, many physiological and cellular barriers need to be overcome to achieve expression of a gene in a certain cell type within the body (figure 1). DNA is a large polyanionic molecule, which in not internalized by eukaryotic cells. Consequently, it has to be condensed by complexation with other molecules to a size that allows it to be taken up into cells[2]. Additionally, the DNA complex should be stable under physiological conditions and not lead to inflammation or any other immunological response. Once the complexes have reached the target cells, they need to be taken up efficiently and then processed in the appropriate fashion to allow efficient transfer from the endosome to the cytoplasm and, finally, the nucleus. This requires effective traversing of intracellular compartments. The lack of efficiency for these steps probably represents the great number of challenges for synthetic gene delivery systems.

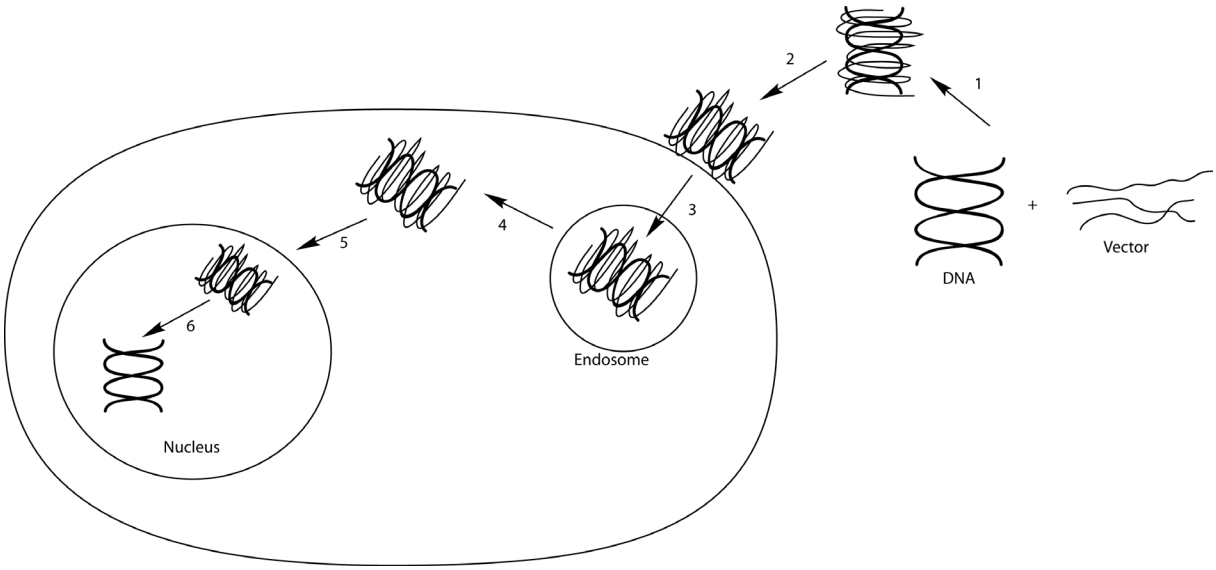

Figure 1. (1) formation of the DNA complex by condensation of DNA with the delivery vector, (2) binding of the DNA complex with the target cell, (3) uptake into intracellular endosomes, (4) release form endosomes intro the cytoplasm, (5) intracellular transport and nuclear localization of the DNA, (6) DNA release.

Gene delivery vehicles can be divided into two categories: recombinant viruses, and synthetic vectors, which can be further subdivided into polymers[3, 4] and lipids[5, 6]. Each delivery method has specific advantages and disadvantages. Safety concerns have been the primary bottleneck to the clinical application of viral gene delivery. Although recombinant viral vectors are rendered non-replicative and therefore non-pathogenic, there still exists the possibility that the virus will revert to a wild-type virion. Furthermore, viruses are inherently immunogenic, leading to the possibility of immune reactions.

Synthetic vectors on the other hand provide opportunities for greater safety and flexibility. In general, synthetic vectors are materials that electrostatically bind DNA or RNA, condense the genetic material into particles of several hundreds of nanometers, protect the genes and mediate in cellular uptake. figure 2 depicts the formation of polyplexes upon mixing solutions of a polycation and DNA. Polyplexes are formed by electrostatic interactions between polycations and DNA. For gene delivery, an excess of polycation is typically used, which generates particles with a positive surface charge. Each particle consists of several plasmid DNA molecules and hundreds of polymer chains and is 100–200 nm in diameter.

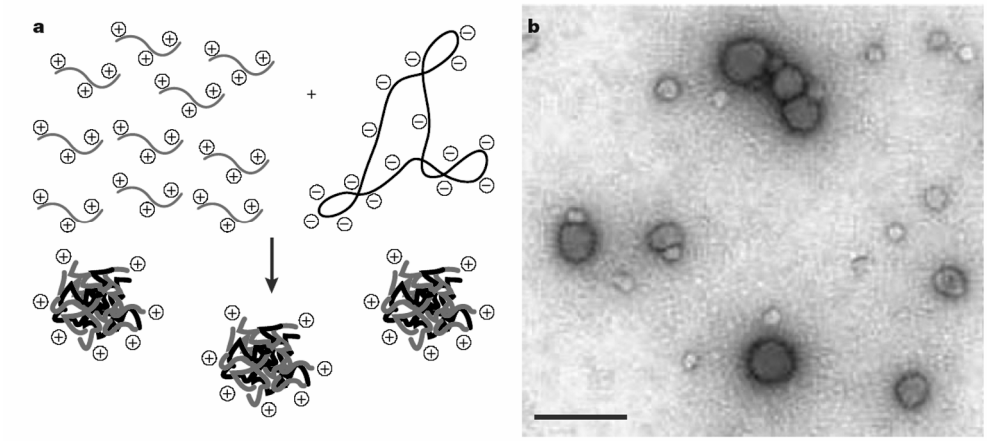

Figure 2. a) Spontaneous polyplex formation between cationic polymers and plasmid DNA b) Transmission electron micrograph of polyplexes comprising plasmid DNA and a polycation.

It is important to note that strong DNA binding and efficient DNA condensation do not correlate directly with gene delivery efficiency, probably because tight binding prevents transcription. A polymer must therefore balance sufficient binding strength, to initially protect the plasmid DNA, with the ability to release the plasmid, perhaps by competition binding of genomic DNA.

A known drawback of polyplexes is that in physiological salt concentrations large aggregates are quickly formed, which are generally inefficient gene-delivery agents, and can even be toxic. Positively charged polyplexes typically remain in solution, however absorption of negatively charged proteins onto these positive complexes causes further aggregation and can lead to rapid clearance of the polyplex from the blood circulation, to organs like lungs and liver.

To circumvent these problems, polyplexes were modified with hydrophilic polymers such as PEG[7-9], N-(2-hydroxypropyl)methacrylate (HPMA)[10, 11] and oligosaccharides[10]. Many of the polymer materials were specifically designed for gene delivery and address a specific issue such as stability or biocompatibility. Although the polymers currently used for gene delivery systems are not as effective as viruses, their versatility and tune-ability offer great opportunities and inspire researchers to continue investigation towards polymer gene and drug delivery systems.

The fact that several studies have found that a reduced polymer/DNA binding strength[12] and conjugation with PEG[13] tails lead to increased gene expressions inspired us to investigate the use of nucleobase functional block copolymers prepared in the previous chapters as gene delivery vehicles.

6.2 DNA binding

The DNA binding studies were all performed with materials PEG-*b*-T10 and PEG-*b*-A10 (figure 3) prepared as described in chapter 3. It was found that these materials have good water solubility and due to the amphiphilic character caused by the PEG (DP=45) and polymethacrylate (DP=10) backbone, the block copolymers produced aggregates in aqueous solutions. It was found that mixing solutions containing PEG-*b*-A10 and PEG-*b*-T10 resulted in a new aggregate, which contained both thymine and adenine functionality. The driving

force for complete mixing of the aggregates is most likely the nucleobase interactions between thymine and adenine moieties.

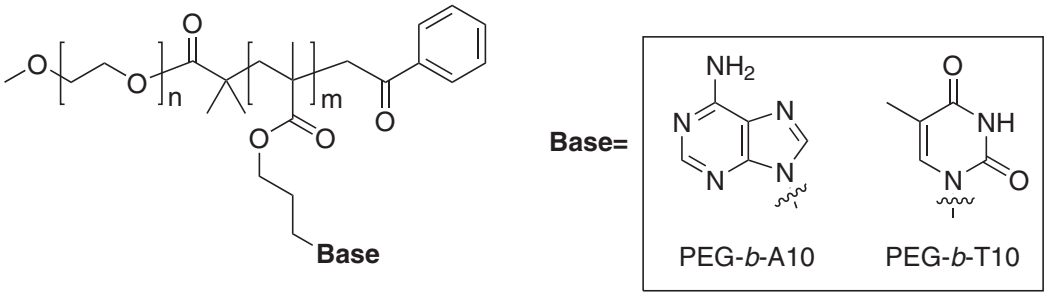

Figure 3. PEG-*b*-A10 and PEG-*b*-T10 used for DNA binding experiments.

6.2.1 Single stranded DNA

To investigate whether the block copolymers could bind to DNA and whether selectivity in binding occurred, the block copolymers PEG-*b*-A10 and PEG-*b*-T10 were mixed in different nucleobase ratios with a 100-mer of single-stranded oligo Thymine DNA ($ssDNA_{T100}$). It is known that ssDNA strands can form loops, which might prevent or obstruct binding with the nucleobase functionalized polymers. Therefore, the samples were mixed and the resulting clear solutions were subjected to heat treatment by annealing them from boiling water to ambient temperature overnight, to facilitate binding and prevent the occurrence of any $ssDNA_{T100}$ conformations that could hinder complex formation with the block copolymers.

If binding of the block copolymers with $ssDNA_{T100}$ would occur, the size of the DNA species would increase by complex formation and the mass to charge ratio would change. As a result, the DNA-polymer complex would have a lower migration speed during electrophoresis than the unbound ssDNA.

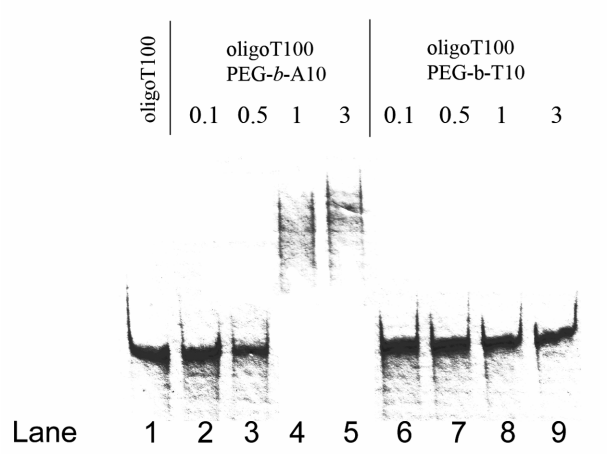

Figure 4. Gel electrophoresis of $ssDNA_{T100}$ (lane 1), mixed with PEG-*b*-A10 (lanes 2 – 5) or PEG-*b*-T10 (lanes 6-9). The numbers above the lanes represent the ratio of polymer-bound nucleobase to DNA nucleobase content.

Depicted in figure 4 is a scan of the obtained gel after electrophoresis after staining with stains-all. As can be clearly seen, PEG-*b*-T10 (lanes 6-9) has no effect on the migration of the non-complementary ssDNAT100 (lane 1), even when up to 10 equivalents of block copolymer were added. Surprisingly, PEG-*b*-A10 (lanes 2-5) affects the migration significantly, since the ssDNAT100 band runs significantly higher upon mixing. As can be seen clearly, mixing DNA with complementary polymer in an equimolar nucleobase ratio completely binds the single stranded DNA.

6.2.2 Plasmid DNA

These successful and selective binding studies with ss-DNA prompted us to expand the scope of DNA binding experiments towards double stranded DNA. Bacterial Blue Script plasmid DNA (pDNA) isolated from *E-coli* bacteria was used to investigate polymer binding. Plasmid DNA is a double stranded circular DNA molecule, which contains about 3000 base pairs and is therefore significantly larger than the block copolymers used. Consequently, the nucleobase block copolymers are not completely complementary with the pDNA sequence and due to the double strand, compete with base pairing or bind to the dsDNA in a different fashion, compared to the single stranded DNA.

Solutions of the block copolymer were mixed with pDNA and binding was analyzed by gel electrophoresis on a 0.8% agarose gel. The DNA was visualized using ethidium bromide, which is a commonly used staining agent. It intercalates into the double-stranded regions of nucleic acids where it will fluoresce upon irradiation with UV light.

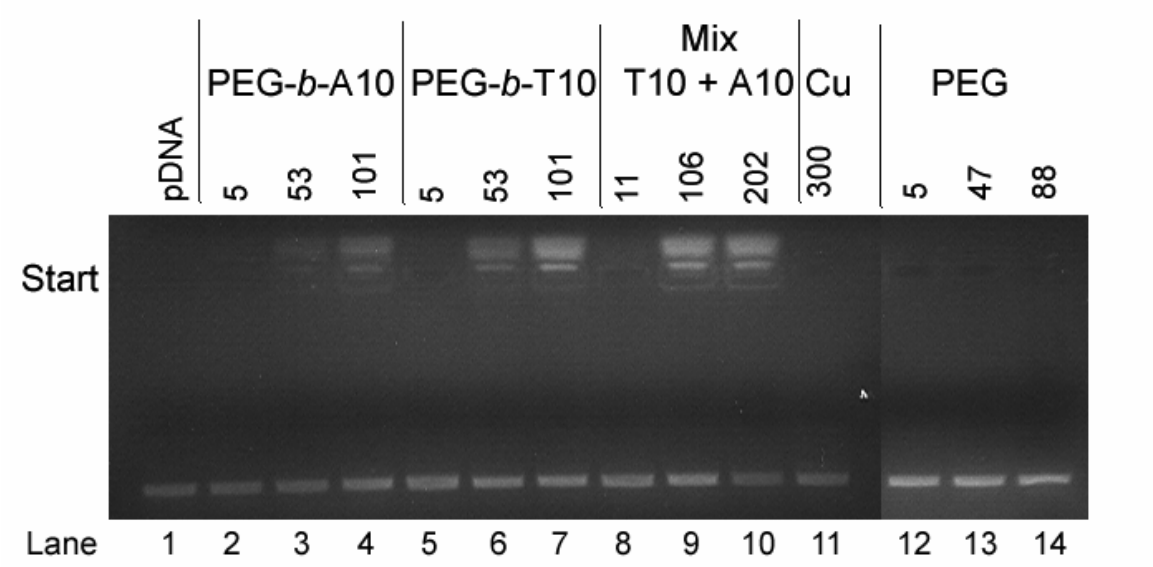

Figure 5. Gel-electrophoresis of pDNA mixed with the different block copolymers. Samples were mixed and loaded at ambient temperature. Lane numbers are depicted below the gel, and the numbers above the gel indicate the molar ratio of nucleobases in the polymer to the total nucleobase content of the pDNA.

As can be seen in figure 5, binding of the block copolymers with pDNA seems to occur. The fluorescence intensity increased in and around the wells with increasing polymer concentration, while the intensity of the unbound pDNA band decreased slightly. This effect was most pronounced when comparing lanes 8, 9 and 10. Although in all cases binding was not complete, the retardation of pDNA migration was most pronounced when an excess of a mixture of PEG-*b*-A10 and PEG-*b*-T10 was used. Control experiments in which only PEG or Cu(II) was added to the DNA, were also performed. Since both the block copolymers contain a PEG chain, the influence of PEG alone was investigated, and because the polymers were prepared using ATRP, the effect of any possible residual copper was studied. As can be seen in figure 5, both control experiments were negative, meaning that both compounds do not affect the migration of pDNA.

In order to investigate whether DNA binding can be enhanced by heat treatment, pDNA was mixed with both block copolymers and allowed to anneal from boiling water to ambient temperature overnight. DNA binding was analyzed using the same conditions as before.

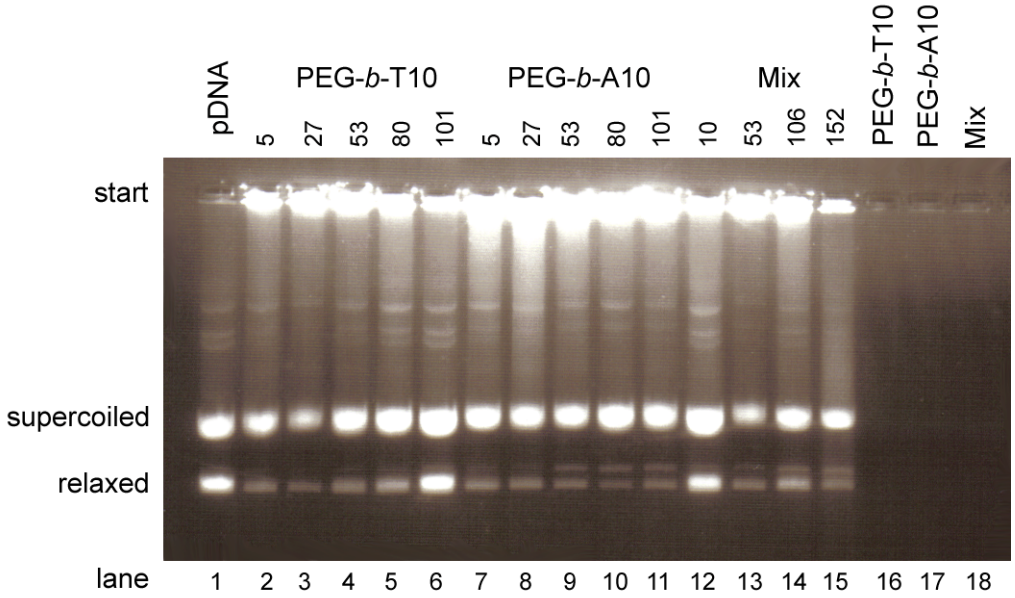

Figure 6. Gel-electrophoresis of pDNA mixed with the different block copolymers. Samples were mixed, annealed from boiling water to ambient temperature and loaded. Numbers above the lanes indicate the molar ratio of nucleobases in the polymer to the total nucleobase content of the pDNA.

As can be seen on the gel depicted in figure 6, an additional band was observed for pDNA when compared to the untreated samples. This is a known phenomenon and occurs when pDNA is annealed. Normally when pDNA is isolated from the bacteria, it is in a relaxed open circular form. When heated, followed by slowly cooling, the DNA strands can twist around each other creating a supercoiled structure. Due to this folding, the size-charge ratio changes, and hence the migration speed on gel will be different.

In all samples some binding of the polymer to the DNA could be observed, however binding was very inconsistent and increasing the polymer nucleobase content up to 202 equivalents did not give complete retardation of DNA migration. Nevertheless, the relaxed pDNA (lowest DNA band) seems to bind more effective to the polymers compared to the supercoiled pDNA. Additionally it could be observed that the fluorescence in the starting slots is caused by pDNA and was not due to residual PEG block copolymer (lanes 16-18).

6.3 Discussion

Since only the PEG block copolymer functionalized with the complementary adenine moiety can affect the electrophoresis properties of the $ssDNA_{T100}$, a logical assumption would be that complex formation occurs via selective complementary base pairing. It must be noted that these experiments do not give any information about the structure of the DNA-polymer complex or the mode of binding between the block copolymer and $ssDNA_{T100}$.

The binding efficiency for double stranded DNA is much lower compared to binding single stranded complementary DNA. Reason for this could be that Blue Script pDNA is relatively much bigger and contains no complementary sequence. Additionally, the polymer has to compete with the completely complementary plasmid DNA itself since the experiment with single stranded DNA has shown that binding predominantly occurs via nucleobase interaction. Therefore, it was estimated that annealing might have a positive effect on the binding efficiency. However, heat treatment upon which the double stranded DNA is melted into two single strands, did not have a significant effect on binding efficiency, although the relaxed DNA seems to bind better. The lower efficiency of binding plasmid DNA compared to single-stranded oligo thymidine is therefore probably predominantly caused by the fact that polymers containing only 2 out of 4 nucleobases were added and that no sequence specificity was introduced.

6.4 Towards DNA transfection

As described in chapter 4 of this thesis, it was found that the thymine and adenine nucleobase functionalized block copolymers PEG-*b*-T10 and PEG-*b*-A10 create small aggregates in aqueous solutions, and it was shown that these block copolymers could bind selectively to single stranded complementary DNA and in a lesser extent to plasmid DNA. In addition, it is known from literature, that polymeric aggregates can be used as gene delivery vectors[11, 2, 8]. These results prompted us to investigate the possibility to apply our PEG block copolymers as gene delivery vectors. Two experiments were conducted. First, both the adenine and thymine PEG block copolymers were used as gene delivery vehicles without the presence of any other transfection agent. In a second attempt, similar to the first experiment PEG block copolymers were added to the DNA after which the DNA-polymer mixture was further condensed with $CaCl_2$. This method is often referred to as PEGylation[14-16].

In order to test the ability to act as gene delivery system and to evaluate the cytotoxicity of a mixture of PEG-b-T10 and PEG-b-A10 experiments were performed with HELA cells (human cancer cell line). Two different plasmids, the EGFP (enhanced green fluorescent protein) and β-gal (beta galactosidase) plasmids were chosen for transfection. Both EGFP and β-gal are not naturally occurring proteins in the cell line, and are therefore suitable for transfection. EGFP can be easily detected using fluorescence microscopy, while β-gal can be detected using a specific assay. pDNA was mixed with both PEG-*b*-A10 and PEG-*b*-T10 polymers, after which the polymer pDNA mixture was incubated with the cells in serum containing culture medium for 24 hours. Using the fluorescence microscope it was observed that after incubation the cells were flourishing, however no fluorescence could be detected, indicating no transfection of the pDNA had occurred.

The next possibility to use the block copolymers as gene transfection carriers is to PEGylate. Using this method, DNA is condensed into small particles using cations or cationic materials, and coated with PEG in order to protect the DNA particles from further coagulation and to enhance the transfection efficiency. As a DNA condensation method we chose to use calcium(II)chloride salts. This is a relative simple and known procedure to condense DNA for transfection, but it has the disadvantage that in the presence of negatively charged proteins coagulation of the condensed DNA salt particles occurs, resulting in large aggregates that are too large for internalization by the cells. This coagulation is especially problematic if transfection needs to be performed *in vivo* or under more physiological conditions. These coagulation problems could be tackled by adding the nucleobase functionalized PEG block copolymers to the condensed calcium DNA particles (PEGylation). The hypothesis is that the DNA is condensed by the calcium salts and the resulting particles are then shielded from protein interactions by the PEG block copolymer.

For the PEGylation studies a mixture of Bluescript, β-gal and luciferase plasmid DNA (80/10/10, BlueScript/β-gal/luciferase) was prepared. The DNA particles were prepared by mixing the pDNA mixture with $CaCl_2$ and different equivalents of PEG-*b*-T10/PEG-*b*-A10 mixture (5 and 10 weight equivalents). HEKS-293 cells were chosen because of their known high transfection efficiencies with calcium chloride. The DNA/polymer particles were then added to the well plates containing HEKS-293 cells. All experiments were conducted in

duplo and additionally at both equivalents of PEG, the transfection mixture was left either on the cells or removed after a certain time period.

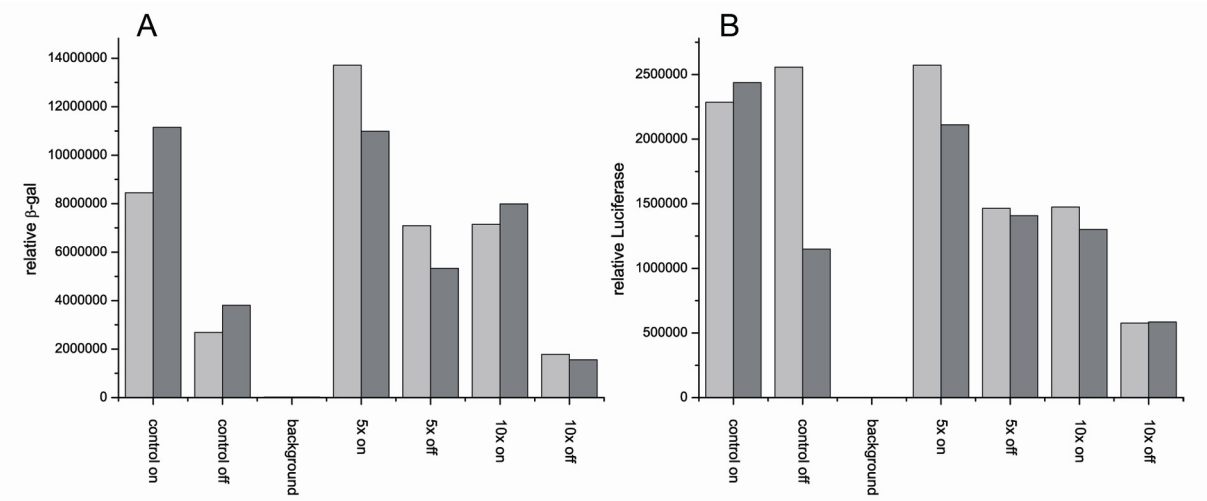

Figure 7. Transfection of HEKS-293 cells using Ca^{2+} with different weight equivalents (5 and 10) of polymer to plasmid DNA, while the transfection mix was left ON or removed (OFF) from the cells.

As can be seen in figure 7, transfection occurred when calcium salts were used to condense DNA, both in the presence and absence of the nucleobase block copolymers. Although the transfection results of the samples in which the PEG nucleobase block copolymers were added did not improve drastically, the transfection does occur at comparable or even slightly higher levels when up to 5 equivalents of PEG block copolymer were used. When 10 equivalents were applied, the transfection efficiency was clearly lowered.

6.5 Discussion and outlook

PEG nucleobase block copolymers alone are not capable of performing gene transfection into human cell lines under the conditions tested. There are a number of reasons possible, but the most probable reason is that DNA is not condensed enough in order to create small particles, capable of internalization by the cells. Therefore, the second possibility to use the PEG block copolymer for PEGylation seems more promising. Calcium(II)chloride was used to condense the pDNA and the PEG block copolymers should shield off the DNA particles to prevent further coagulation.

The problem occurring with calcium chloride DNA condensation is that large aggregates of the DNA calcium salts can be formed in the presence of negatively charged proteins, commonly present under physiological conditions. The *in vitro* conditions we tested however, do not have the aggregation problem, but were used to see whether the PEG nucleobase block copolymers could influence the calcium transfections.

It was observed that the PEG block copolymers did not have a negative effect on the transfection efficiency when up to 5 equivalents were added. Increasing the amount of PEG block copolymer reduced the transfection efficiency.

Obviously, more detailed studies concerning particle sizes and different ratios of polymer/DNA/salt need to be performed, as well as an in vivo evaluation of the shielding effect of the PEG nucleobase block copolymers, to have a better understanding of the added value of this approach. Nevertheless, these preliminary results are encouraging enough to validate further research in this area.

6.6 Experimental

Materials
Stains-All was obtained from Aldrich, Pen Strep (500x) obtained from Roche Diagnostics Netherlands, Fetal Bovine Serum Gold (fetal calf serum): PAA via New Brunswick, EMEM (BioWhitaker TM) from Cambrex Bio Science and pDNA was kindly provided by Mark Damen.

sDNA binding studies
For electrophoresis $1.65*10^{-6}$, $8.25*10^{-6}$, $1.65*10^{-5}$ and $4.95*10^{-5}$ molar samples of PEG-*b*-A10 and PEG-*b*-T10 were prepared by diluting a 1 mg/mL PEG-*b*-T10 and PEG-*b*-A10 stock solution with 4 μL binding buffer (10mM TRIS 0.1mM EDTA + 10% glycerol), 1 μL $ssDNA_{T100}$ ($3.3*10^{-5}$ μmol) and water to a total sample volume of 20 μL. The samples were put in boiling water and allowed to cool to ambient temperature overnight by switching off the heater, before loading onto a 10% acryl amide gel containing 1 mL 10xTBE (Tris, BoricAcid, EDTA), 1.5 mL 40% acryl amide, 7.5 mL water, 4μL TEMED. The gel was run at 150V for approximately 4 min after which it was stained using Stains-All. As a control, a sample containing only the $ssDNA_{T100}$ was also run. .

pDNA binding experiments

$1.1*10^{-4}$, $1.1*10^{-3}$ and $2.1*10^{-3}$ molar samples of PEG-*b*-T10 and PEG-*b*-A10 were prepared by diluting a 10 mg/mL polymer stock solution with 1 μg BlueScript pDNA and TRIS buffer to a total sample volume of 20μL. for the mixed samples $2.2*10^{-4}$, $2.2*10^{-3}$ and $4.2*10^{-3}$ molar (PEG-*b*-T10 + PEG-*b*-A10) were prepared by diluting a 10 mg/mL stock solution of PEG-b-T10 with a 10 mg/mL PEG-b-A10, 1 μg BlueScript pDNA and TRIS buffer to a total sample volume of 20μL. To all samples was added 2.5 μL binding buffer (50 mM TRIS, 0.5 mM EDTA with 10% (v/v) glycerol and 0.4% (w/v) bromophenol blue) before loading onto a 0.8% agarose gel containing ethidium bromide and run at 120 V. As reference naked pDNA was also run. After electrophoresis, pDNA was visualized by exposure to UV light and photographed.

The annealed samples were prepared in a similar fashion as described above but were put into a water bath (at boiling temperature) and allowed to cool overnight by immediate removal of the heat source before loading buffer was added and run according to the procedure described above

Transfection studies of HEKS-293 cells using $CaCl_2$

HEKS-293 cells were cultured in standard DMEM + 10% FCS (fetal calf serum) + Pen/Strep at 37°C and 5% CO_2. 2 hours prior to transfection the cell culture was split to about 20-30% confluency per well.
Three transfection mixtures containing 0, 80 and 344 μL of a polymer mixture (1 μg polymer/μL, containing a 1:1 weight ratio of PEG-*b*-T10 and PEG-*b*-A10) were all diluted with 16 μL of a DNA stock solution (containing 4.8 μg/μL Luciferase, 4.8 μg/μL b-galactose, 38.4 μg/μL BlueScript), 40 μl of 2.5M $CaCl_2$ and enough water (milliQ) to bring the total volume to 0.4 mL. The $CaCl_2$/DNA/polymer mixture was added slowly to 0.4 mL 2xHBS (8 g NaCl, 0.2 g Na2HPO4.7H2O, 6.5 g HEPES, dissolved in distilled water. Adjust pH to 7.0 and bring up to 500 mL with distilled water) while mixing gently during the addition followed directly by dropwise addition of the diluted $CaCl_2$/DNA/polymer mixture to the well plates containing the HEKS cells (100 μL per well) and incubated at 37°C/5% CO_2 for 16 hours. For the ON samples fresh growth medium was added without removal of the transfection medium while incase of the OFF samples the media was removed and cells were washed once with warm PBS, followed by addition of fresh medium and resume incubation for 24 hours prior to assaying.

6.7 References

1. I. M. Verma and N. Somia. *Nature* **1997**, *389*, 239-242.
2. M. D. Brown, A. G. Schatzlein and I. F. Uchegbu. *Int. J. Pharm.* **2001**, *229*, 1-21.
3. C. Dufes, I. F. Uchegbu and A. G. Schatzlein. *Adv. Drug Delivery Rev.* **2005**, *57*, 2177-2202.
4. D. W. Pack, A. S. Hoffman, S. Pun and P. S. Stayton. *Nat. Rev. Drug Discovery* **2005**, *4*, 581-593.
5. P. L. Felgner, T. R. Gadek, M. Holm, R. Roman, H. W. Chan, M. Wenz, J. P. Northrop, G. M. Ringold and M. Danielsen. *Proc. Natl. Acad. Sci. U. S. A.* **1987**, *84*, 7413-7417.
6. I. Koltover, T. Salditt, J. O. Radler and C. R. Safinya. *Science* **1998**, *281*, 78-81.
7. M. Ranger, M. C. Jones, M. A. Yessine and J. C. Leroux. *J. Polym. Sci., Part A: Polym. Chem.* **2001**, *39*, 3861-3874.
8. A. M. Funhoff, S. Monge, R. Teeuwen, G. A. Koning, N. M. E. Schuurmans-Nieuwenbroek, D. J. A. Crommelin, D. M. Haddleton, W. E. Hennink and C. F. van Nostrum. *J. Controlled Release* **2005**, *102*, 711-724.
9. G. W. M. Vandermeulen, C. Tziatzios, R. Duncan and H. A. Klok. *Macromolecules* **2005**, *38*, 761-769.
10. V. Toncheva, M. A. Wolfert, P. R. Dash, D. Oupicky, K. Ulbrich, L. W. Seymour and E. H. Schacht. *Biochimica Et Biophysica Acta-General Subjects* **1998**, *1380*, 354-368.
11. D. Oupicky, K. A. Howard, C. Konak, P. R. Dash, K. Ulbrich and L. W. Seymour. *Bioconjugate Chem.* **2000**, *11*, 492-501.
12. P. Erbacher, A. C. Roche, M. Monsigny and P. Midoux. *Biochimica Et Biophysica Acta-Biomembranes* **1997**, *1324*, 27-36.
13. M. G. Banaszczyk, C. P. Lollo, D. Y. Kwoh, A. T. Phillips, A. Amini, D. P. Wu, P. M. Mullen, C. C. Coffin, S. W. Brostoff and D. J. Carlo. *J. Macromol. Sci., Pure Appl. Chem.* **1999**, *A36*, 1061-1084.
14. T. Blessing, M. Kursa, R. Holzhauser, R. Kircheis and E. Wagner. *Bioconjugate Chem.* **2001**, *12*, 529-537.
15. J. H. v. Steenis, E. M. v. Maarseveen, F. J. Verbaan, R. Verrijk, D. J. A. Crommelin, G. Storm and W. E. Hennink. *J. Controlled Release* **2003**, *87*, 167-176.
16. S. Pirotton, C. Muller, N. Pantoustier, F. Botteman, B. Collinet, C. Grandfils, G. Dandrifosse, P. Degee, P. Dubois and M. Raes. *Pharm. Res.* **2004**, *21*, 1471-1479.

Summary

DNA replication and transcription as it occurs in nature is one of the most exquisite examples of control over macromolecular features such as molecular length, monomer composition and consequently material properties.

Not surprisingly, many scientists have become inspired by the unique properties of DNA and have started to investigate the use of DNA as a building block for use in materials science. Described in chapter 1 are several examples in which DNA, nucleotides or nucleobases are incorporated in different materials.

Methacrylate monomers functionalized with the four nucleobases thymine, adenine, cytosine and guanine were prepared and described in chapter 2. Application of Atom Transfer Radical Polymerization in deuterated DMSO allowed controlled polymerization of the adenine-, thymine-, and, for the first time, also of the cytosine- and guanine-modified monomers. The guanine and cytosine monomers appeared to form a complex with the copper catalyst, as could be observed with ^{1}H-NMR spectroscopy. In case of guanine this did not cause any problems for the polymerization process, while in case of cytosine a stronger copper binding ligand, PMDETA, needed to be applied to gain control over polymerization.

Chapter 3 describes the preparation of a thymine functionalized block copolymer, starting from a poly(ethylene glycol) macro initiator, using ATRP. Polymerization of adenine monomer in DMSO-*d*6 showed a significant increase in polymerization rate when polymeric thymine template was present, while thymine monomer did not show a polymerization rate enhancement. Varying the template to monomer ratio demonstrated that the polymerization rate increased even further if an excess of template was applied. Surprisingly, the addition of monomeric complementary moieties resulted in an even greater rate enhancement. These findings led to our conclusion that non-covalent interaction between adenine and thymine in DMSO-d_6 protects the adenine monomer from interaction with the copper catalyst, thus resulting in a faster polymerization.

Using a similar procedure for block copolymer synthesis as was illustrated in chapter 3, chapter 4 described the preparation of both thymine and adenine block copolymers using ATRP. The aggregation behavior in aqueous medium of the separate block copolymers as well as a mixture was investigated with respect to nucleobase type and possible interaction between thymine and adenine. It was observed that the separate block copolymers

assembled into spherical aggregates, with a bimodal size distribution, indicating the presence of both polymeric micelles and large compound micelles. Upon mixing of the two block copolymers, the critical aggregation concentration increased, and a monomodal particle size distribution was observed. With UV Vis spectroscopy furthermore an interaction between the complementary nucleobases could be detected. These observations demonstrate that the amphiphilic behavior of this class of block copolymers is affected by the interaction between the complementary nucleobases, which leads to an unexpected increase in hydrophilicity of the block copolymer ensemble.

Chapter 5 describes and compares different methods to prepare tri-block copolymers. For the first method, the linear build method, two center polymer blocks were prepared. Both end groups of PEG were chemically modified into α-bromo esters. Additionally, telechelic PMMA was prepared by ATRP using a bifunctional initiator. Both telechelic polymers were used as a macro initiator for the polymerization of the outer nucleobase functionalized blocks. It was found that for the sequential buildup method, macro initiation from a telechelic PEG was the most successful. The second, modular build up method, investigated the use of an isocyanate end group as a reactive handle for the preparation of triblock copolymers. To this end, the α-bromo end groups of telechelic PMA, prepared by ATRP, and the hydroxyl end groups of telechelic PEG were both transformed into isocyanate groups. The coupling between a primary aliphatic amine group of a short nucleobase functionalized polymer and the telechelic isocyanate PEG and PMA was explored. It was found that thymine nucleobase polymers could be successfully coupled to both PEG and PMA. However, coupling of adenine nucleobase polymers was hampered due to solubility problems.

Chapter 6 describes the exploration of waters soluble PEG nucleobase functionalized block copolymers prepared in chapter 3 as gene delivery vehicles. Binding experiments with single stranded Thymine DNA showed complete binding of only the complementary adenine block copolymer upon addition of a 1 to 1 ratio between polymer and DNA nucleobases. As expected binding efficiency of non-complementary double stranded plasmid DNA was significantly less, but nonetheless, some binding was observed. Unfortunately, gene delivery using only the PEG block copolymers as gene delivery vehicles failed. However, promising results were obtained when the PEG block copolymers were used as pegylation agents upon condensation of DNA with Ca^{2+} salts.

Samenvatting

DNA verdubbeling en transcriptie zoals dat in de natuur gebeurt, is een van de meest spraakmakende voorbeelden van controle over macromoleculaire eigenschappen zoals molecuul- lengte, samenstelling en de daaruit voortvloeiende materiaaleigenschappen.

Het is dan ook niet verwonderlijk dat vele wetenschappers geïnspireerd zijn door de unieke eigenschappen van het DNA molecuul, en begonnen zijn met het onderzoeken van DNA als een bouwsteen voor nieuwe materialen. Hoofdstuk 1 beschrijft verschillende voorbeelden waarin DNA, nucleotides en nucleobasen ingebouwd worden in verschillende materialen.

Methacrylaat monomeren gefunctionaliseerd met de vier nucleobasen thymine, adenine, cytosine en guanine zijn gesynthetiseerd en beschreven in hoofdstuk 2. Door toepassing van Atoom Transfer Radicaal Polymerisatie in gedeutereerde DMSO kon een gecontroleerde polymerisatie van de adenine-, thymine-, en voor de eerste keer ook de cytosine en guanine monomeren aangetoond worden. Vooral cytosine en guanine monomeren bleken een complex te vormen met koper. In het geval van het guanine monomeer leverde dit geen problemen op voor het polymerisatie proces, echter in geval van het cytosine monomeer was het sterk koper bindende ligand PMDETA nodig om de polymerisatie gecontroleerd te laten verlopen.

Hoofdstuk 3 beschrijft de bereiding van een thymine gefunctionaliseerd blockcopolymeer, met behulp van ATRP, startend vanaf een poly(ethyleen glycol) macro initiator. Polymerisatie van het adenine monomeer in DMSO-d_6 liet een significante versnelling in polymerisatie snelheid zien in aanweigheid van thymine sjabloon polymeer, terwijl het thymine monomeer deze versnelling in polymerisatie snelheid niet liet zien. Wijzigen van sjabloon-monomeer verhouding liet zien dat de polymerisatie snelheid verder verhoogd werd als een overmaat aan sjabloon gebruikt werd. Verrassend was dat additie van een complementaire monomere eenheid resulteerde in een nog grotere polymerisatie snelheidsverhoging. Deze bevindingen leiden tot de conclusie dat een niet covalente interactie tussen adenine en thymine in DMSO-d6 zorgt voor bescherming van het adenine monomeer tegen interactie met koper, waardoor uiteindelijk de polymerisatie van adenine sneller verloopt.

In hoofdstuk 4 wordt, gebruikmakend van de in hoofdstuk 3 beschreven procedures om blokcopolymeren te maken, de bereiding van zowel thymine als adenine blokcopolymeren met behulp van ATRP beschreven. Het aggregatie gedrag in waterig medium van zowel de losse blokcopolymeren als het mengsel werd bestudeerd. Hierbij werd onder andere gekeken naar nucleobase type en mogelijkheid van interactie tussen adenine en thymine, en werd waargenomen dat de losse blokcopolymeren aggregeren tot sferische aggregaten met een bimodale verdeling. Dit was een indicatie voor de aanwezigheid van micellen en grotere multilaag micellaire structuren. Door de complementaire blokcopolymeren te mengen werd een verhoogde kritische micel concentratie en een monomodale deeltjesgrootte verdeling gevonden. Daarnaast werd met UV Vis spectroscopie een interactie tussen de complementaire nucleobasen waargenomen. Al deze bevindingen demonstreren dat het amfifiele gedrag van de blokcopolymeren beïnvloed werd door de interacties tussen complementaire nucleobasen, die leiden tot onverwachte toenames in hydrofiliciteit van de blokcopolymere ensembles.

Hoofdstuk 5 beschrijft en vergelijkt verschillende methodes om triblok copolymeren te bereiden. Voor de eerste methode, de lineaire opbouwmethode, zijn twee polymere middenblokken gesynthetiseerd. Beide eindgroepen van PEG werden chemisch gemodificeerd in α-bromoesters. Daarnaast werd een telecheel PMMA center polymeer gemaakt door middel van ATRP vanaf een bifunctionele initiator. Beide centrum polymeren zijn vervolgens gebruikt als macro initiator voor de polymerisatie van nucleobase gefunctionaliseerde polymere blokken. Hierbij werd gevonden dat voor de lineaire opbouwmethode macroinitiatie van een telecheel PEG het meest succesvol was. De tweede, modulaire opbouwmethode, bestudeerde het gebruik van isocyanaat eindgroepen als reactieve handvaten voor de opbouw van de triblokcopolymeren. Met dit als doel werden de α-broomgroepen van een telecheel PMA, verkregen met behulp van ATRP, en de hydroxy eindgroepen van een bifunctioneel PEG gemodificeerd tot isocyanaat eindgroepen. De koppeling van korte nucleobase-gefunctionaliseerde polymeren met een primaire amine eindgroep met telecheel isocyanaat PEG en PMA werd bestudeerd. Hierbij werd gevonden dat de thymine nucleobase polymeren succesvol gekoppeld konden worden, maar dat koppeling met adenine nucleobase polymeren verhinderd werd door ernstige oplosbaarheidsproblemen.

Hoofdstuk 6 beschrijft de exploratie van de wateroplosbare PEG nucleobase gefunctionaliseerde blokcopolymeren uit hoofdstuk 3 als gen-aflever-systemen. Bindingsexperimenten met enkelzijdig thymine DNA resulteerde in een volledige binding met alleen het complementaire adenine PEG blokcopolymeer in een 1 op 1 verhouding tussen polymeer en DNA nucleobasen. Zoals verwacht was de binding met niet-complementair dubbel strengs plasmide DNA veel minder efficiënt, echter binding met het plasmide DNA kon wel worden waargenomen. Helaas mislukte gentransfectie bij HELA cellen wanneer gebruik gemaakt werd van alleen de blokcopolymeren als gen-aflever-systeem. Desalniettemin leverde een gen therapie experiment waarbij de PEG block copolymeren gebruikt werden als PEG-ylerings agens tijdens een Ca^{2+} transfectie een positief resultaat op.

Dankwoord

Na een lange periode van studeren, en hard werken komt er dan toch een einde aan een lange loopbaan als scholier, student en uiteindelijk AIO (assistent in opleiding), met het schrijven van dit proefschrift. Het is vooral tijdens de schrijfperiode dat je tot realisatie komt hoeveel mensen in meer of mindere mate tijdens de onderzoeksperiode bijgedragen hebben aan dit proefschrift. Graag wil ik deze gelegenheid aangrijpen om iedereen hiervoor hartelijk te bedanken en een aantal mensen in het bijzonder.

Allereerst ben ik mijn promotor Jan van Hest zeer dankbaar dat hij mij de kans heeft gegeven om na mijn stage periode als eerste student in de van Hest groep, het leerproces van een promotie onderzoek door te maken. Jan jouw creativiteit en enthousiasme voor een breed onderzoeksveld hebben op mij een zeer grote indruk gemaakt. Het vertrouwen dat jij in mij had om dit onderzoek zelfstandig uit te voeren en de altijd aanmoedigende woorden "nog even die reactie en dan kunnen we dit zo publiceren" wat er in de praktijk altijd op neer kwam dat het idee veel makkelijker gezegd werd dan gedaan was, hebben mij door de promotie tijd heen geleid.

Floris van Delft wil ik bedanken voor de begeleiding tijdens mijn stage periode waardoor ik klaar gestoomd was voor mijn promotie. Daarnaast is jouw hulp bij de synthese route van het guanine monomeer onmisbaar geweest, want blijkbaar hebben sommige (☹☠💣✂☠) Mitsunobu reacties toch een soort van "fingerspitzengefühl" nodig, die ik nog niet heb.

Lee Ayres, bedankt voor alle nuttige discussies over ATRP, maar vooral voor het levendig en wakker houden van de rest. Samen met Dennis Vriezema wens ik jou heel veel succes met jullie bedrijf Encapson, wie weet kunnen we ooit zaken doen.

Mark Lambermon wil ik graag bedanken voor zijn hulp bij de gel electroforese experimenten en Mark Damen wil ik bedanken voor zijn hulp bij de cel transfectie studies.

Tijdens mijn promotie heb ik het genoegen gehad om verscheidene studenten te mogen begeleiden. Een aantal daarvan wil ik in het bijzonder bedanken. Joost Opsteen, ik mocht jou al begeleiden als student toen ik zelf formeel nog niet eens als AIO begonnen was. Jouw resultaten zijn verwerkt in hoofdstuk 5 van dit proefschrift, en je hebt dit als basis voor jouw eigen promotie onderzoek kunnen gebruiken. In al die jaren heb ik je als collega, en vriend leren kennen en ik ben dan ook blij dat jij een van mijn paranimfen wil zijn.

Ton, jij was de tweede fulltime student die ik mocht begeleiden. Hiervoor ben ik erg dankbaar, want dankzij jouw enorme werklust en enthousiasme zijn jouw stageresultaten uiteindelijk verwerkt in maarliefst twee artikelen en hoofdstukken van dit proefschrift. Het verbaast mij nog steeds dat je naast je dagelijkse werk als AIO nog voldoende tijd overhebt voor Halfvol, iWings en je vriendin Susanne, dus ik wil jou dan ook met al die dingen heel veel succes wensen. Roy, jij was de laatste student die ik gedeeltelijk mocht begeleiden. Helaas zijn jou resultaten van het gedeelde project met Matthijs niet in dit proefschrift verwerkt, maar ik wil jou toch bedanken voor jou inzet, en veel succes wensen met je eigen onderzoek.

Verder wil ik de overige studenten en leden van de van Hest groep met name: Dennis, Hans, Jeffrey, Joris, Marjolein, Jurgen, Rosalie, Kaspar, Pieter, Erik, Hefziba, Bertil, Mariska en Femke bedanken voor de gezelligheid en de nuttige discussies. Minstens zo belangrijk waren de mensen die zorgden voor de analytische ondersteuning. Peter van Dijk als er weer eens met spoed een stofje besteld moest worden, Ad Swolfs voor de NMR ondersteuning, en Peter van Galen en Helene Amatdjais-Groenen voor het meten van de massa spectra. De secretaresses Jacky en Desiree omdat je daar altijd voor van alles en nog wat terecht kan. Daarnaast wil ik vrienden en collega's die het werk op de derde verdieping van het UL tot een groot plezier maakten bedanken: Hester, Jeroen, Sjef, Christien, Bart, Koen, Stan, Brian, Sander, Roel, Valeria, Sander H, Daniel, Guuske, Jan D, Bas, Maarten, Dani, Leon, Rene, Richard, Jasper, Denis. Verder wil ik uiteraard alle andere studenten en AIO's die ik vergeten ben in dit lijstje en ontmoet heb tijdens mijn periode bedanken voor de nodige gezelligheid tijdens de gezamenlijke uitjes en borrels.

Omdat een deel van dit proefschrift geschreven is toen ik al bezig was met mijn huidige werk wil ik naast mijn oude collega's ook mijn nieuwe collega's Vincent, Patrick, John en Tijl bedanken voor hun steun en motivatie (nimmer eindigend geouwehoer) over de snelle afwikkeling van mijn proefschrift. We hebben er in ieder geval een prachtige smurfenmop en een mooie barbecue met rare helikopter insecten aan over gehouden.

Mijn familie kan ik nooit genoeg bedanken voor hun fantastische steun zowel tijdens mijn studie als tijdens mijn promotie. Al blijft voor jullie scheikunde een onbegrijpelijk terrein, nooit heeft dat jullie er van weerhouden om belangstelling te tonen. Francis en Michel, bedankt voor alle steun, in het bijzonder tijdens de moeilijke periode na het overlijden van papa. Ik ben daarom ook erg blij dat Michel mij als paranimf wil bijstaan.

Mam, al is papa er nu helaas niet meer bij, zonder jullie beide steun zou dit proefschrift er nooit zijn gekomen. De passie en het enthousiasme die pap altijd voor zijn vakgebied, de bouw had, blijft voor mij altijd een groot voorbeeld. Het feit dat jullie altijd voor mij klaar stonden als ik iets nodig had, en het vertrouwen dat jullie in mij hadden, hebben mij gebracht waar ik nu ben.

Henri

List of publications

1. J. C. M. van Hest, H. Spijker, L. Ayres, J. Opsteen, M. Vos and H. Adams. Well-defined bio-related polymer structures, prepared by ATRP *Polym. Prepr. (Am. Chem. Soc., Div. Polym. Chem.)* **2002**, *43*, 42-43.

2. J. C. M. van Hest, L. Ayres, H. Spijker, M. Vos and J. Opsteen. Bioinspired triblock copolymers prepared by atom transfer radical copolymerization *ACS Symp. Ser.* **2003**, *854*, 394-410.

3. J. C. M. van Hest, H. Spijker, L. Ayres, J. Opsteen, J. Smeenk and H. Adams. Biomolecular building blocks for well-defined polymer architectures *Polym. Prepr. (Am. Chem. Soc., Div. Polym. Chem.)* **2003**, *44*, 628-629.

4. H. J. Spijker, A. J. Dirks and J. C. M. van Hest. Unusual rate enhancement in the thymine assisted ATRP process of adenine monomers *Polymer* **2005**, *46*, 8528-8535.

5. H. J. Spijker, T. J. Dirks, F. L. Van Delft and J. C. M. van Hest. Nucleobase directed template polymerizations *Polym. Prepr. (Am. Chem. Soc., Div. Polym. Chem.)* **2005**, *46*, 157-158.

6. H. J. Spijker, A. J. Dirks and J. C. M. van Hest. Synthesis and assembly behavior of nucleobase-functionalized block copolymers *J. Polym. Sci., Part A: Polym. Chem.* **2006**, *44*, 4242-4250.

7. H. J. Spijker, F. L. van Delft, J. C. M. van Hest. Atom Transfer Radical Polymerization of Adenine, Thymine, Cytosine and Guanine Nucleobase Monomers. *Macromolecules* **2007**, *40*, 12-18.

Curriculum Vitae

Henri Johannes Spijker is geboren op 31 maart 1976 te Enschede. In 1992 behaalde hij zijn MAVO diploma (D-Niveau) aan het Dr. A. Ariëns college te Enschede. In datzelfde jaar begon hij aan de Middelbare Laboratorium Opleiding (MLO) te Hengelo waarna hij in 1995 doorgestroomd is naar de Hogere Laboratorium Opleiding (HLO) te Enschede die hij in 1998 afrondde in de richting Organische Chemie na zijn afstudeerstage bij AKZO Nobel te Arnhem. Aansluitend begon de auteur aan een versnelde studie scheikunde aan de Radboud Universiteit te Nijmegen die hij in 2001 voltooide met het doctoraalexamen. De hoofdvakstage werd op de afdeling organische chemie uitgevoerd onder leiding van Dr. Floris van Delft en Prof. Jan van Hest.

Het stage onderwerp vormde vervolgens de basis voor de werkzaamheden die verricht zijn tussen maart 2001 en juni 2005 als Junior Onderzoeker te Nijmegen. De resultaten van het onderzoek staan in dit proefschrift beschreven en zijn uitgevoerd onder de leiding van Prof. Jan van Hest. Hij heeft het NSRIM opleidingsprogramma gevolgd en was betrokken bij het onderwijs aan studenten.

Sinds 1 oktober 2005 is Henri werkzaam als projectleider bij Syntarga B.V. te Nijmegen.